UNIVERSITY OF CALIFORNIA,
IRVINE

LYVE1 as a Marker for Definitive Hematopoietic Stem Cell Ontogeny

DISSERTATION

submitted in partial satisfaction of the requirements
for the degree of

DOCTOR OF PHILOSOPHY

in Biological Sciences

by

Yasamine Ghorbanian

Dissertation Committee:
Associate Professor Matthew A. Inlay, Chair
Associate Professor Kim N. Green
Professor Craig M. Walsh

2019

DEDICATION

To my parents for their abundance of encouragement, support, and love.
To my sister for being my best friend, my motivator, and my distraction when I needed it.
To Coco for all the love and cuddles.

I could not have done any of this without you.

TABLE OF CONTENTS

LIST OF FIGURES AND MOVIES

LIST OF TABLES

ACKNOWLEDGMENTS

I first would like to express my sincerest thank you to my thesis advisor, Dr. Matthew Inlay, for his encouragement and guidance. His mentorship has helped to shape me into the scientist that I have become today. I will forever be grateful for his support, understanding, and friendship.

I would also like to thank my committee members, Drs. Green and Walsh, for their input and insights regarding my various research projects. They have been instrumental in shaping my dissertation.

There are a few other UCI professors I would like to thank. First, I'd like to thank Dr. Pavan Kadandale, Dr. Brian Sato, and Dr. Daniel Mann for their incredible mentorship in pedagogy. I have learned so much from them and have grown into a more confident instructor as a result. I would also like to thank Dr. Andrea Tenner and Dr. Alex Boiko for their guidance as members of my advancement committee. I'd like to thank Dr. Melissa Lodoen and Dr. David Fruman for their incredible mentorship and support during my undergraduate years here at UCI. They were really the motivation for me to apply to graduate school. A very special thank you goes to my undergraduate research mentor, Dr. David Gardiner, for giving me a chance and allowing me to conduct research in his lab.

In addition, I would like to thank all the incredibly intelligent and talented people who I had the pleasure of working with. My lab mates, Dr. Ankita Shukla, Dr. Alborz Karmizadeh, Dr. Tannaz Faal, and Erika Varady, made the lab a fun and positive environment to work in. I will always value them as not only great scientists, but as cherished friends as well. I also had the wonderful opportunity to collaborate with the Green Lab. Dr. Lindsay Hohsfield, Dr. Allison Najafi, and Joshua Crapser made the Green Lab feel like a second lab family. I learned so much from all of them and am so grateful for their friendship. I'd also like to thank Dr. Shiva Othy for his incredible expertise on 2 photon microscopy and for the great scientific discussions that we had. To all the students I mentored- Andrew Pop, Shailey Patel, Angela Nguyen, and Rocio Barahona- thank you for all your hard work. I would like to extend a special thank you to Vanessa Scarfone. She was not only a great resource as the SCRC Flow Core manager, but she was also a source of support and friendship that I will always be thankful for. I'd like to thank Dr. Laura McIntyre as well for being one of my best friends throughout this whole experience.

I'd like to thank me fiancée, Vincent, for his love, understanding, and support. It's been such a fun journey over the past few years and I'm so glad we've been able to help each other succeed.

Lastly I would like to thank my family. You have all shown me nothing but love, support, and encouragement throughout my entire life and I am so thankful. To my parents and my sister, for whom this work is dedicated, I have no way of ever expressing how much I love you all. Thank you for everything that you have done for me and for shaping me into the person that I have become today. My only hope is that I have made you proud.

I would like to thank Cell Press for permission to include Chapter One of my dissertation, which was originally published in Cell Reports. This work was supported by the National Institutes of Health (T32NS082174 to YG and R56HL133656 to MAI) and the UCI Sue and Bill Gross Stem Cell Research Center Seed Grant.

CURRICULUM VITAE

Yasamine Ghorbanian
linkedin.com/in/yasamine-ghorbanian

Education

PhD **University of California, Irvine**
Molecular Biology and Biochemistry, November 2019

BS **University of California, Irvine**
Microbiology and Immunology, June 2013

Research Experience

Inlay Lab, 2014-Present

Graduate Thesis Lab; Department of Molecular Biology and Biochemistry; University of California, Irvine

My thesis project focused on determining if the yolk sac contributes to definitive hematopoiesis in the mouse. In collaboration with the Mikkola lab, we used a Lyve1-Cre lineage tracing reporter and showed that Lyve1 is a marker that is enriched in the yolk sac endothelium. These Lyve1-derived cells contribute to each *definitive* wave of embryonic hematopoiesis. About one-third of adult hematopoietic stem cells are derived from Lyve1-expressing precursors and these HSCs are engraftable and multipotent. This lineage tracing system can also be used to mark microglia, a project that we are pursuing in collaboration with the Green lab.

Gardiner Lab, June 2012-June 2013

Undergraduate Research; Department of Developmental and Cell Biology; University of California, Irvine

My project was to characterize regenerative and scar-like responses in the axolotl (*Ambystoma mexicanum*) following injury.

Publications

Lee LK, **Ghorbanian Y**, Wang W, Wang Y, Kim YJ, Weissman IL, Inlay MA, Mikkola HK. LYVE1 marks the divergence of yolk sac definitive hemogenic endothelium from the primitive erythroid lineage. Cell Rep. 2016 Nov 22;17(9):2286-2298. doi: 10.1016/j.celrep.2016.10.080. PubMed PMID: 27880904.

Hohsfield LA, Najafi AR, **Ghorbanian Y**, Soni N, Crapser J, Figueroa Velez DX, Jiang S, Royer SE, Kim SJ, Anderson AJ, Gandhi SP, Mortazavi A, Inlay MA, Green KN. Complete microglial elimination stimulates recruitment of distinct meningeal-associated myeloid cells (MAMs) that fully reconstitute the adult brain in a wave that originates from the SVZ. *Manuscript in revision for Cell.*

Hohsfield LA, Najafi AR, **Ghorbanian Y**, Soni N, Hingco EE, Kim SJ, Jue AD, Swarup V, Inlay MA, Green KN. Effects of long-term replacement if the microglial tissue with peripheral bone marrow-derived myeloid cells on the neuronal landscape and cognition. *Manuscript in submission.*

Karimzadeh A, Varady ES, Scarfone VM, Chao C, Grathwohl K, Nguyen PU, **Ghorbanian Y**, Serwold T, Inlay MA. CD11a identifies embryonic pre-HSCs via neonatal transplant system. *Manuscript in submission.*

Ghorbanian Y, Othy S, Shukla A, Barahona R, Patel S, Pop A, Chen F, Chao C, Karimzadeh A, Parker I, Cahalan MD, Mikkola HK, Inlay MA. LYVE1 identifies a population of cells in the embryo that contributes to a third of the adult hematopoietic stem cell pool. *Manuscript in preparation.*

Ghorbanian Y, Shukla AK, Fabello J. Extraembryonic mesoderm derived hematopoietic stem cells. *Manuscript in preparation.*

Ghorbanian Y, Patel S, Nguyen A, Barahona R, Inlay MA. Lineage bias seen in the Lyve1Cre model is specific to the reporter system used. *Manuscript in preparation.*

Fellowships and Honors

2017-2019	National Institute of Neurological Disorders and Stroke pre-doctoral fellowship (NINDS/NIH T32)
2018-2019	University of California, Irvine Teaching Apprenticeship in STEM
2018	Edward Steinhaus Teaching Award Recipient
2017	Associated Graduate Students Travel Award
2017	University of California, Irvine Center for Engaged Instruction Pedagogical Fellowship

Professional Memberships

2017-2018	International Society for Experimental Hematology, Member
2016-2017	International Society for Stem Cell Research, Member

Professional Development

2018	iPSC Reprogramming and Culturing Techniques Course through the University of California, Irvine's Stem Cell Research Center (Certificate)
2018	Effective Communications for Scientists at the University of California, Irvine (Certificate)
2018	Reviewed manuscript for EMBO Reports with Dr. Inlay
2018	Reviewed manuscript for Stem Cell Reports with Dr. Inlay
2017	UCI Center for Integration of Research, Teaching, and Learning (CIRTL) Associate Level Certificate

Presentations

Abstract Selected Talks

UCI Immunology Fair, *December 2017* **Talk awarded first place**
"Tracing the emergence of hematopoietic stem cells from the extra-embryonic yolk sac"
SoCal Flow Summit, *April 2017* **Excellence in Cytometry Award**
"Hematopoietic stem cells and their downstream effector immune cells have yolk sac origins"

Oral Presentations

Associated Graduate Students Symposium, *April 2017*
Immunology Department Seminar, *March 2017*
Molecular Biology and Biochemistry Department Seminar, *November 2016, February 2016, April 2015*
UCI Stem Cell Awareness Day Scientific Symposium, *October 2016*
UCI Stem Cell Research Center High School Program (Pilot), *August 2015*

Poster Presentations

La Jolla Immunology Conference, *October 2018, October 2017, October 2016* ***AAI Young Investigator award****, October 2015*
ISEH Annual Meeting, *August 2018, August 2017*
Molecular Biology and Biochemistry Departmental Retreat, *March 2018, March 2017, March 2015*
ISSCR Annual Meeting, *June 2017*
Gavin Herbert Eye Institute Bench to Bedside Symposium, *March 2017* ***1st place poster***
SoCal Flow Summit, *April 2016, April 2015*
UCI Immunology Fair, *December 2015*

Teaching Experience

Molecular Biology
Instructor of Record, *Summer 2019*
Molecular Biology
Teaching Assistant, *Spring 2015, Spring 2016, Spring 2019*
Guest lecturer, *Spring 2017, Spring 2019*
Teaching Assistant Professional Development Program
Instructor, *Fall 2017, Fall 2018*
Immunology Lab
Head Teaching Assistant and guest lecturer, *Spring 2016, Spring 2017*
Teaching Assistant*, Spring 2015*
Molecular Biology Lab
Guest lecturer*, Spring 2016, Fall 2017 (flipped lecture)*
Teaching Assistant, *Fall 2015*
Immunology with Hematology
Teaching Assistant, *Fall 2015*

Mentorship

Rocio Barahona
June 2019-September 2019, First year PhD student at UCI
Angela Nguyen
September 2018-June 2019, Undergraduate at UCI; received the Undergraduate Research Opportunities Program fellowship; Currently a research technician for the Blumberg Lab at UCI
Shailey Patel
July 2017-July 2018, Undergraduate at UCI; received the Undergraduate Research Opportunities Program fellowship; Currently a research technician for the St Pierre Schneider Lab at UNLV
Andrew Pop
March 2016-June 2017, Undergraduate at UCI; received the Undergraduate Research Opportunities Program fellowship; Currently a medical student at Loma Linda Medical School
Leanne Hildebrand
January - July 2016, Undergraduate at CalState Fullerton, California Institute for Regenerative Medicine Fellow; Received her Master's degree from UCI

Science Outreach

Southern California Flow Cytometry Association Social Media Outreach Team
2018-2019, Instagram and Twitter account manager
Ask-A-Scientist Night
October 2013, October 2014, October 2015, October 2017, October 2018, Volunteer for elementary school science fair project planning
Stem Cell Awareness Day
November 2014, October 2016, October 2018, Volunteer for high school, community college, and general public science education and engagement (tours, talks, science demonstrations)
Project Based Learning Showcase
May 2018, Volunteer judge for middle school TED talk projects
21st Century Career Conference
December 2017, Presenter to middle school audience
COSMOS Tour
August 2017, Presenter for summer high school program
UCI Stem Cell Research Center High School Program (Pilot)
August 2015, Chair of organizational committee for summer high school program and helped to write CIRM SPARK grant application
Stem Cells Offer Hope
May 2015, Volunteer for general public education and engagement

ABSTRACT OF THE DISSERTATION

LYVE1 as a Marker for Definitive Hematopoietic Stem Cell Ontogeny

By

Yasamine Ghorbanian

Doctor of Philosophy in Biological Sciences

University of California, Irvine, 2019

Associate Professor Matthew A. Inlay, Chair

The question of the developmental origins of hematopoietic stem cells (HSCs) is an actively investigated topic in the hematopoiesis field. It is an important subject to address because of its potential impact on identifying and treating the root cause of hematopoietic disorders and diseases. It had been found that LYVE1, which is most commonly known as a lymphatic vessel marker, identifies a population of blood vessel endothelial cells in the embryo and hematopoietic cells in the adult mouse (Pham et al. 2010). Over the course of my dissertation research, we sought to determine the contribution of LYVE1-derived cells to the adult (definitive) HSC population. We utilized a lineage tracing system and identified that LYVE1 marks definitive hemogenic endothelium— a subset of endothelial cells that gives rise to hematopoietic cells early in development— in the yolk sac and the AGM. We found that these LYVE1-derived pre-HSCs take longer to mature than their non-LYVE1-derived counterparts and need to receive maturation signals from the intra-embryonic environment in order to become fully functional. These LYVE1-derived cells persist to adulthood and contribute to approximately a third of the adult murine HSC pool. During the course of these studies, we also found the

importance of utilizing different reporter systems in order to validate the phenotypes identified using Cre-Lox recombination systems. Overall, the findings in these studies indicate that there are multiple pools of HSCs (Lyve1-derived and not) and that each pool has a unique origin. The heterogeneity of the HSC pool should be considered when differentiating these cells from iPSCs for both research and clinical translational purposes. It should also be something that is considered during the treatment of different hematopoietic disorders, as there may be a healthy and diseased pool of HSCs that corresponds with their developmental origins.

INTRODUCTION

Hematopoietic stem cells (HSCs) are an incredibly important cell type that generates the entire blood system. When this system becomes diseased or fails the outcome is most often fatal. The ultimate treatment for a hematopoietic illness is a blood and marrow transplant (BMT), which is transfer of healthy, donor HSCs into the patient. This involves ablating the patient's diseased blood system and replacing it with the newly transplanted one. However, the largest hurdle towards the success of this transplant is finding a source of donor cells that will not be rejected or fail due to an incompatible immune (HLA) match. The best solution for this problem is to use patient derived cells —a perfect HLA match— reprogram them into induced pluripotent stem cells (iPSCs), and then differentiate those into HSCs for transplantation. This has been an elusive treatment thus far because reliable differentiation of HSCs to be used in a clinical setting has yet to be achieved. The biggest contribution to this inability to differentiate HSCs from iPSCs is the lack of understanding of how HSCs are first created during embryonic development. The ontogeny of HSCs has been debated since the 1970s. Early work contributed definitive HSC production to the yolk sac (YS) where the first hematopoietic cells are seen, but in the 1990s this was contested as many started to find evidence of other sources of HSCs, namely the aorta-gonad-mesonephros (AGM) and the placenta. It is important to understand the embryonic origins of HSCs in order to elucidate the signals and microenvironment necessary for their creation. It is only then can we hope to recreate this process *in vitro* as a potential therapy to cure any disease or disorder that has a hematopoietic cause.

In this work we have identified a population of cells that are LYVE1-derived and contribute to the murine definitive HSC pool. LYVE1 labels a subset of definitive hemogenic

endothelium that gives rise to cells of all waves of definitive hematopoiesis in the embryo and to HSCs in the adult. A third of the adult HSC pool is LYVE1-derived and these cells possess the hallmark properties of a definitive HSC (self renewing, multipotent, and engraftable). We believe that we have identified a source of hemogenic endothelium that is found in both the YS and the AGM that contributes to the adult HSCs. This may have implications in that it is not necessarily the tissue that these cells are found in that is important for their creation, but the specific cells, signals, and the microenvironment that they create in multiple tissues that is vital to the creation of definitive HSCs.

Hematopoietic stem cells constitute the entire blood system

Hematopoietic stem cells are the blood (*hemato-*) forming *(-poietic*) cells in the body. These stem cells are multipotent as they are able to undergo asymmetric division. They divide and differentiate into downstream hematopoietic progenitors, which then produce erythrocytes, platelets, and leukocytes (monocytes, granulocytes, and lymphocytes). These effector cells are responsible for carrying oxygen, responding to blood vessel injury, and protecting the body from disease, infection, and cancer.

In addition to being able to produce all the cells in the blood system, HSCs are able to undergo symmetric division to create more of themselves. This self-renewal process is essential in maintaining the stem cell pool for the life of the organism. In fact, it is one of the reasons why BMT is used clinically to treat many hematopoietic diseases. BMT is essentially transplantation of HSCs from one person (the donor) to another (the recipient). This is largely successful because HSCs are engraftable, meaning that they can home to their bone marrow

(BM) niche and be maintained there. Their multipotency allows them to reconstitute the recipient's entire blood system and the transplantation only needs to be performed once because the HSCs are self-renewing and are able to sustain the HSC pool.

These properties (multipotency, self renewal, and engraftability) are true of HSCs not only in the adult, but in the embryo as well. During developmental hematopoiesis, the HSCs and their precursors are responsible for creating the blood cells that keep the embryo alive. Which effector cells are produced is dictated by the needs of the embryo at that particular developmental stage. As the embryo matures and develops, so does the lineage potential of the HSCs and their precursors.

Embryonic hematopoiesis occurs in waves

Early on in development, at 7.5 days into gestation (E7.5), the first wave of hematopoiesis arises (Moore and Metcalf 1970). This "primitive" wave gives rise to nucleated erythrocytes containing fetal hemoglobin to provide oxygen to the cells of the developing embryo (Moore and Metcalf 1970; Auerbach, Huang, and Lu 1996; Lux et al. 2008). The yolk sac (YS) is the source of these primitive HSC precursors (Moore and Metcalf 1970). The next wave of hematopoiesis, which begins to appear around E8.5 and is the first "definitive" wave, is the erythromyeloid progenitor (EMP) wave (Lux et al. 2008). The HSC precursors in this wave differentiate into enucleated erythrocytes and myeloid cells (monocytes and granulocytes). These are the cells of the innate immune system and are evolutionarily the first type of immune system to emerge. These cells help with embryonic development, as they are involved in tissue remodeling.

Following the EMP wave is the pre-HSC wave. These HSC precursors (pre-HSCs) start to appear at E10, but have controversial origins (McGrath and Palis 2005; Lux et al. 2008; Batsivari et al. 2017). They have the hallmark properties of HSCs in that they are multipotent self-renewing cells, but they can only be transplanted successfully into embryonic or neonatal recipients. These pre-HSCs can differentiate to make up cells of the entire blood system, much like their HSC counterparts (Yoder et al. 1997; Yoder and Hiatt 1998; Yoder, Hiatt, and Mukherjee 1997).

By E11.5, the definitive HSCs are present in the embryo. These cells have all the characteristic properties of their adult counterparts and can therefore engraft into adult recipients (Palis 2001; Batsivari et al. 2017). Because the BM niche is not yet established at this time point, the embryonic definitive HSCs reside in the fetal liver (FL). The FL, which contains hematopoietic cells starting at E10, is the main site for hematopoiesis in the embryo by E12 and these cells migrate to the BM from E15 until shortly after birth (Johnson and Moore 1975; Palis 2001; Ghiaur et al. 2008).

These hematopoietic stem and precursor cells all have an initial non-hematopoietic origin. There is a specific subset of endothelial cells with hematopoietic potential, called the hemogenic endothelium, which gives rise to embryonic HSCs and their precursors (Dieterlen-Lièvre 1998; Ottersbach and Dzierzak 2005). The tissue, or tissues, that contains the hemogenic endothelial population from which the definitive waves originate is a topic of intense debate in the hematopoiesis field and is an active area of research. There has been conflicting evidence that implicates the YS, aorta-gonad-mesonepheros (AGM), and the placenta as potential sources of definitive HSCs in the embryo, the history of which are detailed in this chapter.

The yolk sac as a hematopoietic tissue

Hemangioblasts, blood islands, and primitive erythropoiesis

Early in embryonic development, around E7.5, the first hematopoietic precursors arise concurrently with vascular endothelial cell precursors in the YS (Auerbach, Huang, and Lu 1996; Moore and Metcalf 1970; McGrath and Palis 2005). The single progenitor that gives rise to these cells, because it has this dual potential, was termed the "hemangioblast" (Auerbach, Huang, and Lu 1996; Palis 2001; McGrath and Palis 2005). The fate of these hemangioblast cells is determined by the presence of vascular endothelial growth factor (VEGF). VEGF binding to its receptor, Flk-1, results in differentiation of endothelial cells, whereas absence of VEGF-Flk-1 binding results in a hematopoietic cell fate (Palis 2001). The primitive blood cells start to develop as small clusters of cells called blood islands (Auerbach, Huang, and Lu 1996; Moore and Metcalf 1970; Palis 2001; Lux et al. 2008). The presence of this form of erythroid cell— large, nucleated, and expressing embryonic hemoglobins— is what defines the primitive wave of hematopoiesis from the definitive wave, which gives rise to smaller, adult hemoglobin expressing erythrocytes (McGrath and Palis 2005; Lux et al. 2008). The early YS is where the primitive wave of hematopoiesis originates (Auerbach, Huang, and Lu 1996; Moore and Metcalf 1970; Palis 2001; McGrath and Palis 2005; Lux et al. 2008), but the contribution of the YS to later definitive waves is highly debated.

Definitive hematopoiesis and transplantation models

Early models of hematopoiesis by Moore, Owen, and Metcalf stated that HSCs are produced in the YS and then migrate to and seed the FL (Moore and Owen 1967; Moore and

Metcalf 1970). More recently, it has been shown that circulation and the ability of definitive hematopoietic stem and progenitor cells (HSPCs) to migrate is necessary for the presence of these cells in the embryo proper (EP) (Lux et al. 2008; Ghiaur et al. 2008). In $Ncx1^{-/-}$ mice, which lack a heartbeat and therefore do not establish circulation, the numbers of definitive HSPCs in the YS were normal when compared to wildtype (WT). However, there were almost no HSPCs in the EP without circulation, which suggests that HSPCs seen in the EP in WT mice migrated there from the YS via circulation (Lux et al. 2008). It has also been shown that Rac1 is necessary for the migration of HSPCs. In $Rac1^{-/-}$ mice there is again a significant decrease in HSPCs in the EP whereas there was no significant change in the YS. This indicates that migration is necessary for intraembryonic hematopoiesis and provides evidence that migrating HSPCs may originate from the YS (Ghiaur et al. 2008).

One of the defining properties of HSCs is their ability to engraft into a host. Cells from the AGM are the first to be able to engraft into a conditioned adult recipient. Their engraftment potential begins at E10, whereas cells from the FL and YS engraft into adults a day later (Müller et al. 1994; A. Medvinsky and Dzierzak 1996). However, cells from E8 or E9 YS can engraft into conditioned embryonic recipients as shown by Weissman and colleagues in 1978, or conditioned neonatal recipients as shown by Yoder and Hiatt (Yoder et al. 1997; Yoder, Hiatt, and Mukherjee 1997; Yoder and Hiatt 1998). In addition to their ability to engraft into conditioned newborn primary recipients, E9 YS derived cells can also engraft into secondary recipients and thus demonstrate definitive HSC repopulating activity (Yoder et al. 1997; Palis 2001). Because early YS cells are able to engraft into embryonic or neonatal recipients, but not adults until later stages, this suggests that the E8-E10.5 hematopoietic stem and precursor cells

in this tissue require additional maturation steps (Yoder et al. 1997; Samokhvalov, Samokhvalova, and Nishikawa 2007). It has been hypothesized that hematopoietic stem and precursor cells in the YS have the potential to become HSCs, but "require a different microenvironment" for further differentiation (Auerbach, Huang, and Lu 1996; Moore and Metcalf 1970; Ghiaur et al. 2008). This new microenvironment may promote differentiation due to the presence of certain factors that were not in the YS or loss of any inhibitory factors secreted in the YS (Auerbach, Huang, and Lu 1996; Moore and Metcalf 1970). The FL, the HSC niche during mid-gestation, appears to be the main contender for this inductive microenvironment (Auerbach, Huang, and Lu 1996; Moore and Metcalf 1970; Palis 2001), but the AGM has been implicated as well (Samokhvalov, Samokhvalova, and Nishikawa 2007; Metcalf 2008; Kumaravelu et al. 2002).

The AGM as a source of definitive HSCs

Early evidence for the AGM as a hematopoietic source

Early experiments have shown that the YS gives rise to the first hematopoietic cells and YS-derived cells have multi-lineage potential (Moore and Metcalf 1970). It has also been shown that in the early embryo an intraembryonic source of hematopoietic cells called the para-aortic splanchnopleura (PAS) also has multi-lineage potential and, like the early YS, these cells do not successfully engraft into a conditioned adult (A. L. Medvinsky and Dzierzak 1998; Kumaravelu et al. 2002). Part of the PAS goes on to form the AGM and this, as well as some other work in avian and amphibian hematopoiesis, laid the groundwork for investigation into the AGM as a

potential source of definitive HSCs (A. L. Medvinsky et al. 1993; A. L. Medvinsky and Dzierzak 1998; Kumaravelu et al. 2002).

Definitive HSC potential and culturing systems

Multipotency is a central characteristic of a definitive HSC and the spleen colony formation unit assay (CFU-S) is one method to determine whether or not a certain subset of cells has this potential. When comparing the CFU-S activity of the YS, AGM, and FL it was found that the AGM has a higher frequency of CFU-S compared to the YS and this begins before the activity found in the FL at late E10.5 (A. L. Medvinsky et al. 1993). This CFU-S activity correlated with stem cell factor (SCF) expression at these stages (E9 and E10) in that it is high in the AGM and low in the YS indicating that SCF may play a role in timing and tissue specificity of definitive HSC emergence or maturation (A. L. Medvinsky et al. 1993).

However, because hematopoietic cells are in circulation this is a confounding variable in determining whether the tissue the cells are found in is the site of maturation or of *de novo* cell synthesis. In order to address this caveat, Medvinsky and Dzierzak developed an *in vitro* organ culturing system. YS, AGM, and FL tissues from E9-11 embryos were harvested, cultured, and then assayed for CFU-S activity. They reported that E10 and E11 AGM tissues were able to generate, maintain, and even increase CFU-S activity whereas YS cultures were only able to maintain CFU-S activity at E10 and minimally increase activity at E11. From this data they proposed that the AGM is the source of CFU-S progenitors that then seed the FL (A. Medvinsky and Dzierzak 1996). This idea was later expanded upon by utilizing a limiting dilution analysis to map the colonization of the FL by definitive HSCs/long-term repopulating units (HSC/RUs). It

was found that at E11 there are about 3 HSC/RUs in the embryo, but this rapidly increases to about 66 HSC/RUs (53 in the FL) at E12. To resolve the contribution of different hematopoietic tissues to FL colonization, HSC/RU numbers in each tissue were quantified and then cultured to determine their generation and expansion potential at E11-12. It was found that the AGM was able to generate HSC/RUs at E11, but that this ability dropped at E12 when the YS potential peaked, suggesting that the AGM and the YS both contribute to FL colonization by HSC/RUs in two sequential waves (Kumaravelu et al. 2002).

Transplantation into conditioned adults

Another indication that AGM-derived definitive HSCs migrate to and colonize the FL prior to colonization by YS-derived cells is given by transplantation experiments. It has been shown that cells from the AGM can engraft into conditioned adults a day earlier (E10) than the FL or YS (E11) (Müller et al. 1994; A. Medvinsky and Dzierzak 1996). Importantly, this has also been demonstrated using human tissue. Cells from the AGM in human tissues demonstrate long-term multilineage engraftment in both primary and secondary recipient immunodeficient mice (Ivanovs et al. 2011).

The CFU-S studies, both with cultured and uncultured tissues, suggest that the AGM is the first site of definitive HSC production and transplantation studies support these findings. However, it cannot be ruled out that pre-HSCs from other tissues migrate to the AGM prior to E10 and then further differentiate and mature in the AGM microenvironment (A. L. Medvinsky and Dzierzak 1998; Müller et al. 1994). The YS is potentially one of these other tissues because it contains pre-HSCs that can engraft into conditioned embryonic or neonatal recipients (Yoder,

Hiatt, and Mukherjee 1997; Yoder et al. 1997; Yoder and Hiatt 1998). This implies that these HSC precursors need to migrate into the embryo to acquire certain differentiation signals (Müller et al. 1994; Batsivari et al. 2017). Because the AGM has higher levels of SCF at E10 than the YS, it has the appropriate conditions for HSC maturation (Müller et al. 1994; Batsivari et al. 2017). These mature cells from the AGM, and potentially the later stage YS, then migrate to and colonize the FL HSC niche (Kumaravelu et al. 2002; Batsivari et al. 2017; Müller et al. 1994).

The placenta is a third origin of HSCs

There have also been studies showing that the placenta, in addition to the YS and AGM, may give rise to definitive HSCs during embryonic development. The first source of evidence for this was that the placenta contains multilineage hematopoietic progenitors between E10 and E12 as demonstrated by a colony formation assay (Alvarez-Silva et al. 2003). Building upon these findings by using a Ly6A-GFP mouse model, it was shown that the vasculature in the placenta is marked by Ly6A (Sca-1). In previous experiments using Ly6A-GFP mice to study hematopoietic tissues like the AGM and YS, it was found that this system labeled endothelial tissues and these GFP+ populations contained definitive HSCs as measured by engraftment into conditioned adult recipients. Similarly, Ly6A-labeled placenta cells from E11 and E12 embryos resulted in multilineage engraftment into primary and secondary recipients (Ottersbach and Dzierzak 2005). Others have confirmed these findings and have found that the engraftment potential of cells from the placenta begins around the same time as that of cells from the AGM (around E10.5) and that HSC pool expands in the placenta until E13.5 (Gekas et al. 2005;

Mikkola et al. 2005). Taken together, these studies suggest that the placenta is an important hematopoietic tissue that contributes to the definitive HSC pool along with the AGM and YS.

LYVE1 as a potential marker for hematopoietic tissues

LYVE1 is the receptor for hyaluronan

Lymphatic vessel endothelial hyaluronan (HA) receptor-1, or LYVE1, is an integral membrane protein that is related to CD44, a HA receptor on leukocytes (Banerji et al. 1999; Prevo et al. 2001; Jackson 2004). HA is a glycosaminoglycan found in the extracellular matrix (ECM) and has important roles in cell migration, wound healing, inflammation, embryonic morphogenesis, and cell differentiation (Prevo et al. 2001; Banerji et al. 1999). This ECM component plays many vital roles and genetic deletion of HA synthetase results in embryonic lethality (Banerji et al. 1999). HA has a very short half-life (approximately 24 hours) and is transported by the lymphatic system for degradation in the lymph nodes and subsequent uptake by the liver (Banerji et al. 1999). The receptor for HA in the lymphatics was identified in 1999 as LYVE1. Because LYVE1 expression seemed to be exclusive to the lymphatic vessels and was not expressed in blood vessels it quickly became a useful marker for this subset of endothelial cells (Banerji et al. 1999).

Role of LYVE1

The actual mechanism by which LYVE1 worked remained elusive for quite some time and is still being actively researched. It is speculated that LYVE1 might “sequester HA” on lymphatic vessel walls or bind to leukocytes that have HA bound CD44 on their surface to

mediate their movement within, into, and out of the lymphatics (Banerji et al. 1999; Lawrance et al. 2016). LYVE1 has also been implicated to have a role in lymphangiogenesis (Lawrance et al. 2016). It was found that LYVE1 was expressed on both the luminal and abluminal sides of the lymphatic vessels *in vivo* and demonstrated the ability to bind to and internalize HA *in vitro* by receptor-mediated endocytosis. This indicated that LYVE1's function was not in the degradation of HA, but in its in transport from the tissue to the lymphatics (Prevo et al. 2001; Jackson 2004).

Lyve1 in embryonic development

The discovery of LYVE1 as a lymphatic vessel marker has enabled research into lymphangiogenesis in both the context of normal embryonic development and cancer (Jackson 2004). It facilitated validation of the hypothesis that lymphatic vessels bud from the cardinal vein during embryogenesis, indicating that they first arise from blood vessels. This was demonstrated by knockout of SLP-76 and Syk, which resulted in mixed blood and lymphatic circulations indicating a failure in complete separation of the lymphatics from their progenitors (Jackson 2004). It was also found that a certain fraction of blood endothelial cells was labeled in embryonic development when a Lyve1-Cre mouse strain was crossed to a YFP reporter strain (Pham et al. 2010). This paper, which generated the Lyve1-Cre mice, also reported that approximately half of the hematopoietic cells (CD45+) were labeled in this system. This included both lymphoid and myeloid cells and they suggested that LYVE1 may be expressed in hematopoietic precursors during embryonic development (Pham et al. 2010). This finding was the preliminary evidence and inspiration for the following work. During the course of my

dissertation research I sought to determine the contribution of LYVE1-derived cells to the definitive hematopoietic pool in order to better elucidate the ontogeny of HSCs.

References

Alvarez-Silva, M., P. Belo-Diabangouaya, J. Salaun, and F. Dieterlen-Lievre. 2003. "Mouse Placenta Is a Major Hematopoietic Organ." *Development* 130: 5437–44.

Auerbach, Robert, Hua Huang, and Lisheng Lu. 1996. "Hematopoietic Stem Cells in the Mouse Embryonic Yolk Sac." *Stem Cells* 14 (3): 269–80. https://doi.org/10.1002/stem.140269.

Banerji, Suneale, Jian Ni, Shu Xia Wang, Steven Clasper, Jeffrey Su, Raija Tammi, Margaret Jones, and David G. Jackson. 1999. "LYVE-1, a New Homologue of the CD44 Glycoprotein, Is a Lymph-Specific Receptor for Hyaluronan." *Journal of Cell Biology* 144 (4): 789–801. https://doi.org/10.1083/jcb.144.4.789.

Batsivari, Antoniana, Stanislav Rybtsov, Celine Souilhol, Anahi Binagui-Casas, David Hills, Suling Zhao, Paul Travers, and Alexander Medvinsky. 2017. "Understanding Hematopoietic Stem Cell Development through Functional Correlation of Their Proliferative Status with the Intra-Aortic Cluster Architecture." *Stem Cell Reports* 8 (6): 1549–62. https://doi.org/10.1016/j.stemcr.2017.04.003.

Dieterlen-Lièvre, Françoise. 1998. "Hematopoiesis: Progenitors and Their Genetic Program." *Current Biology* 8 (20): 727–30. https://doi.org/10.1016/s0960-9822(98)70460-9.

Gekas, Christos, Francoise Dieterlen-Lièvre, Stuart H. Orkin, and Hanna K.A. Mikkola. 2005. "The Placenta Is a Niche for Hematopoietic Stem Cells." *Developmental Cell* 8 (3): 365–75. https://doi.org/10.1016/j.devcel.2004.12.016.

Ghiaur, Gabriel, Michael J. Ferkowicz, Michael D. Milsom, Jeff Bailey, David Witte, Jose A. Cancelas, Mervin C. Yoder, and David A. Williams. 2008. "Rac1 Is Essential for Intraembryonic Hematopoiesis and for the Initial Seeding of Fetal Liver with Definitive Hematopoietic Progenitor Cells." *Blood* 111 (7): 3322–30. https://doi.org/10.1182/blood-2007-09-078162.

Ivanovs, Andrejs, Stanislav Rybtsov, Lindsey Welch, Richard A. Anderson, Marc L. Turner, and Alexander Medvinsky. 2011. "Highly Potent Human Hematopoietic Stem Cells First Emerge in the Intraembryonic Aorta-Gonad-Mesonephros Region." *Journal of Experimental Medicine* 208 (12): 2417–27. https://doi.org/10.1084/jem.20111688.

Jackson, David G. 2004. "Biology of the Lymphatic Marker LYVE-1 and Applications in Research into Lymphatic Trafficking and Lymphangiogenesis." *Apmis* 112 (7–8): 526–38. https://doi.org/10.1111/j.1600-0463.2004.apm11207-0811.x.

Johnson, G. R., and M. A.S. Moore. 1975. "Role of Stem Cell Migration in Initiation of Mouse Foetal Liver Haemopoiesis." *Nature* 258 (5537): 726–28. https://doi.org/10.1038/258726a0.

Kumaravelu, Parasakthy, Lilian Hook, Aline M. Morrison, Jan Ure, Suling Zhao, Sergie Zuyev, John Ansell, and Alexander Medvinsky. 2002. "Quantitative Developmental Anatomy of Definite Haematopoietic Stem Cells/Long-Term Repopulating Units (HSC/RUs): Role of the

Aorta-Gonad-Mesonephros (AGM) Region and the Yolk Sac in Colonisation of the Mouse Embryonic Liver." *Development* 129 (21): 4891–99.
Lawrance, William, Suneale Banerji, Anthony J. Day, Shaumick Bhattacharjee, and David G. Jackson. 2016. "Binding of Hyaluronan to the Native Lymphatic Vessel Endothelial Receptor LYVE-1 Is Critically Dependent on Receptor Clustering and Hyaluronan Organization." *Journal of Biological Chemistry* 291 (15): 8014–30. https://doi.org/10.1074/jbc.M115.708305.
Lux, Christopher T., Momoko Yoshimoto, Kathleen McGrath, Simon J. Conway, James Palis, and Mervin C. Yoder. 2008. "All Primitive and Definitive Hematopoietic Progenitor Cells Emerging before E10 in the Mouse Embryo Are Products of the Yolk Sac." *Blood* 111 (7): 3435–38. https://doi.org/10.1182/blood-2007-08-107086.
McGrath, Kathleen, and James Palis. 2005. "Hematopoiesis in the Yolk Sac: More than Meets the Eye." *Experimental Hematology* 33 (9): 1021–28. https://doi.org/10.1016/j.exphem.2005.06.012.
Medvinsky, Alexander, and Elaine Dzierzak. 1996. "Definitive Hematopoiesis Is Autonomously Initiated by the AGM Region." *Cell* 86 (6): 897–906. https://doi.org/10.1016/S0092-8674(00)80165-8.
Medvinsky, Alexander L., and Elaine A. Dzierzak. 1998. "Development of the Definitive Hematopoietic Hierarchy in the Mouse." *Developmental & Comparative Immunology* 22 (3): 289–301. https://doi.org/10.1016/S0145-305X(98)00007-X.
Medvinsky, Alexander L., Nina L. Samoylina, Albrecht M. Müller, and Elaine A. Dzierzak. 1993. "An Early Pre-Liver Intraembryonic Source of CFU-S in the Developing Mouse." *Nature* 364 (6432): 64–67. https://doi.org/10.1038/364064a0.
Metcalf, Donald. 2008. "AGM: Maternity Ward or Finishing School?" *Blood*. American Society of Hematology. https://doi.org/10.1182/blood-2007-11-124412.
Mikkola, H.K.A., C. Gekas, S. Orkin, and F. Dieterlen-Lievre. 2005. "Placenta as a Site for Hematopoietic Stem Cell Development." *Experimental Hematology* 33 (9): 1048–54. https://doi.org/10.1016/j.exphem.2005.06.011.
Moore, Malcolm A.S., and Donald Metcalf. 1970. "Ontogeny of the Haemopoietic System: Yolk Sac Origin of In Vivo and In Vitro Colony Forming Cells in the Developing Mouse Embryo." *British Journal of Haematology* 18 (3): 279–96. https://doi.org/10.1111/j.1365-2141.1970.tb01443.x.
Moore, Malcolm A.S., and J Owen. 1967. "Stem-Cell Migration in Developing Myeloid and Lymphoid Systems." *Lancet* 11: 658–59.
Müller, Albrecht M., Alexander Medvinsky, John Strouboulis, Frank Grosveld, and Elaine Dzierzakt. 1994. "Development of Hematopoietic Stem Cell Activity in the Mouse Embryo." *Immunity* 1 (4): 291–301. https://doi.org/10.1016/1074-7613(94)90081-7.
Ottersbach, Katrin, and Elaine Dzierzak. 2005. "The Murine Placenta Contains Hematopoietic Stem Cells within the Vascular Labyrinth Region." *Developmental Cell* 8 (3): 377–87. https://doi.org/10.1016/j.devcel.2005.02.001.
Palis, J. 2001. "Yolk-Sac Hematopoiesis The First Blood Cells of Mouse and Man." *Experimental Hematology* 29 (8): 927–36. https://doi.org/10.1016/S0301-472X(01)00669-5.
Pham, Trung H.M., Peter Baluk, Ying Xu, Irina Grigorova, Alex J. Bankovich, Rajita Pappu, Shaun R. Coughlin, Donald M. McDonald, Susan R. Schwab, and Jason G. Cyster. 2010. "Lymphatic

Endothelial Cell Sphingosine Kinase Activity Is Required for Lymphocyte Egress and Lymphatic Patterning." *The Journal of Experimental Medicine* 207 (1): 17–27. https://doi.org/10.1084/jem.20091619.

Prevo, Remko, Suneale Banerji, David J.P. Ferguson, Steven Clasper, and David G. Jackson. 2001. "Mouse LYVE-1 Is an Endocytic Receptor for Hyaluronan in Lymphatic Endothelium." *Journal of Biological Chemistry* 276 (22): 19420–30. https://doi.org/10.1074/jbc.M011004200.

Samokhvalov, Igor M., Natalia I. Samokhvalova, and Shin-ichi Nishikawa. 2007. "Cell Tracing Shows the Contribution of the Yolk Sac to Adult Haematopoiesis." *Nature* 446 (7139): 1056–61. https://doi.org/10.1038/nature05725.

Yoder, Mervin C., and Kelly Hiatt. 1998. "Engraftment of Embryonichemato- Poietic Cells in Conditioned Newborn Recipients." *Blood* 89: 2176–83.

Yoder, Mervin C., Kelly Hiatt, Parmesh Dutt, Pinku Mukherjee, David M. Bodine, and Donald Orlic. 1997. "Characterization of Definitive Lymphohematopoietic Stem Cells in the Day 9 Murine Yolk Sac." *Immunity* 7 (3): 335–44. https://doi.org/10.1016/S1074-7613(00)80355-6.

Yoder, Mervin C., Kelly Hiatt, and Pinku Mukherjee. 1997. "In Vivo Repopulating Hematopoietic Stem Cells Are Present in the Murine Yolk Sac at Day 9.0 Postcoitus." *Proc. Natl. Acad. Sci.* 94: 6776–80.

CHAPTER ONE

LYVE1 Marks the Divergence of Yolk Sac Definitive Hemogenic Endothelium from the Primitive Erythroid Lineage

Lydia K. Lee[1,2], Yasamine Ghorbanian[3], Wenyuan Wang[1], Yanling Wang[1], Yeon Joo Kim[1], Irving L. Weissman[4], Matthew A. Inlay[3], Hanna K.A. Mikkola[1, 5]

[1]Dept. of Molecular, Cell & Developmental Biology at UCLA, Los Angeles, CA, 90095; [2]Dept. of Obstetrics and Gynecology at UCLA, Los Angeles, CA, 90095, [3]Sue and Bill Gross Stem Cell Research Center, Dept. of Molecular Biology & Biochemistry at UCI, [4]Institute of Stem Cell Biology and Regenerative Medicine and Ludwig Center at Stanford University, Stanford, CA 94305, USA [5]Eli and Edythe Broad Center for Regenerative Medicine and Stem Cell Research at UCLA, Los Angeles, CA, 90095.

***The following chapter was published in *Cell Reports* 17, 2286-2298 (2016)**

Abstract

The contribution of the different waves and sites of developmental hematopoiesis to fetal and adult blood production remain uncharted. We identified LYVE1 as a marker of yolk sac (YS) endothelium and definitive hematopoietic stem/progenitor cells (HS/PC). LYVE1-Cre labeled endothelium in mid-gestation YS and vitelline vessels while sparing the dorsal aorta and placenta. Whereas most YS HS/PCs and erythro-myeloid progenitors were LYVE1-Cre lineage-traced, primitive erythroid cells were not, suggesting they represent distinct lineages. Fetal liver (FL) and adult HS/PCs showed 35-40% LYVE1-Cre marking. Analysis of circulation-deficient *Ncx1*$^{-/-}$ concepti identified the YS as a major source of LYVE1-Cre labeled HS/PCs. FL pro-erythroblast compartment was extensively labeled at E11.5-13.5, whereas by E16.5, proerythroblast marking decreased to levels equivalent to HSCs, suggesting that HSCs from multiple sources became responsible for erythropoiesis. LYVE1-Cre thus marks the divergence between YS primitive and definitive hematopoiesis and provides a tool to target YS definitive hematopoiesis and FL colonization.

Introduction

Developmental hematopoiesis is comprised of temporally orchestrated programs that generate both the differentiated blood cells to support embryonic growth, and the undifferentiated hematopoietic stem cells (HSCs) to sustain post-natal hematopoiesis. This challenge is met by segregating hematopoiesis into multiple waves that occur in different anatomical locations. The earliest ("primitive") hematopoietic wave starts in the extra-embryonic yolk sac (YS) at E7.5 and gives rise to erythroid cells that fulfill the immediate

metabolic needs of the embryo (Moore and Metcalf, 1970). They are characterized by the expression of embryonic β globin (betaH1 in mice) (Haar and Ackerman, 1971). At E8.5-9.5, the YS also generates an intermediate ("transient-definitive") wave of erythro-myeloid progenitors (EMP) (McGrath et al., 2015; Mikkola and Orkin, 2006; Palis et al., 1999) that produce red cells that express "definitive" adult type β-globins (beta-major in mice)(McGrath et al., 2003). However, YS EMPs lack self-renewal ability and lymphoid potential, the hallmarks of HSCs. It has been proposed that EMPs initiate fetal liver (FL) definitive hematopoiesis and function in supporting embryonic survival (Chen et al., 2011), inflammatory signaling during HSC emergence (Espín-Palazón et al., 2014), and adult tissue-resident macrophage development (Gomez Perdiguero et al., 2015). However, the duration and significance of this second wave are not fully understood.

The final ("definitive") wave generates self-renewing, multipotent HSCs that sustain lifelong production of all blood cell types. Transplantable HSCs were first identified at E10.5-11.5 in the intra-embryonic para-aortic splanchnopleural/aorta-gonad-mesonephros region (pSP/AGM), and the vitelline and umbilical vessels that connect the pSP/AGM to extra-embryonic tissues (Medvinsky and Dzierzak, 1996; Muller et al., 1994) . Several studies have proposed that the YS and the placenta (PL) can also generate multipotent HS/PCs *de novo* (Inlay et al., 2014; Rhodes et al., 2008; Samokhvalov et al., 2007; Weissman et al., 1978; Weissman et al., 1977; Zeigler et al., 2006). Direct transplantation of pre-circulation YS tissues into congenic embryos and inducible *Runx1* lineage-tracing both supported the hypothesis that YS contributes to adult hematopoiesis (Samokhvalov et al., 2007; Weissman et al., 1978; Weissman et al., 1977). Moreover, *in vitro* experiments with placental tissues isolated before the onset of

circulation or from heartbeat-deficient *Ncx1*$^{-/-}$ concepti demonstrated multi-lineage hematopoietic potential (Rhodes et al., 2008; Zeigler et al., 2006). However, the degrees to which each organ contributes to the post-natal HSC pool remain to be determined.

The identity of the precursors for the different hematopoietic waves has been studied intensely. Recently, lineage tracing and time-lapsed imaging of HS/PC emergence *in vitro* and *in vivo* evidenced that definitive HS/PCs arise from specialized endothelial cells, named hemogenic endothelium (Bertrand et al., 2010; Boisset et al., 2010; Chen et al., 2009; Eilken et al., 2009; Lancrin et al., 2009; Zovein et al., 2008). Hemogenic competence in the endothelium is established by the bHLH factor SCL/TAL1 (Stem cell leukemia gene/T-cell acute leukemia gene 1), which activates a broad transcriptional network of hematopoietic regulators and prevents misspecification of the endothelium to cardiac fate (Van Handel et al., 2012). Together with GATA factors, SCL turns on *Runx1* and other transcription factors that enable HS/PC emergence from hemogenic endothelium (Org et al., 2015). SCL is also essential for the generation of primitive erythroid cells, and controls the terminal maturation of erythroid cells at all stages of ontogeny (Mikkola et al., 2003a; Schlaeger et al., 2005; Shivdasani et al., 1995). However, the identity of the immediate precursors for the primitive erythroid cells, and the timing when they diverge from the definitive hematopoietic lineages is not known. The presumption that these hematopoietic waves represent distinct lineages that arise from their own precursors ("lineage switch" model) has been challenged by studies that show sequential expression of both the primitive and definitive globins ("maturational switch" model) during erythroid maturation (Kingsley et al., 2006; McGrath et al., 2011; Palis, 2008; Qiu et al., 2008).

Although the fundamentals of the developmental hematopoietic hierarchy are gradually

being revealed, the contributions of each wave and hemogenic tissue to fetal and post-natal hematopoiesis remain poorly defined. This is due to the lack of wave- and tissue-specific tools to prospectively isolate and track the progeny of the temporally and spatially overlapping blood precursors. Most surface antigens expressed in hemogenic endothelium or emerging HS/PCs – e.g. *Flk1*, *CD31*, *VE-Cadherin*, *Tie2*, *CD41*, *ckit* and *Sca1*--, are not specific to individual wave or anatomical site (McKinney-Freeman et al., 2009; Mikkola and Orkin, 2006). Although many of these markers are developmentally regulated, none of them is wave-specific. The use of inducible lineage-tracing studies using regulatory elements of hematopoietic transcription factors (e.g. *Runx1*) is complicated by the fact that the expression of such factors is not restricted to a particular hemogenic tissue (Samokhvalov et al., 2007). Thus, there are no robust methods to separate or genetically target *in vivo* individual hematopoietic waves or hemogenic tissues.

Here we identify the lymphatic vessel endothelial hyaluronan receptor-1 (LYVE1) as a marker that is differentially and highly expressed in YS endothelium during HS/PC development. Lineage tracing using reporter gene expression and conditional deletion of hematopoietic regulators *Scl* and *Runx1* by LYVE1-Cre distinguished YS endothelium, EMPs and definitive HS/PCs from the primitive erythroid lineage. Our data suggest that LYVE1-Cre labeled cells primarily originate from the YS and/or vitelline vessels, and contribute to 35-40% of fetal and adult HSC compartments. At E11.5 the FL pro-erythroblast pool is dominated by LYVE1-lineage cells, whereas by late gestation the level of marking is similar to the HSC compartment, implying a temporal switch in the precursors responsible for FL erythropoiesis. LYVE1-Cre thus

provides a unique tool to investigate the contribution of YS hemogenic endothelium to fetal and adult hematopoiesis, and the factors that regulate the fate of these cells.

Results

LYVE1 protein is expressed in YS endothelium and definitive hematopoietic cells

To map the complex hierarchy of developmental hematopoiesis and define the precursors and respective contributions of the different waves to fetal and adult hematopoiesis, we sought to identify cell surface markers expressed in hemogenic endothelium that are tissue- or wave-specific. From a list of genes encoding surface proteins highly expressed in YS endothelium (Van Handel et al., 2012), *LYVE1* (lymphatic vessel endothelial hyaluronan receptor-1) emerged as a promising candidate. Initially reported as a marker for lymphatic vasculature, LYVE1 expression was later documented also in mid-gestation YS vasculature, FL sinusoids, intersomitic vessels and cardinal vein, while being minimal in the dorsal aorta (Banerji et al., 1999; Gordon et al., 2008).

As LYVE1 expression has not been assessed in the context of developmental hematopoiesis, LYVE1 protein expression was surveyed in hemogenic organs by immunostaining and flow cytometry. Immunofluorescence (IF) at E10.5 demonstrated robust LYVE1 protein expression in YS and vitelline vasculature, whereas no signal was observed in the placenta, umbilical vessels and the dorsal aorta (**Figure 1.1A**). LYVE1 protein expression was ubiquitous in $CD31^+$ endothelial cells of E9.5 YS (**Figures 1.1B and 1.1C**). In contrast, minimal LYVE1 protein was identified in embryo (EM) and PL endothelium (**Figure 1.1C**). Very little LYVE1 protein was discernible in PL vasculature during HS/PC emergence (E11.5) and

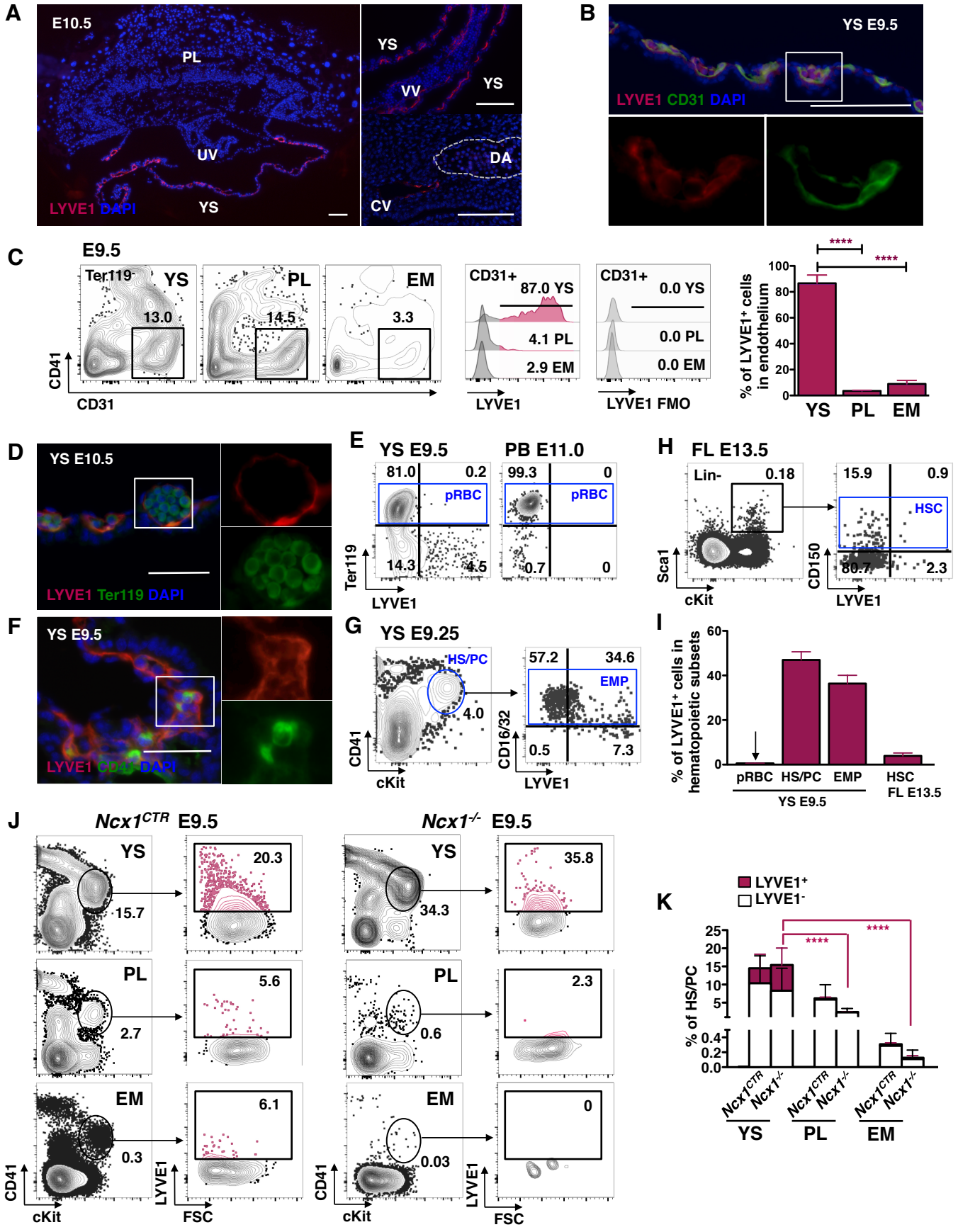
A
E10.5
PL
UV
YS
LYVE1 DAPI
YS
VV
YS
DA
CV
B
YS E9.5
LYVE1 CD31 DAPI
C
E9.5
Ter119-
YS
13.0
PL
14.5
EM
3.3
CD41
CD31
CD31+
87.0 YS
4.1 PL
2.9 EM
LYVE1
CD31+
0.0 YS
0.0 PL
0.0 EM
LYVE1 FMO
****
****
% of LYVE1+ cells in endothelium
YS
PL
EM
D
YS E10.5
LYVE1 Ter119 DAPI
E
YS E9.5
PB E11.0
81.0
0.2
pRBC
14.3
4.5
99.3
0
pRBC
0.7
0
Ter119
LYVE1
H
FL E13.5
Lin-
0.18
15.9
0.9
HSC
80.7
2.3
Sca1
cKit
CD150
LYVE1
F
YS E9.5
LYVE1 CD41 DAPI
G
YS E9.25
HS/PC
4.0
57.2
34.6
EMP
0.5
7.3
CD41
cKit
CD16/32
LYVE1
I
% of LYVE1+ cells in hematopoietic subsets
pRBC
HS/PC
EMP
HSC
YS E9.5
FL E13.5
J
Ncx1CTR E9.5
Ncx1-/- E9.5
YS
15.7
20.3
PL
2.7
5.6
EM
0.3
6.1
YS
34.3
35.8
PL
0.6
2.3
EM
0.03
0
CD41
cKit
LYVE1
FSC
K
LYVE1+
LYVE1-
****
****
% of HS/PC
Ncx1CTR
Ncx1-/-
YS
PL
EM

Figure 1.1 LYVE1 protein is expressed in YS endothelium and HS/PCs
(A) LYVE1 protein is detected by immunofluorescence (IF) in E10.5 yolk sac (YS), vitelline vessels (VV) and cardinal vein (CV), but is absent from the placenta (PL), umbilical vessels (UV) and dorsal aorta (DA). Representative images from 3 independent experiments. Scale bar, 100µm.
(B) IF staining shows co-localization of LYVE1 in E9.5 YS $CD31^+$ endothelium. Representative image from 3 independent experiments. Scale bar, 100µm.
(C) FACS analysis of $CD31^+CD41^-Ter119^-$ endothelium in YS, PL and caudal half of the embryo (EM) of one representative E9.5 conceptus. Corresponding histograms of $LYVE1^+$ endothelial cells show robust LYVE1 expression in YS endothelium only. Data from n=11, from 3 independent experiments are represented as mean ± SD; p values of ≤0.001 are shown as ***.
(D) LYVE1 protein is not discernable by IF in $Ter119^+$ primitive erythroid cells in E10.5 YS. Representative image from 2 independent experiments is shown. Scale bar, 50µm.
(E) Representative FACS plots indicate that $Ter119^+$ primitive erythroid cells (pRBC) do not express LYVE1 in E9.5 YS or E11.0 peripheral blood (PB).
(F) IF staining of E9.5 YS shows co-expression of LYVE1 protein with HS/PC marker CD41. Representative image from 3 independent experiments is shown. Scale bar, 50µm.
(G) Representative FACS plots show LYVE1 expression in $CD41^{mid}cKit^+Ter119^-$ HS/PCs and its subset, $CD16/32^+$ erythro-myeloid progenitors (EMP) in E9.25 YS.
(H) Representative FACS plots of E13.5 fetal liver (FL) document minimal LYVE1 expression in $Lin^-Sca1^+cKit^+$ $CD150^+$ HSC compartment.
(I) LYVE1 expression is prominent in mid-gestation YS HS/PCs and EMPs. Data from n=8, 3 independent experiments for YS pRBC; n=28, 10 independent experiments for YS HS/PC; n=8, 3 independent experiments for YS EMP; n=6, 2 independent experiments for FL HSC subset are shown as mean ± SD.
(J) Representative FACS plots of hemogenic tissues in *Ncx1*$^{-/-}$ E9.5 concepti demonstrate the enrichment of LYVE1-expressing $CD41^{mid}cKit^+Ter119^-$ HS/PCs in the YS.
(K) Significantly higher fraction of YS HS/PCs than PL or EM (embryo) HS/PCs expresses LYVE1 protein in *Ncx1*$^{-/-}$ concepti. Quantification of n=23 for control and n=11 for *Ncx1*$^{-/-}$, from 5 independent experiments is represented as mean ± SD. P values of the difference of $LYVE1^+$ fractions at ≤0.0001 are shown as ****.
See also Figure S1.1

expansion/maturation (E13.5); however, some LYVE1 protein was detected in PL endothelium at late gestation (E16.5), when PL HSC pool has already diminished (Gekas et al., 2005) (**Figure S1.1A**). As reported previously, LYVE1 expression was identified in the cardinal vein at E10.5, but spared from the dorsal aorta and umbilical vessels (**Figure 1.1A**). At E13.5, LYVE1 expression was also abundant in FL sinusoids and azygous vein --tissues incapable of de novo generation of HS/PCs-- but not the aorta (**Figure S1.1B**).

Analysis of the early concepti revealed LYVE1 expression by E7.5 in $Tie2^{+}CD31^{+}$ angioblasts (**Figure S1.1C**). At E8.5, LYVE1 was expressed in YS $Tie2^{+}CD31^{+}$ angioblasts and excluded from $Ter119^{+}$ primitive erythroid cells (**Figure S1.1C**), and the embryo proper or allantois (data not shown).

These data show that the YS is the primary site containing LYVE1 expressing endothelium during HS/PC emergence. Moreover, these data imply that LYVE1 protein is expressed already at the time when primitive hematopoiesis begins and the endothelium that gives rise to definitive lineages in the YS is specified.

We next assessed the expression of LYVE1 protein in YS hematopoietic cells. IF and flow cytometry analysis showed that $Ter119^{+}$ primitive erythroid cells were devoid of LYVE1 expression (**Figures 1.1D, 1.1E and 1.1I**). In contrast, LYVE1 surface expression was observed in 47.0 ± 19.1% SD of E9.25-9.5 YS $CD41^{mid}cKit^{+}Ter119^{-}$ cells (**Figures 1.1F, 1.1G and 1.1I**), which predominantly consists of erythro-myeloid progenitors (EMP) (Ferkowicz et al., 2003; Mikkola et al., 2003b). Co-staining for the EMP marker CD16/32 (McGrath et al., 2015) suggested that most $LYVE1^{+}$ HS/PCs in E9.25 YS are EMPs (**Figure 1.1G**). In contrast to YS HS/PCs, the E13.5 FL

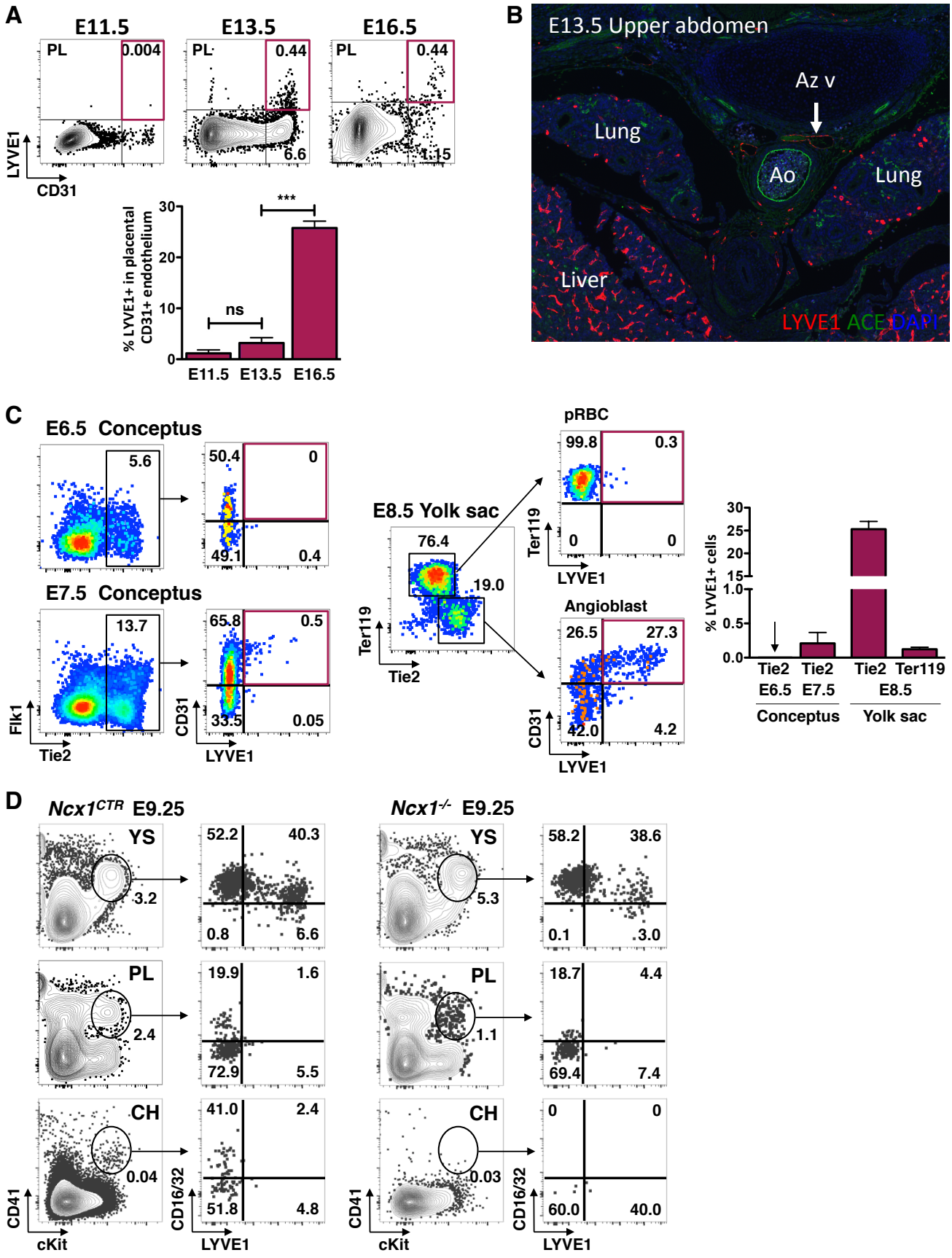
A
E11.5
E13.5
E16.5
PL
0.004
0.44
6.6
1.15
LYVE1
CD31
% LYVE1+ in placental CD31+ endothelium
ns
***
E11.5 E13.5 E16.5
B
E13.5 Upper abdomen
Az v
Lung
Ao
Lung
Liver
LYVE1 ACE DAPI
C
E6.5 Conceptus
5.6
50.4
0
49.1
0.4
E7.5 Conceptus
13.7
65.8
0.5
33.5
0.05
Flk1
Tie2
CD31
LYVE1
E8.5 Yolk sac
76.4
19.0
Ter119
Tie2
pRBC
99.8
0.3
0
0
Ter119
LYVE1
Angioblast
26.5
27.3
42.0
4.2
CD31
LYVE1
% LYVE1+ cells
Tie2 E6.5
Tie2 E7.5
Tie2 E8.5
Ter119 E8.5
Conceptus
Yolk sac
D
Ncx1CTR E9.25
Ncx1-/- E9.25
YS
PL
CH
3.2
2.4
0.04
5.3
1.1
0.03
52.2
40.3
0.8
6.6
19.9
1.6
72.9
5.5
41.0
2.4
51.8
4.8
58.2
38.6
0.1
3.0
18.7
4.4
69.4
7.4
0
0
60.0
40.0
CD41
cKit
CD16/32
LYVE1

Supplementary Figure 1.1 LYVE1 protein expression in endothelial and hematopoietic compartments during development

(A) Representative FACS plots of $CD31^{+}CD45^{-}$ endothelium in the placenta (PL) at E11.5, E13.5 and E16.5. Bar graphs show a significant increase in the fraction of placental endothelium expressing LYVE1 in late gestation. Data from 3 independent experiments for E11.5 and E13.5 each and one experiment with 9 concepti for E16.5 are represented as mean ± SD; p values are shown as ns if >0.05 and *** if ≤0.001.

(B) Immunofluorescence co-staining of embryonic upper abdomen at E13.5 highlights LYVE1 protein expression in fetal liver sinusoids, lungs, and azygous vein (Az v) but sparing in fetal aorta (Ao; outlined by expression of angiotensin converting enzyme, ACE).

(C) Representative FACS plots of $Tie2^{+}CD31^{+}$ early angioblasts reveal appearance of LYVE1 protein in the conceptus by E7.5, when primitive hematopoiesis begins and the endothelium that gives rise to definitive hematopoiesis is becoming specified. By E8.5, LYVE1 expression in the yolk sac (YS) is confined to endothelial cells while being absent from $Ter119^{+}$ primitive erythroid cells. Data are from n=XXX, 3 independent experiments.

(D) Representative FACS plots of hemogenic tissues with (*Ncx1*^{CTR}) and without heart beat (*Ncx1*$^{-/-}$) demonstrate the enrichment of LYVE1-expressing $CD41^{mid}cKit^{+}CD16/32^{+}$ erythro-myeloid progenitors at E9.25 in the YS in the absence of blood circulation.

LSK ($Lin^-Sca1^+cKit^+$) $CD150^+$ HSC subset showed minimal expression of LYVE1 protein (**Figures 1.1H and 1.1I**).

To assess whether the YS is the main source of $LYVE1^+$ HS/PCs, LYVE1 surface expression was examined in the different hemogenic tissues in embryos defective for the sodium calcium exchanger NCX1, in which a defective heartbeat prevents the circulation of cells (Koushik et al., 2001). Flow cytometry analysis of *Ncx1*$^{-/-}$ tissues showed that LYVE1 expression was robust in $CD41^{mid}cKit^+$ HS/PCs in the YS but scant in the PL or EM (**Figures 1.1J and 1.1K**). Comparable results were observed with $CD16/32^+CD41^{mid}cKit^+$ EMPs (**Figure S1.1D**). These data suggested that the YS is the primary source of $LYVE1^+$ expressing HS/PCs, including EMPs, in mid-gestation concepti.

LYVE1-Cre labels YS endothelium and vitelline vessels

To define the contribution of $LYVE1^+$ candidate hemogenic endothelial cells in fetal and adult hematopoiesis, lineage tracing was performed by breeding *LYVE1-eGFP-hCre* knock-in mice (Pham et al., 2010) (referred as "LYVE1-Cre" hereafter) with reporter mouse lines. eGFP expression from LYVE1-Cre-line was very weak, as originally reported. To follow Cre-mediated marking, we first used *Rosa*$^{mT/mG}$ fluorescent reporter mice (**Figure 1.2A**), in which all cells initially express tdTomato. Upon activation of Cre recombinase, the floxed membrane-targeted tdTomato cassette is excised allowing the expression of the downstream membrane-targeted EGFP in Cre-expressing cells and their progeny (Muzumdar et al., 2007).

Analysis of *LYVE1-Cre;Rosa*$^{mT/mG}$ concepti by fluorescence microscopy demonstrated LYVE1-Cre labeling already in E8.5 YS (**Figure 1.2B**). By E10.5, marking was apparent in YS and

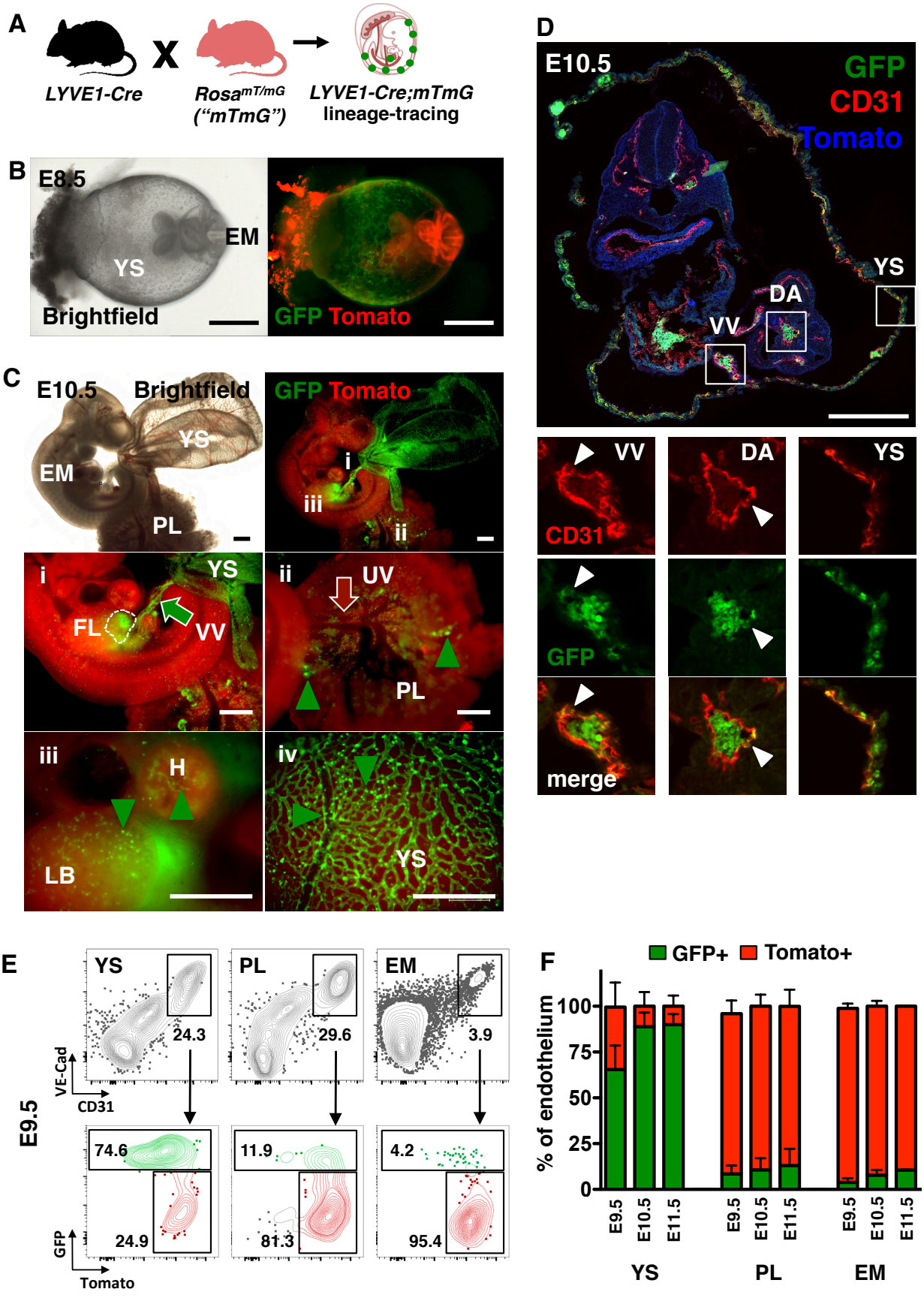
A
LYVE1-Cre
x
Rosa^mT/mG ("mTmG")
LYVE1-Cre;mTmG lineage-tracing
B
E8.5
YS
EM
Brightfield
GFP Tomato
C
E10.5
Brightfield
GFP Tomato
YS
EM
PL
i
ii
iii
FL
VV
UV
H
LB
iv
D
E10.5
GFP
CD31
Tomato
YS
DA
VV
CD31
GFP
merge
E
E9.5
YS
PL
EM
24.3
29.6
3.9
VE-Cad
CD31
74.6
24.9
11.9
81.3
4.2
95.4
GFP
Tomato
F
GFP+
Tomato+
% of endothelium
100
75
50
25
0
E9.5
E10.5
E11.5
YS
PL
EM

Figure 1.2 LYVE1-Cre labels YS endothelium and vitelline vessels
(A) Schematic of mouse model for tracing LYVE1-Cre lineage cells using the *Rosa*$^{mT/mG}$ reporter line
(B) Brightfield and whole mount fluorescence microscopy images of *LYVE1-Cre;mTmG* E8.5 concepti show the replacement of Tomato (red) expression by GFP (green) in the YS. Representative image from n=8 concepti from 2 independent experiments. Scale bar, 500µm.
(C) Brightfield and whole mount fluorescence microscopy images of EM, YS and PL at E10.5. Panel (i) shows GFP expression in the FL (dashed outline) and the vitelline vessels (VV; green arrow). Panel (ii) shows intact Tomato activity in placental and umbilical vessels (UV; red arrow), and in the dorsal aorta (DA). GFP$^+$ hematopoietic cells (green arrowheads) are found in placental vasculature (panel ii), heart (H), and limb bud (LB; dashed outline) (panel iii), and YS (panel iv). GFP expression is prominent throughout YS vasculature (iv). Representative image of n=18 embryos from 3 independent experiments. Scale bar, 500µm.
(D) At E10.5, GFP labeling is robust in YS and VV CD31$^+$ endothelium but minimal in the dorsal aorta (DA). Representative image from 2 independent experiments. Scale bar, 250µm.
(E) Representative FACS plots of GFP labeling of VE-Cad$^+$CD31$^+$ endothelial cells in E9.5 YS, PL and caudal half of the embryo (EM).
(F) Bar graphs of endothelial cells show robust LYVE1-Cre lineage-tracing in YS at E9.5-E11.5. EM includes the caudal half at E9.5 and the aorta-gonado-mesonephros region at E10.5 and E11.5. Data are from pools of embryos from n=3 (E9.5), n=7 (E10.5), and n=3 (E11.5), independent experiments and are represented as mean ± SD.

vitelline vessels as well as the FL rudiment (**Figures 1.2Ci, iii, iv**); however, no labeling was discernable in umbilical vessels or the placental large vessels (**Figure 1.2Cii**). Contrasting the robust labeling of $CD31^+$ YS and vitelline vessels, the dorsal aorta showed minimal LYVE1-Cre labeling (**Figures 1.2C and 1.2D**).

FACS analysis of hemogenic tissues from *LYVE1-Cre;Rosa*$^{mT/mG}$ concepti at E9.5-E11.5 further documented that VE-Cad^+CD31^+ endothelial cells were GFP-labeled abundantly in the YS but minimally in the PL and EM (caudal half at E9.5, and aorta-gonad-mesonephros region at later ages) (**Figures 1.2E and 1.2F**). These data raised the hypothesis that LYVE1-Cre targets YS hemogenic endothelium.

LYVE1-Cre lineage traces YS definitive HS/PCs but bypasses the primitive erythroid lineage

We next interrogated the origin of the different hematopoietic compartments. LYVE1-Cre was crossed with a *R26-stop-YFP* strain*,* where deletion of the transcriptional stop preceding the YFP sequence in the Rosa26 locus leads to marking of all progenies with YFP (**Figure 1.3A**) (Friedrich and Soriano, 1991).

Flow cytometry analysis of E8.5 *LYVE1-Cre;YFP* YS showed no labeling in $Ter119^+$ primitive red blood cells, whereas one third of angioblasts were already labeled (**Figure 1.3B**) in concordance with the LYVE1 protein expression at this stage (**Figure S1.1C**). Whereas no labeling was observed in $Ter119^+$ cells in E9.0 *LYVE1-Cre;YFP* YS, 90% of erythroid cells were labeled when the YFP reporter strain was crossed with strain that expresses Cre from the regulatory elements of the gene encoding the receptor tyrosine kinase *TIE2/TEK,* a known regulator of endothelial development. In *TIE2/TEK-Cre* mouse, Cre is activated in hemato-

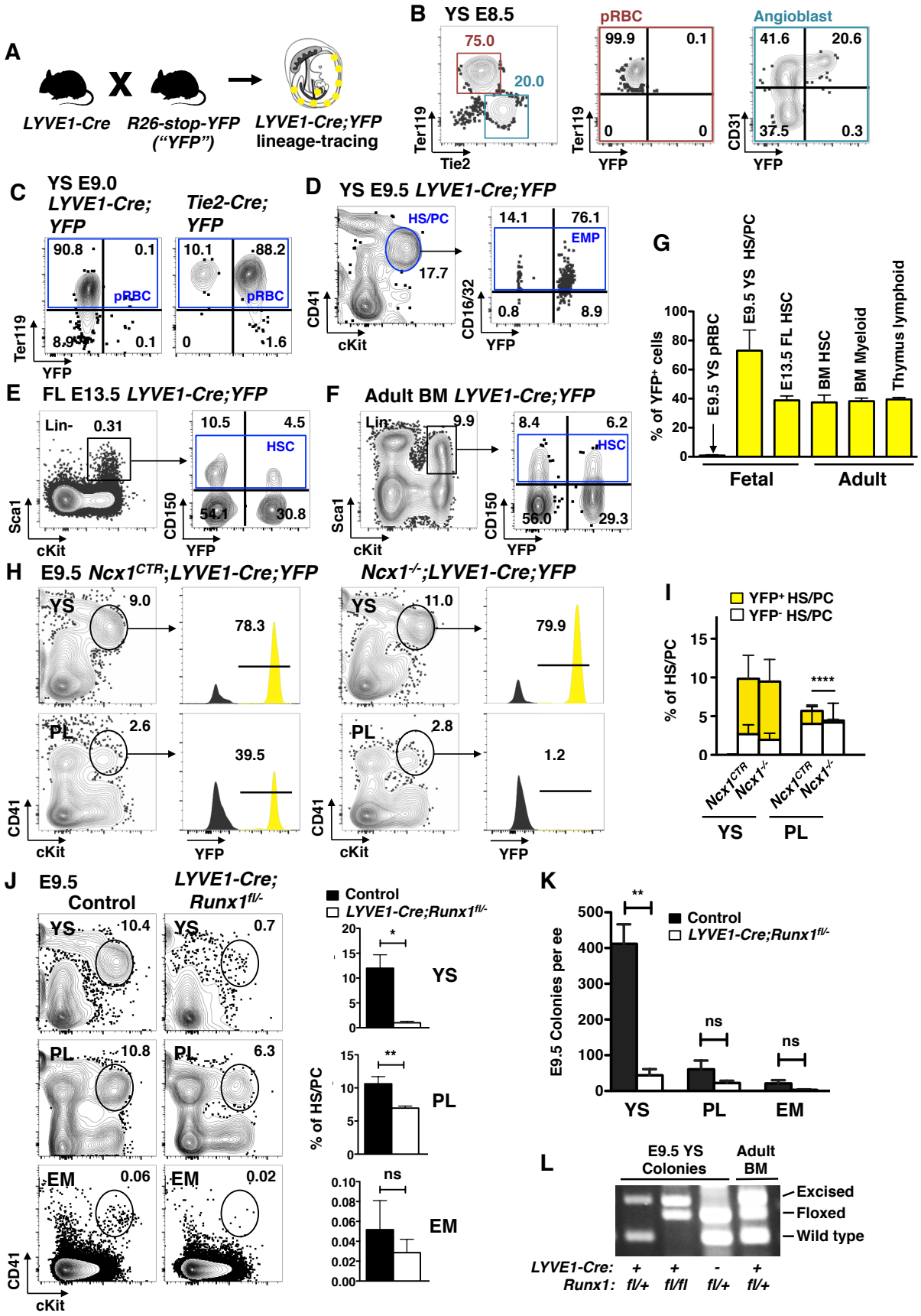
A
LYVE1-Cre
R26-stop-YFP ("YFP")
LYVE1-Cre;YFP lineage-tracing
B YS E8.5
75.0
20.0
Ter119
Tie2
pRBC
99.9
0.1
0
0
Ter119
YFP
Angioblast
41.6
20.6
37.5
0.3
CD31
YFP
C YS E9.0
LYVE1-Cre; YFP
Tie2-Cre; YFP
90.8
0.1
pRBC
8.9
0.1
10.1
88.2
pRBC
0
1.6
Ter119
YFP
D YS E9.5 LYVE1-Cre;YFP
HS/PC
17.7
CD41
cKit
14.1
76.1
EMP
0.8
8.9
CD16/32
YFP
G
% of YFP+ cells
E9.5 YS pRBC
E9.5 YS HS/PC
E13.5 FL HSC
BM HSC
BM Myeloid
Thymus lymphoid
Fetal
Adult
E FL E13.5 LYVE1-Cre;YFP
Lin-
0.31
10.5
4.5
HSC
54.1
30.8
Sca1
cKit
CD150
YFP
F Adult BM LYVE1-Cre;YFP
Lin-
9.9
8.4
6.2
HSC
56.0
29.3
Sca1
cKit
CD150
YFP
H E9.5 Ncx1CTR;LYVE1-Cre;YFP
Ncx1-/-;LYVE1-Cre;YFP
YS
9.0
78.3
PL
2.6
39.5
CD41
cKit
YFP
YS
11.0
79.9
PL
2.8
1.2
CD41
cKit
YFP
I
YFP+ HS/PC
YFP- HS/PC
% of HS/PC
****
Ncx1CTR
Ncx1-/-
YS
PL
J E9.5
Control
LYVE1-Cre; Runx1fl/-
YS
10.4
0.7
PL
10.8
6.3
EM
0.06
0.02
CD41
cKit
Control
LYVE1-Cre;Runx1fl/-
YS
PL
EM
% of HS/PC
ns
K
E9.5 Colonies per ee
Control
LYVE1-Cre;Runx1fl/-
ns
ns
YS
PL
EM
L
E9.5 YS Colonies
Adult BM
Excised
Floxed
Wild type
LYVE1-Cre: + + - +
Runx1: fl/+ fl/fl fl/+ fl/+

Figure 1.3 LYVE1-Cre targets YS definitive hematopoiesis
(A) Schematic of mouse model for tracing LYVE1-Cre marked cells using the *R26-stop-YFP* reporter.
(B) Representative FACS plots of E8.5 conceptus show LYVE1-Cre;YFP labeling in the angioblasts ($Tie2^+$) but not in $Ter119^+$ primitive erythroid cells (pRBC). N=9, 3 independent experiments.
(C) Representative FACS plots of E9.0 YS demonstrate labeling of $Ter119^+$ pRBC by *TIE2-Cre*, but not by *LYVE1-Cre*.
(D) Representative FACS plot of E9.5 YS $CD41^{mid}cKit^+Ter119^-$ HS/PC and $CD16/32^+$ EMP by LYVE1-Cre.
(E and F) Representative FACS plots display similar YFP marking in the $Lin^-Sca1^+cKit^+CD150^+$ HSC in E13.5 FL (E) and 8 month-old adult bone marrow (BM) (F).
(G) Quantification shows a contrast of YFP marking between pRBCs (n=4, 2 independent experiments) and YS HS/PCs (n=15, 7 independent experiments). LYVE1-Cre marking in E13.5 FL $Lin^-Sca1^+cKit^+CD150^+$ HSCs (n=15, 4 independent experiments) is similar to 8 month-old adult BM HSCs, BM $Mac1^+Gr1^+$ myeloid cells (n=8, 2 independent experiments) and thymus $CD4^+CD8^+$ T lymphocytes (n=7, 2 experiments). No comparison of marking between populations yielded statistical difference. Data are represented as mean ± SD.
(H) Representative FACS plots of E9.5 *LYVE1-Cre;YFP* $Ncx1^{-/-}$ concepti show decrease of YFP^+ HS/PCs in the PL in the absence of circulation.
(I) Quantification of HS/PCs in E9.5 $Ncx1^{-/-}$ concepti show diminished YFP^+ fraction in the PL with impaired circulation. Data from n=16 for $Ncx1^{CTR}$ and n=5 for $Ncx1^{-/-}$ from 3 independent experiments are represented as mean ± SD; p value of the difference in YFP^+ fractions at ≤0.01 is shown as **.
(J) Representative FACS plots and quantification of HS/PCs in hemogenic organs of E9.5 *LYVE1-Cre;*$Runx1^{fl/-}$ tissues show depletion of YS HS/PCs upon LYVE1-Cre mediated deletion of *Runx1*. The depletion is partial in the PL and not significant in the EM. Data from n=4 for mutants and n=9 for controls from 3 independent experiments are represented as mean ± SD. P values are shown as ns if >0.05, * if ≤0.05, ** if ≤0.01.
(K) Quantification of myelo-erythroid colonies per embryo equivalent (ee) from each organ. Data from n=4 for mutants and n=3 for controls from 2 independent experiments are represented as mean ± SD.
(L) Genotyping of *Runx1* alleles in representative colonies.
See also Figure S1.2.

vascular precursors after gastrulation (**Figure 1.3C**) (Kisanuki et al., 2001). 100% labeling was observed with the germ cell specific *VASA-Cre* mouse, in which Cre is active during fertilization enabling recombination in all cells of the conceptus (data not shown) (Gallardo et al., 2007). Hence, using two different Cre lines, we verified that the lack of LYVE1-Cre marking in YS $Ter119^{+}$ cells was not explained by silencing of the Rosa26 locus.

Lack of LYVE1-Cre labeling in primitive erythroid cells was confirmed by analyzing E9.5 *LYVE1-Cre;Rosa*$^{mT/mG}$ concepti. While many $CD43^{+}$ hematopoietic cells in YS had switched from tdTomato to GFP expression, $CD71^{+}Ter119^{+}$ primitive erythroid cells retained tdTomato expression (**Figures S1.2A**), documenting lack of LYVE1-Cre marking despite intact activity of the Rosa26 locus. As expected, *Rosa*$^{mT/mG}$ maternal $CD71^{-}Ter119^{+}$ red blood cells in the PL had downregulated expression of tdTomato. These data confirm that the primitive erythroid lineage does not originate from LYVE1-expressing hemogenic endothelium. LYVE1-Cre marking of primitive erythroid cells in later development could not be followed using reporter gene expression because the YFP expression from the *Rosa26* locus was silenced in primitive erythroid cells as they matured in circulation, irrespective of the Cre line used (data not shown).

In contrast to the unlabeled primitive erythroid cells, the majority (69.7 ± 14.8% SD) of $CD41^{mid}cKit^{+}$ HS/PCs in E9.5 *LYVE1-Cre;YFP* YS was marked by YFP (**Figures 1.3D and 1.3G**). These data imply that LYVE1-Cre marks the point when the precursors generating YS definitive hemogenic endothelium and HS/PCs have separated from the primitive erythroid lineage.

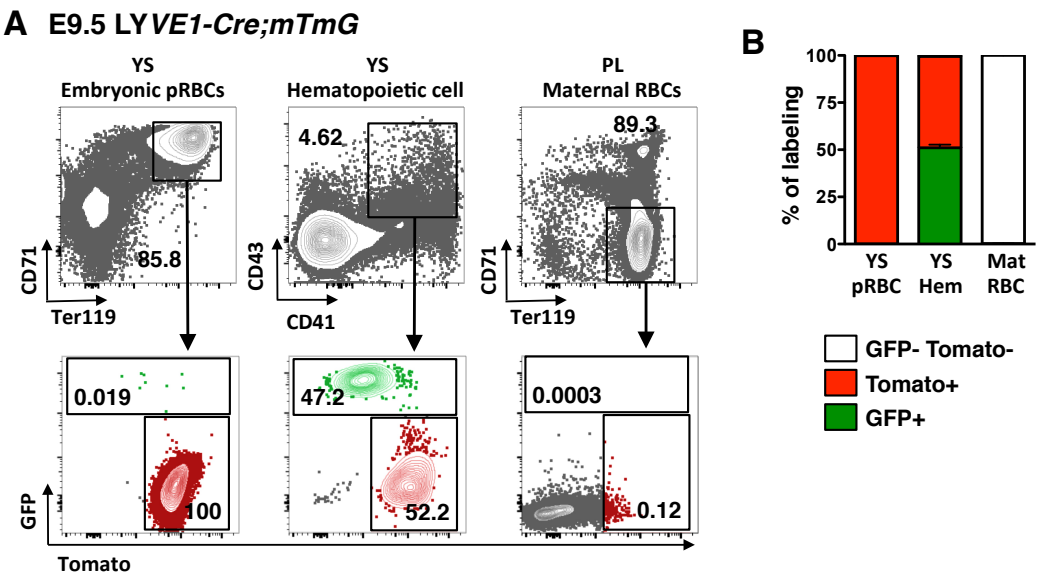

Supplementary Figure 1.2 Primitive erythroid cells do not derive from the LYVE1-Cre lineage

(A and B) Representative FACS plots and bar graph of *LYVE1-Cre;mTmG* tissues at E9.5. Yolk sac (YS) contains embryonic CD71^{+} Ter119^{+} primitive red blood cells (pRBC) that express Tomato only, tracing their lineage to LYVE1-Cre-negative precursors. A subset of Ter119^{-} CD43^{+} CD41^{+} hematopoietic (Hem) cells in the YS has substituted Tomato with GFP expression. Maternal RBCs phenotyped as Ter119^{+} FSC^{small} CD71^{-} CD43^{-}CD41^{-} subset within the placenta (PL) downregulate expression of Tomato, hence, appear as negative for both Tomato and GFP, enabling separation of maternal RBCs from embryonic Tomato^{+} pRBCs. Data from n=**MATT,** 3 independent experiments.

LYVE1-Cre labels a subset of fetal and adult HSCs

To investigate if LYVE1-Cre marking is restricted to EMPs or also marks HSCs, we assessed the contribution of lineage-traced cells to fetal and adult HSC. At E13.5, when the FL HSC compartment has become established and is rapidly expanding, 38.9 ± 11.6% SD of the LSK $CD150^+$ HSCs were YFP-marked (**Figures 1.3E and 1.3G**). In the adult, comparable fractions of YFP labeling were found in BM LSK $CD150^+$ HSCs (37.4 ± 11.1% SD) and $Mac1^+Gr1^+$ myeloid cells (38.2 ± 6.0% SD), and the thymus $CD4^+CD8^+$ T lymphocytes (39.4 ±3.5% SD) (Figures 1.3F and 1.3G). Uniform degree of post-natal LYVE1-Cre marking in all major lineages is in stark contrast to the absent or low expression of LYVE1 protein in HSCs or in cells committed to the different hematopoietic lineages (**Figure S1.2B**). These data establish that more than one-third of long-term repopulating HSCs derive from the LYVE1-Cre lineage, and that the cells were labeled during embryonic development.

YS is the primary source of LYVE1-Cre lineage derived HS/PCs at mid-gestation

Although the YS was the only hemogenic organ that showed extensive labeling of endothelium during HS/PC emergence (**Figure 1.2F**), analysis of the $CD41^{mid}cKit^+$ HS/PCs in different hemogenic tissues evidenced LYVE1-Cre labeling also in E9.5 PL (**Figures 1.3H and 1.3I**) and EM (data not shown). To examine how circulating cells contribute to HS/PC census in each hemogenic organ, YFP expression was mapped in heartbeat-deficient *Ncx1*$^{-/-}$ embryos. The YS maintained YFP^+ labeled HS/PC pool (79 ± 2.8% SD) regardless of heartbeat. In contrast, the absence of circulation in *Ncx1*$^{-/-}$ mutants depleted YFP^+ labeled HS/PCs from the PL (**Figures 1.3H and 1.3I**). CD16/32 expressing EMPs in *Ncx1*$^{-/-}$ mutants showed similar redistribution of

YFP^{+} fractions (**Figure S1.2C**). These data suggested that the YS is the main source of LYVE1-Cre lineage traced HS/PCs and EMPs at mid-gestation. Due to the severely defective generation of HS/PCs in the embryo proper of *Ncx1*$^{-/-}$ mutants, labeling of HS/PC could not be reliably assessed.

To target the hematopoietic cells derived from the LYVE1-lineage, LYVE1-Cre was used to delete the Runt-related transcription factor 1 (*Runx1*) gene, which is required for the generation of EMPs and HSCs. Comparison of *LYVE1-Cre;Runx1*$^{fl/-}$ concepti to control tissues at E9.5 showed near depletion of CD41^{mid}ckit^{+} HS/PCs in the conditional knockout YS. Both the PL and caudal half of the EM showed partial reduction in HS/PC population, likely reflecting the loss of HS/PCs migrating from the YS but retention of resident HS/PCs unaffected by LYVE1-Cre mediated *Runx1* deletion (**Figure 1.3J**). A parallel defect in myelo-erythroid colony formation was evident in *LYVE1-Cre;Runx1*$^{fl/-}$ YS (**Figure 1.3K**). As expected from the known function of *Runx1* in hemogenic endothelium (Chen et al., 2009), genotyping of YS colonies confirmed that only rare cells that had escaped LYVE1-Cre-mediated *Runx1* deletion formed colonies (**Figure 1.3L**). These genetic labeling and gene ablation data verified that YS HS/PCs are efficiently targeted by LYVE1-Cre, whereas the PL and EM harbor endogenous HS/PCs that do not originate from the LYVE1 lineage.

LYVE1-Cre lineage tracing identifies a temporal switch in precursors responsible for FL erythropoiesis

To investigate the contribution of LYVE1-Cre lineage cells to FL hematopoiesis, we assessed the fraction of lineage-traced cells in different hematopoietic compartments from mid

to late gestation. LYVE1-Cre marking in the $Lin^{-}cKit^{+}CD34^{+}Sca1^{+}$ HS/PC compartment peaked at E11.5 (61.3 ± 17.8% SD), when the FL is first seeded by HSCs, and leveled to 36.4 ± 11.7% at E13.5 and 41.4 ± 10.4% at E16.5 (**Figures 1.4A, 1.4D**). Of note, CD150, the Slam family marker that identifies long-term reconstituting HSCs in mice (Kiel et al., 2005) could not be used to further define the HSC compartment during early FL colonization as this marker is not reliably expressed in HSCs at E11.5 (McKinney-Freeman et al., 2009). Including CD150 expression to further define the HSC compartment at E13.5 did not change the level of LYVE1-Cre marking (data not shown). These data suggest that LYVE1-lineage cells are major contributors to initially establish the FL HSC compartment, whereas by E13.5, non-lineage-traced HSCs co-seed the FL. The uniform marking in HSC compartments from E13.5 FL to adult implies that the contribution of LYVE1-Cre labeled and non-labeled HSCs to the HSC pool remains stable after the FL HSC compartment has been established at E13.5.

In addition to serving as a site for HSC expansion, the FL supports definitive erythropoiesis through most of fetal life. Whereas the primitive erythroid cells differentiate in the YS and continue maturation in circulation, the progenitors for definitive erythroid cells must transit through the FL to differentiate and enucleate (McGrath et al., 2011). The precursors that first colonize the FL and initiate fetal definitive erythropoiesis have been proposed to originate from the YS, but their origin and the duration of their contribution has not been experimentally proven.

Flow cytometry analysis from *LYVE1-Cre;YFP* mice revealed that at E11.5, the FL contained $CD71^{+}Ter119^{-}$ pro-erythroblasts (ProE) and $ckit^{+}CD34^{-}$ erythroid precursors (HPC) with high YFP marking levels (76.7 ± 4.7% and 79.3 ± 3.0%, respectively) (**Figures 1.4A and 1.4D**)

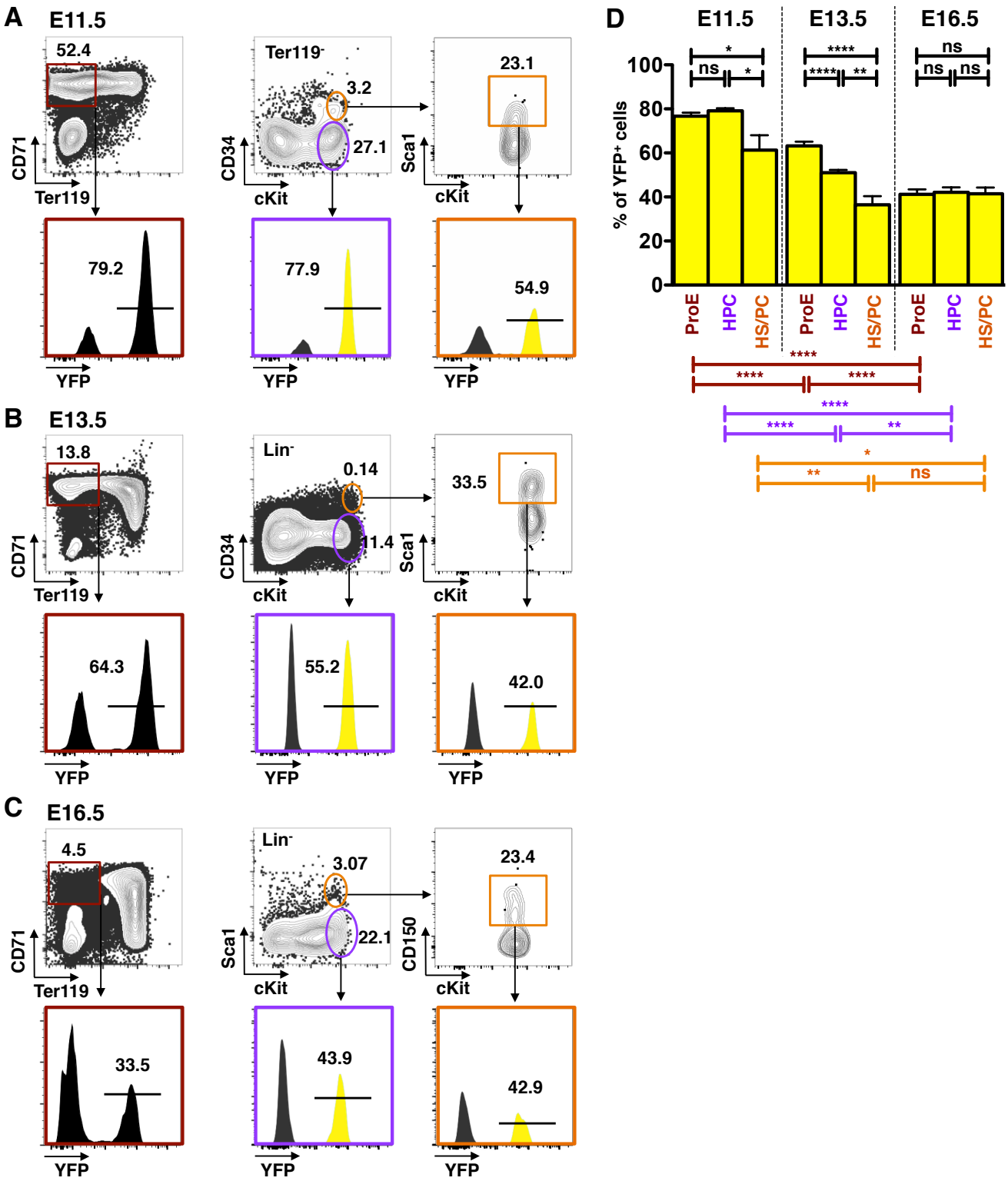
A
E11.5
52.4
CD71
Ter119
79.2
YFP
Ter119-
3.2
27.1
CD34
cKit
77.9
YFP
23.1
Sca1
cKit
54.9
YFP
B
E13.5
13.8
CD71
Ter119
64.3
YFP
Lin-
0.14
11.4
CD34
cKit
55.2
YFP
33.5
Sca1
cKit
42.0
YFP
C
E16.5
4.5
CD71
Ter119
33.5
YFP
Lin-
3.07
22.1
Sca1
cKit
43.9
YFP
23.4
CD150
cKit
42.9
YFP
D
E11.5
E13.5
E16.5
% of YFP+ cells
100
80
60
40
20
0
ProE
HPC
HS/PC
ns
*
****
**

Figure 1.4 Progenitors of LYVE1-Cre lineage initiate FL hematopoiesis
(A) Representative FACS plots of LYVE1-Cre marking in hematopoietic subpopulations in one representative E11.5 FL. $Ter119^{-}$ $CD71^{+}$ proerythroblasts (ProE). $Ter119^{-}cKit^{+}$ hematopoietic progenitor cells (HPC), $Ter119^{-}CD34^{+}cKit^{+}Sca1^{+}$ hematopoietic stem and progenitor cells (HS/PC).
(B) Representative FACS plots of FL subsets at E13.5.
(C) Representative FACS plots of FL subsets at E16.5.
(D) Comparative analysis of E11.5, E13.5 and E16.5 FL illustrates a shift in hematopoietic populations derived from the LYVE1-Cre lineage. Data from n=9, 3 independent experiments for E11.5, n=18, 3 independent experiments for E13.5, and n=13, 2 independent experiments for E16.2 are represented as mean ± SD. P values are shown as ns if >0.05, * if ≤0.05, ** if ≤0.01, *** if ≤0.001, and **** if ≤0.0001.

comparable to the E9.25 YS CD41^{mid}cKit^{+} HS/PCs (**Figures 1.3D and 1.3G**). This suggests that the YS supplies EMPs that first colonize the FL to initiate erythropoiesis. At E13.5, 63.2 ± 8.7% SD of the ProE and 51.0 ± 5.5% SD of HPCs in the FL were derived from the LYVE1 lineage (**Figures 1.4B and 1.4D**). These compartments displayed significantly higher marking than Lin^{-} Sca1^{+}cKit^{+}CD34^{+} HSC subset (36.4 ± 11.7%) at E13.5, implicating that the progenitors responsible for FL definitive erythropoiesis derive from a different source than most HSCs at this stage. By E16.5, the FL erythroblast and HSC enriched populations exhibited similar degrees of LYVE1-Cre marking (41.2 ± 8.1% and 41.4 ± 10.3%, respectively), suggesting that in late gestation, HSC become responsible for FL erythropoiesis (**Figures 1.4C and 1.4D**).

LYVE1-Cre mediated deletion of Scl/Tal1 targets early FL definitive erythropoiesis but spares the primitive erythroid lineage

To confirm that the LYVE1-Cre model can be used to study early definitive erythropoiesis without affecting primitive erythropoiesis, we used the LYVE1-Cre to deplete the bHLH transcription factor SCL. SCL is essential for the specification of hemogenic endothelium (Porcher et al., 1996; Van Handel et al., 2012) but dispensable for HSC maintenance (Mikkola et al., 2003a) due to redundancy with LYL1 (Souroullas et al., 2009). As SCL is required for the terminal differentiation of all erythroid cells, inactivation of *Scl* by TIE2-Cre results in defects in both primitive and definitive erythropoiesis (Schlaeger et al., 2005). May-Grunwald Giemsa stain of E12.5 peripheral blood from *TIE2-Cre;Scl$^{fl/-}$* mutants displayed abnormal primitive erythroid cells that were mitotic, binucleated, or had larger nucleus-to-cytoplasm ratio than control littermates, implying defective maturation (**Figure 1.5A**). Two-hour BrDU pulse analysis

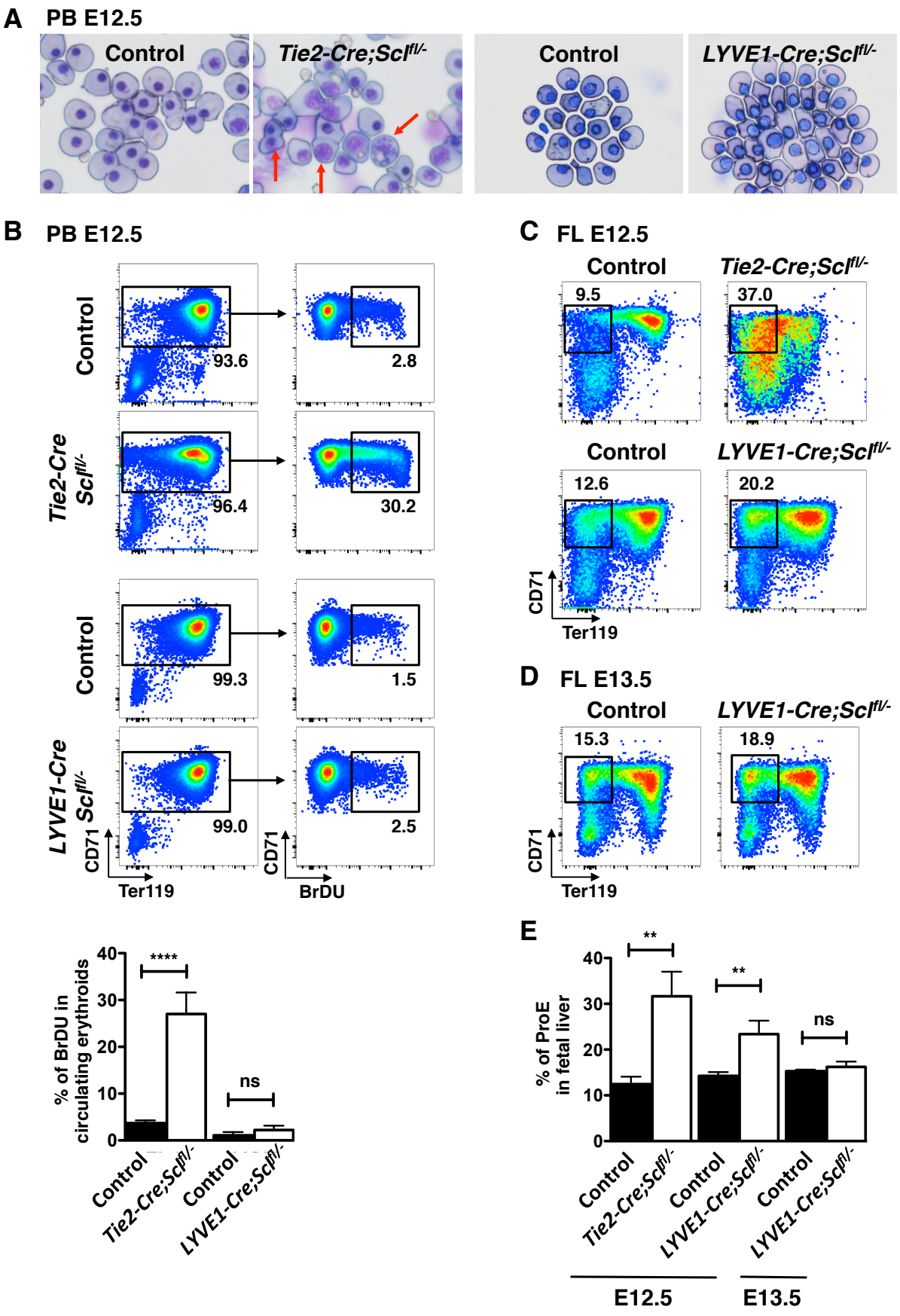
A
PB E12.5
Control
Tie2-Cre;Scl fl/-
Control
LYVE1-Cre;Scl fl/-
B
PB E12.5
Control
Tie2-Cre Scl fl/-
Control
LYVE1-Cre Scl fl/-
93.6
2.8
96.4
30.2
99.3
1.5
99.0
2.5
CD71
Ter119
CD71
BrDU
C
FL E12.5
Control
Tie2-Cre;Scl fl/-
9.5
37.0
Control
LYVE1-Cre;Scl fl/-
12.6
20.2
CD71
Ter119
D
FL E13.5
Control
LYVE1-Cre;Scl fl/-
15.3
18.9
CD71
Ter119
% of BrDU in circulating erythroids
****
ns
Control
Tie2-Cre;Scl fl/-
Control
LYVE1-Cre;Scl fl/-
E
% of ProE in fetal liver
**
**
ns
Control
Tie2-Cre;Scl fl/-
Control
LYVE1-Cre;Scl fl/-
Control
LYVE1-Cre;Scl fl/-
E12.5
E13.5

Figure 1.5 LYVE1-Cre targets early FL definitive hematopoiesis
(A) May-Grunwald Giemsa stain of E12.5 peripheral blood (PB) shows primitive erythroid defects in *TIE2-Cre;Scl$^{fl/-}$* blood cells (arrows) but not in *LYVE1-Cre;Scl$^{fl/-}$* blood. Representative images from 3 independent experiments are shown.
(B) Representative FACS plots of BrDU staining of E12.5 PB illustrates excessive proliferative activity in *TIE2-Cre;Scl$^{fl/-}$* primitive erythroid cells but not in *LYVE1-Cre;Scl$^{fl/-}$* cells. Bar graphs from n=22 (control) and n=4 (knockout) from 3 independent *TIE2-Cre;Scl$^{fl/-}$* experiments and n=6 (control) and n=3 (knockout) from 2 independent *LYVE1-Cre;Scl$^{fl/-}$* experiments are shown as mean ± SD.
(C) E12.5 FL from both *TIE2-Cre;Scl$^{fl/-}$* (upper panel) and *LYVE1-Cre;Scl$^{fl/-}$* (lower panel) embryos exhibit accumulation of pro-erythroblasts (ProE).
(D) At E13.5 the defect in ProE fraction in *LYVE1-Cre;Scl$^{fl/-}$* FL has corrected.
(E) Quantification of ProE fractions in E12.5 and E13.5 FL. Data from n=2 (E12.5 *TIE2-Cre;Scl$^{fl/-}$*) and n=6 (control), n=3 (E12.5 *LYVE1-Cre;Scl$^{fl/-}$*) and n=7 (control), n=4 (E13.5 *LYVE1-Cre;Scl$^{fl/-}$*) and n=14 (control) from 2 independent experiments for each genotype and age are shown as mean ± SD.

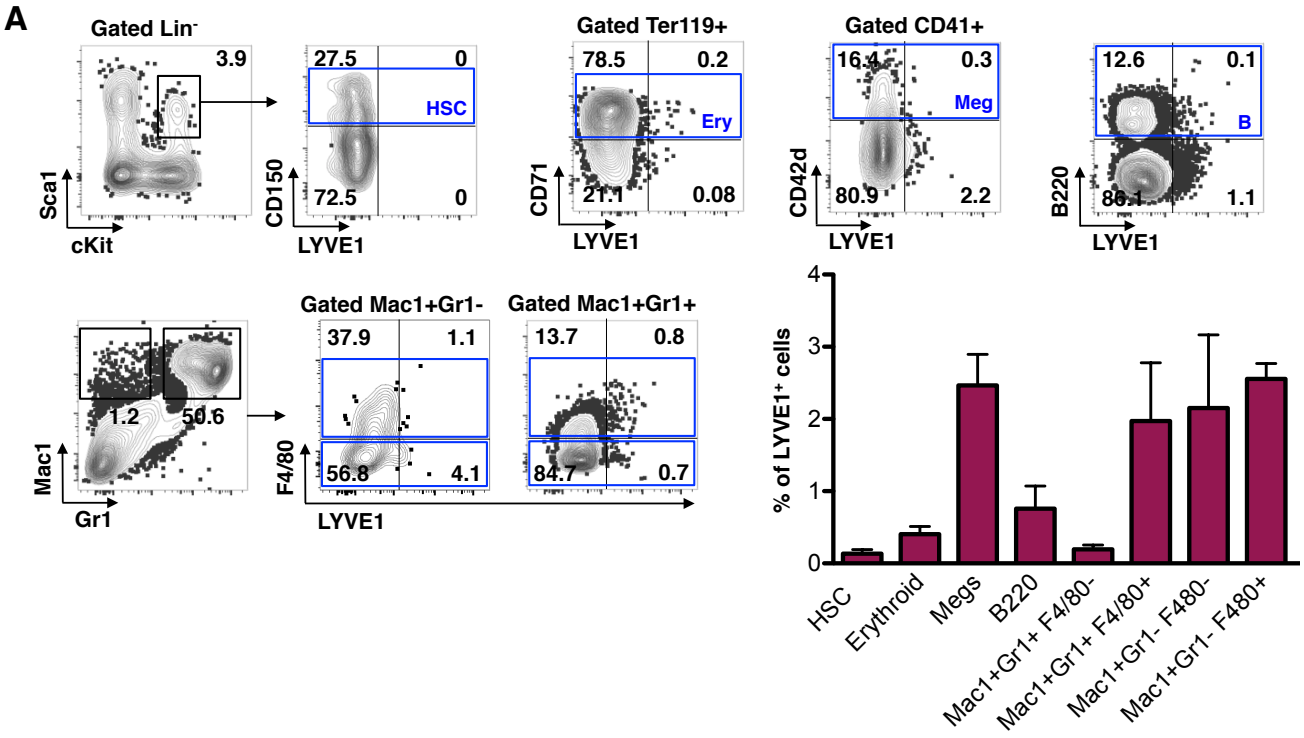

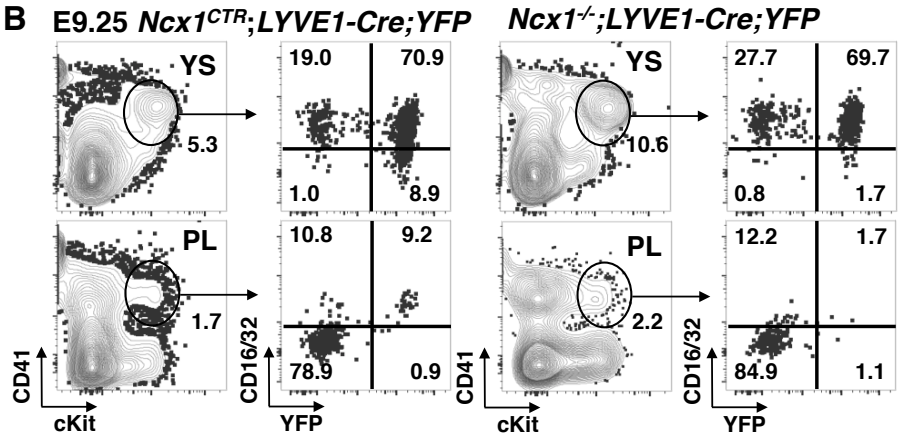

Supplementary Figure 1.3

(A) Representative FACS plots and bar graph of hematopoietic compartments in adult bone marrow. Data are from n=8 mice from 2 independent experiments.

(B) Representative FACS plots of E9.25 circulation-deficient *Ncx1*$^{-/-}$ tissues show the presence of LYVE1-Cre marker CD41^{mid}cKit^{+}CD16/32^{+} erythro-myeloid progenitors in the yolk sac (YS). Placenta, PL. Data from n=7 Ncx1 control, and n=5 null concepti from 2 independent experiments.

showed a higher fraction of cycling cells among primitive erythroid cells that underwent *Scl* deletion by TIE2-Cre (**Figure 1.5B**). In contrast, when *Scl* was excised in LYVE1-Cre expressing cells, the primitive erythroid cells did not show abnormal morphology or proliferation activity, indicating that primitive erythroid cells had been spared from *Scl* inactivation (**Figures 1.5A and 1.5B**).

FACS analysis of FL of both *TIE2-Cre;Scl*$^{fl/-}$ and *LYVE1-Cre;Scl*$^{fl/-}$ embryos at E12.5 showed accumulation of CD71^{+}Ter119^{-} pro-erythroblasts (**Figures 1.5C and 1.5E**), consistent with delayed maturation reported with *Scl* deficient definitive erythroid cells (Mikkola et al., 2003a; Schlaeger et al., 2005). This defect in definitive erythropoiesis was ameliorated at E13.5 (**Figures 1.5D and 1.5E**), likely due to replenishment of the FL proerythroblast pool by a new source of unaffected precursors. This data verified that LYVE1-Cre deletes *Scl* specifically from the transient-definitive, but not primitive erythroid cells, enabling studies that address the impact of the different erythroid waves on embryonic development.

Discussion

The difficulty to track the origin and contribution of the different waves of developmental hematopoiesis *in vivo* has limited the understanding of their unique roles in embryo and adult. We report that LYVE1 expression and lineage tracing can be used to examine definitive hematopoiesis originating from the YS and vitelline vessels, without targeting the primitive erythroid lineage and the majority of the HSC compartment generated elsewhere in the conceptus.

LYVE1 protein expression and LYVE1-Cre fate mapping distinguished endothelial cells from the YS and vitelline vessels from those from other hemogenic organs at the developmental window when HS/PCs emerge. Although LYVE1^{+} EMPs and HS/PCs could be detected in all hemogenic organs with normal circulation, analysis of heartbeat deficient *Ncx1*$^{-/-}$ concepti implied that the YS is the main source of LYVE1^{+} HS/PC and EMPs. These data propose that at least some, if not all LYVE1-Cre labeled HSCs, which constitute more than one third of the fetal and the adult HSC pools, originate from the YS and/or vitelline vessels. However, as LYVE1 protein expression appears in PL vasculature at late gestation, and minor LYVE1-Cre marking is noted in the endothelium in the PL and the EM at mid-gestation, our data do not exclude possible contribution from other hemogenic sites to the LYVE1-lineage traced HSC pool. The *Ncx1*$^{-/-}$ model cannot be used to assess adult-repopulating HSC activity of LYVE1-Cre marked cells because these embryos die by E10.0 --before transplantable HSCs can be obtained-- and because heartbeat is critical for proper HSC development (North et al., 2009). Hence, the question of whether all, or most, of the 35-40% LYVE1-Cre marked fetal and adult HSCs arise from the YS and/or vitelline vessels requires further studies using different experimental systems. Nevertheless, as the YS predominantly generates LYVE1 marked HS/PCs, and the PL and the EM generate a substantial fraction of LYVE1-negative HS/PCs, our data propose that HSCs from multiple anatomical sites contribute to adult hematopoiesis. How these different lineages of HSCs contribute to various hematopoietic subsets in the adult *in vivo* can now be approached experimentally using the LYVE1-Cre model. This is of importance as HSCs are heterogeneous and can show cell intrinsic biases to different lineages in age dependent

manner (Beerman et al., 2010; Benz et al., 2012; Pang et al., 2011; Sieburg et al., 2006; Yamamoto et al., 2013).

Our data document that the LYVE1^{+} endothelium in the YS does not give rise to primitive erythroid cells. The absence of LYVE1 protein expression and marking in primitive erythroid cells contrasts the abundant protein expression and marking in YS definitive HS/PCs. These data imply that these two hematopoietic lineages have separated from common mesodermal precursor before LYVE1-Cre becomes active. The YS thus gives rise to at least two lineages of erythroid cells that originate from distinct precursors. The LYVE1-Cre lineage trace may thus provide clarity to studies that show that the types of globins expressed in primitive or definitive erythroid lineages are not mutually exclusive, as there is a maturational globin switch as the cells undergo erythroid differentiation (Kingsley et al., 2006; McGrath et al., 2011; Palis, 2008; Qiu et al., 2008).

LYVE1 expression and lineage tracing offers a powerful tool to separate primitive erythropoiesis from early fetal definitive erythropoiesis even after circulation has been established. The defects in primitive and definitive erythroid cell differentiation caused by TIE2-Cre-specific *Scl* deletion (Schlaeger et al., 2005) were uncoupled using LYVE1-Cre, which only affected early FL definitive erythropoiesis. Selective inactivation of key hematopoietic regulators in LYVE1-Cre progeny makes it possible to study the requirement of such factors in early FL erythropoiesis without the confounding effects of early embryonic lethality -- as in *Scl* null embryos (Porcher et al., 1996; Shivdasani et al., 1995)-- or primitive erythroid defects -- as in *TIE2-Cre;Scl*$^{fl/fl}$ concepti.

The LYVE1-Cre model also provides *in vivo* evidence that the earliest progenitors seeding and initiating FL erythropoiesis are products of a distinct lineage that likely originates from the YS. However, the deletion of *Scl* from LYVE1-lineage cells causes only temporary effect on FL erythropoiesis, possibly because cells not targeted by LYVE1-Cre converge to the FL from other sources and replenish the affected erythroid compartment. Future studies will inform if the erythroid progenitors, or HSCs, originating from the LYVE1-lineage exhibit different properties than those arising from non-LYVE-lineage precursors.

LYVE1 is expressed abundantly in lymphatic vessels and lymph node sinus endothelial cells, but its expression has also been described in other cell types such as liver blood sinusoids and tissue macrophages (Carreira et al., 2001; Pham et al., 2010; Schledzewski et al., 2006). In the YS, LYVE1 expression is not related to lymphatic identity, as the YS does not contain lymphatic vasculature (Banerji et al., 1999; Gordon et al., 2008). It is unknown how the YS and vitelline vessel restricted expression pattern of LYVE1 among hemogenic vessels is established, and whether this is intrinsically regulated, or involves signals from the microenvironment. It will be interesting to determine if LYVE1 expression is limited to YS and vitelline vessels and HS/PCs also during human development, and how the expression pattern is preserved during ES cell differentiation.

The functional significance of LYVE1 expression in YS endothelium is unknown. Although it was suggested to serve in cell adhesion/transmigration and as a scavenger for hyaluronan turnover, mouse knockout studies were unable to verify a critical function for LYVE1 in these processes, or in embryonic development in general, in the 129/C57Bl/6, or C57Bl/6 backgrounds (Gale et al., 2007). The Cre cassette was inserted into the 3'UTR of the

endogenous *Lyve1* locus, and does not affect LYVE1 function in that allele. Hence, our model cannot be used to answer whether loss of LYVE1 causes subtle effects in hematopoiesis that would be observed upon more detailed examination or back-crossing to different genetic backgrounds. However, because of the lineage and tissue restricted expression of LYVE1 within the hematopoietic compartment, the LYVE1-Cre model can be exploited to uncover new functions for the different blood progenitor waves and HSC sources during developmental and adult hematopoiesis.

Materials and Methods

Mouse models

LYVE1-eGFP-hCre knockin mice (C57BL/6) (Pham et al., 2010) were crossed with two reporter lines: 1) *R26-YFP* carrying a floxed transcriptional stop upstream of the YFP in Rosa26 locus (Srinivas et al., 2001), and 2) double-fluorescent reporter (*Rosa*$^{mT/mG}$*)* where cells express Tomato constitutively but switch to GFP upon excision (Muzumdar et al., 2007). Whereas YFP or GFP fluorescence rendered from crossing with the reporter lines intensely highlighted the Cre-excised cells, eGFP from *LYVE1-eGFP-hCre* alone could not be discerned by fluorescence microscopy, as previously reported (Pham et al., 2010). FACS analysis confirmed the low eGFP signal from *LYVE1-eGFP-hCre,* which did not overlap with the intense YFP or GFP signal. Hence, for simplicity, the *LYVE1-eGFP-hCre* is referred as *LYVE1-Cre.* To label the entire hemato-vascular compartment, *TIE2/TEK-Cre* mice (Kisanuki et al., 2001) were bred with the *R26-YFP* line. To label all cells of the conceptus, the germ-cell specific VASA-Cre was crossed with the *R26*-YFP line. *LYVE1-Cre;YFP* mice were further crossed with *Ncx1*$^{+/-}$ mice (Koushik et al., 2001)

to generate *Ncx1*$^{-/-}$ mutants that underwent LYVE1-Cre labeling and lacked circulation. Although some contaminating embryonic RBCs could occasionally be found in the embryo proper of *Ncx1*$^{-/-}$ concepti, only embryos with less than 5% RBC contamination were used in the analysis. *LYVE1-Cre* was also bred with *Runx1*$^{fl/-}$ (Growney et al., 2005; Wang et al., 1996) and *Scl*$^{fl/-}$ (Mikkola et al., 2003a; Shivdasani et al., 1995). Embryos were not separated based on sex, and both female and male embryos were studies. Mice were maintained according to protocols of Animal Research Committee at the University of California, Los Angeles, and the University of California, Irvine, who approved these studies.

Preparation of tissue sections

After isoflurane-induced anesthesia, mice were sacrificed by cervical dislocation. Intact embryos were imaged using a Keyence BZ-X700 fluorescence microscope prior to tissue harvesting. Fetal hematopoietic organs were dissected and fixed in 4% paraformaldehyde at 4°C for 4-6 hours, followed by 30% sucrose in PBS solution overnight, 1:1 30% sucrose:OCT (Tissue-Tek, Electron Microscopy Sciences) for 1 hour at 4°C, and embedded and frozen in 100% OCT. Frozen sections were cut at 5-7 µm with a Leica CM3050 S cryostat. For paraffin-embedded blocks, tissues were fixed in 4% paraformaldehyde at 4°C overnight and processed by standard protocol at the Tissue Procurement and Histology Core Laboratory of the Pathology and Laboratory Medicine at UCLA. Paraffin sections were cut at 5 µm.

Immunostaining

Fixed frozen and paraffin-embedded sections were prepared and immunostained as described (Rhodes et al., 2008) using the following antibodies: LYVE1 conjugated to eFluor 770, c. ALY7 (1:200; BD Pharmingen), Ter119, c. TER119 (1:500, BD Pharmingen), CD41, c. MWReg30 (1:100; BD Pharmingen), ACE (1:100; R&D), and CD31, c. MEC 13.3 (1:500; BD Pharmingen). Biotinylated secondary antibodies (1:500; Vector) and Tyramide Signal Amplification kit (PerkinElmer) were used as directed by manufacturer's protocol. Immunofluorescent images were obtained on a Zeiss Axio Imager.A1 with a Zeiss Axiocam MRm camera or a Zeiss LSM 510 microscope equipped with 405 nm, 488 nm, 543 nm, and 633 nm lasers, or a Keyence BZ-X700 fluorescence microscope.

Flow cytometry

Tissues were dissociated with collagenase (Worthington), DNase (Qiagen) and dispase (Invitrogen) at 37° C for 20 minutes. Cells were stained with rat anti-mouse monoclonal antibodies against Ter119, CD71, CD41, CD16/32, cKit, Sca1, CD34, CD150, CD31, Flk1, and LYVE1 (See Table 1.1). Dead cells were excluded with DAPI. Cells were assayed on a Becton Dickinson Biosciences LSRII or Fortessa flow cytometer and data was analyzed with FlowJo software (Tree Star Inc.). FMO (fluorescence minus one) controls were used to determine the gate for each population.

Clonogenic progenitor assay

Methylcellulose colony-forming assays were performed as described previously (Chhabra et al.,

2012). Briefly, single cell suspensions were plated in MethoCult 3434 (Stem Cell Technologies) supplemented with TPO (PeproTech) and colonies were enumerated in 5-7 days. Clustering of 30 or more cells was defined as one colony. Colonies were imaged using a Canon PowerShot G6 camera connected to Zeiss Axiovert 40 CFL microscope. *Lyve1-Cre;Runx1*$^{fl/-}$ colonies were genotyped by PCR using the following primers: Runx1 F563: 5'- CCC ACT GTG TGC ATT CCA GAT TGG; Runx1 Ex4-R837: 5'- GAC GGT GAT GGT CAG AGT GAA GC; Runx1 Int3-2: 5' - CAC CAT AGC TTC TGG GTG CAG (Chen et al., 2009)

Cytospin

Peripheral blood cells were mounted on frosted microscope glass slides (Fisherbrand) using a Shandon Cytospin 4 (Thermo Electron). Slides were air-dried and stained with MGG solutions (Sigma Aldrich). Images were taken using an Olympus BX51 microscope with a DP72 camera.

Cell proliferation assay

Pregnant mice were injected intraperitoneally with BrdU two hours before sacrificing them (FITC BrdU Flow Kit;BD Pharmingen). Tissues were then harvested and treated as described in Flow Cytometry.

Statistical analysis

Mathematical analysis and statistics were performed using GraphPad Prism Software. P values and data reported as mean ± SD were calculated using the Student's unpaired two-tailed *t* tests.

Antibody	Fluorochrome	Clone	Dilution	Manufacturer	Catalog
B220	APC-Cy7	RA3-6B2	1:200	BD Pharmingen	552094
B220	Per-CP-Cyanine5.5	RA3-6B2	1:100	eBioscience	45-0452-82
B220	PE-Cy5	RA3-6B2	1:100	BD Pharmingen	553091
cKit	APC-Cy7	2B8	1:100	Biolegend	105825
F4/80	FITC	BM8	1:100	eBioscience	11-4801-82
Flk1	APC	Avas 12a1	1:50	BD Pharmingen	560070
Flk1	Per-CP-Cyanine5.5	Avas 12a1	1:50	BD Pharmingen	560681
GR1	PE-Cy7	RB6-8C5	1:100	eBioscience	25-5931-82
LYVE1	PE	223322	1:200	R&D	FAB2125P
LYVE1	eFluor 660	ALY7	1:200	eBioscience	50-0443-82
Mac1	PE-Cy5	M1/70	1:200	eBioscience	15-0112-83
Mac1	PE	M1/70	1:200	BD Pharmingen	553311
Sca1	PE-Cy7	D7	1:100	eBioscience	25-5981-82
Sca1	Per-CP-Cyanine5.5	D7	1:100	eBioscience	45-5981-82
Ter119	Per-CP-Cyanine5.5	TER-119	1:200	eBioscience	45-5921-82
Ter119	PE-Cy5	TER-119	1:200	eBioscience	15-5921-83
Ter119	PE	TER-119	1:200	BD Pharmingen	553673
Tie2	PE	TEK4	1:100	eBioscience	12-5987-82
VE-Cadherin	Biotin	BV13	1:400	Biolegend	138008
Streptavidin	eFluor 710	n/a	1:400	eBioscience	49-4317-80
CD3e	PE-Cy5	145-2C11	1:100	eBioscience	15-0031-83
CD4	APC	RM4-5	1:200	BD Pharmingen	553051
CD8a	PE	53-6.7	1:200	BD Pharmingen	553033
CD16/32	PE	2.4G2	1:100	BD Pharmingen	553145
CD19	PE-Cy7	1D3	1:100	BD Pharmingen	552854
CD31	PE	MEC 13.3	1:100	BD Pharmingen	553373
CD31	PE-Cy7	390	1:100	eBioscience	25-0311-82
CD31	PerCP-eFluor710	390	1:400	eBioscience	46-0311-80
CD34	Alexa Fluor 647	MEC14.7	1:100	BD Pharmingen	560230
CD41	PE-Cy7	eBioMWReg30	1:100	eBioscience	25-0411-82
CD42d	PE	1C2	1:200	eBioscience	12-0421-80
CD45	PE-Cy7	30-F11	1:200	eBioscience	25-0451-82
CD71	PE	C2	1:200	BD Pharmingen	553267
CD71	APC	R17217	1:200	eBioscience	17-0711-82
CD150	PE	TC15-12F12.2	1:100	Biolegend	115904

Table 1.1 Antibodies

Author Contributions

Conceptualization, H.K.M., M.A.I., I.L.W. and L.K.L.; Methodology, H.K.M., L.K.L., M.A.I., Y.G.; Investigation, L.K.L., M.A.I., Y.G., Y.W., Y.J.K.; Writing – Original draft, H.K.M. and L.K.L.; Writing – Review and Editing, M.A.I., I.L.W.; Visualization, L.K.L., W.W., M.A.I., Y.G.

Acknowledgements

We thank Dr. Calvanese, Dr. Montecino-Rodriguez and Dr. Dorshkind for discussions. We thank the UCLA Translational Pathology Core Laboratory for preparing the paraffin tissue sections, and Vanessa Scarfone and the UCI Sue and Bill Gross Stem Cell Research Center FACS core for flow cytometry. We thank Dr. Speck and Dr. Gilliland for providing the *Runx1*$^{fl/fl}$ and *Runx1* knockout mice, and Dr. Orkin for providing the *Scl*$^{fl/fl}$ and *Scl* knockout mice.

This work was supported by the following funding: NIH R01 HL097766-01 and Leukemia Lymphoma Society Scholar Award to H.K.A.M, TG2-01169 CIRM Type I Training Grant, the American Association of Obstetricians and Gynecologists Foundation Scholarship and the Specialty Training and Advanced Research (STAR) Training Fellowship at UCLA to L.K.L, and by Eli and Edythe Broad Center of Regenerative Medicine and Stem Cell Research at UCLA and Jonsson Cancer Center Foundation.

References

Banerji, S., Ni, J., Wang, S.X., Clasper, S., Su, J., Tammi, R., Jones, M., and Jackson, D.G. (1999). LYVE-1, a new homologue of the CD44 glycoprotein, is a lymph-specific receptor for hyaluronan. J Cell Biol *144*, 789-801.

Beerman, I., Bhattacharya, D., Zandi, S., Sigvardsson, M., Weissman, I.L., Bryder, D., and Rossi, D.J. (2010). Functionally distinct hematopoietic stem cells modulate hematopoietic

lineage potential during aging by a mechanism of clonal expansion. Proc Natl Acad Sci U S A *107*, 5465-5470.

Benz, C., Copley, M.R., Kent, D.G., Wohrer, S., Cortes, A., Aghaeepour, N., Ma, E., Mader, H., Rowe, K., Day, C*., et al.* (2012). Hematopoietic stem cell subtypes expand differentially during development and display distinct lymphopoietic programs. Cell Stem Cell *10*, 273-283.

Bertrand, J.Y., Chi, N.C., Santoso, B., Teng, S., Stainier, D.Y., and Traver, D. (2010). Haematopoietic stem cells derive directly from aortic endothelium during development. Nature *464*, 108-111.

Boisset, J.C., van Cappellen, W., Andrieu-Soler, C., Galjart, N., Dzierzak, E., and Robin, C. (2010). In vivo imaging of haematopoietic cells emerging from the mouse aortic endothelium. Nature *464*, 116-120.

Carreira, C.M., Nasser, S.M., Tomaso, E. di, Padera, T.P., Boucher, Y., Tomarev, S.I., and Jain, R.K. (2001). LYVE-1 Is Not Restricted to the Lymph Vessels Expression in Normal Liver Blood Sinusoids and Down-Regulation in Human Liver Cancer and Cirrhosis. Cancer Res. *61*, 8079–8084.

Chen, M.J., Li, Y., De Obaldia, M.E., Yang, Q., Yzaguirre, A.D., Yamada-Inagawa, T., Vink, C.S., Bhandoola, A., Dzierzak, E., and Speck, N.A. (2011). Erythroid/myeloid progenitors and hematopoietic stem cells originate from distinct populations of endothelial cells. Cell Stem Cell *9*, 541-552.

Chen, M.J., Yokomizo, T., Zeigler, B.M., Dzierzak, E., and Speck, N.A. (2009). Runx1 is required for the endothelial to haematopoietic cell transition but not thereafter. Nature *457*, 887-891.

Chhabra, A., Lechner, A.J., Ueno, M., Acharya, A., Van Handel, B., Wang, Y., Iruela-Arispe, M.L., Tallquist, M.D., and Mikkola, H.K. (2012). Trophoblasts regulate the placental hematopoietic niche through PDGF-B signaling. Dev Cell *22*, 651-659.

Eilken, H.M., Nishikawa, S., and Schroeder, T. (2009). Continuous single-cell imaging of blood generation from haemogenic endothelium. Nature *457*, 896-900.

Espín-Palazón, R., Stachura, D.L., Campbell, C.A., García-Moreno, D., Del Cid, N., Kim, A.D., Candel, S., Meseguer, J., Mulero, V., and Traver, D. (2014). Proinflammatory signaling regulates hematopoietic stem cell emergence. Cell *159*, 1070-1085.

Ferkowicz, M.J., Starr, M., Xie, X., Li, W., Johnson, S.A., Shelley, W.C., Morrison, P.R., and Yoder, M.C. (2003). CD41 expression defines the onset of primitive and definitive hematopoiesis in the murine embryo. Development *130*, 4393–4403.

Friedrich, G., and Soriano, P. (1991). Promoter traps in embryonic stem cells: a genetic screen to identify and mutate developmental genes in mice. Genes Dev *5*, 1513-1523.

Gale, N.W., Prevo, R., Espinosa, J., Ferguson, D.J., Dominguez, M.G., Yancopoulos, G.D., Thurston, G., and Jackson, D.G. (2007). Normal lymphatic development and function in mice deficient for the lymphatic hyaluronan receptor LYVE-1. Mol Cell Biol *27*, 595-604.

Gallardo, T., Shirley, L., John, G.B., and Castrillon, D.H. (2007). Generation of a germ cell-specific mouse transgenic Cre line, Vasa-Cre. Genesis *45*, 413-417.

Gekas, C., Dieterlen-Lièvre, F., Orkin, S.H., and Mikkola, H.K. (2005). The placenta is a niche for hematopoietic stem cells. Dev Cell *8*, 365-375.

Gomez Perdiguero, E., Klapproth, K., Schulz, C., Busch, K., Azzoni, E., Crozet, L., Garner, H., Trouillet, C., de Bruijn, M.F., Geissmann, F.*, et al.* (2015). Tissue-resident macrophages originate from yolk-sac-derived erythro-myeloid progenitors. Nature *518*, 547-551.

Gordon, E.J., Gale, N.W., and Harvey, N.L. (2008). Expression of the hyaluronan receptor LYVE-1 is not restricted to the lymphatic vasculature; LYVE-1 is also expressed on embryonic blood vessels. Dev Dyn *237*, 1901-1909.

Growney, J.D., Shigematsu, H., Li, Z., Lee, B.H., Adelsperger, J., Rowan, R., Curley, D.P., Kutok, J.L., Akashi, K., Williams, I.R., et al. (2005). Loss of Runx1 perturbs adult hematopoiesis and is associated with a myeloproliferative phenotype. Blood *106*, 494–504.

Haar, J.L., and Ackerman, G.A. (1971). A phase and electron microscopic study of vasculogenesis and erythropoiesis in the yolk sac of the mouse. Anat Rec *170*, 199-223.

Inlay, M.A., Serwold, T., Mosley, A., Fathman, J.W., Dimov, I.K., Seita, J., and Weissman, I.L. (2014). Identification of multipotent progenitors that emerge prior to hematopoietic stem cells in embryonic development. Stem Cell Reports *2*, 457-472.

Keller, G. (2005). Embryonic stem cell differentiation: emergence of a new era in biology and medicine. Genes Dev *19*, 1129-1155.

Kiel, M.J., Yilmaz, O.H., Iwashita, T., Terhorst, C., and Morrison, S.J. (2005). SLAM family receptors distinguish hematopoietic stem and progenitor cells and reveal endothelial niches for stem cells. Cell *121*, 1109-1121.

Kingsley, P.D., Malik, J., Emerson, R.L., Bushnell, T.P., McGrath, K.E., Bloedorn, L.A., Bulger, M., and Palis, J. (2006). "Maturational" globin switching in primary primitive erythroid cells. Blood *107*, 1665-1672.

Kisanuki, Y.Y., Hammer, R.E., Miyazaki, J., Williams, S.C., Richardson, J.A., and Yanagisawa, M. (2001). Tie2-Cre transgenic mice: a new model for endothelial cell-lineage analysis in vivo. Dev Biol *230*, 230-242.

Koushik, S.V., Wang, J., Rogers, R., Moskophidis, D., Lambert, N.A., Creazzo, T.L., and Conway, S.J. (2001). Targeted inactivation of the sodium-calcium exchanger (Ncx1) results in the lack of a heartbeat and abnormal myofibrillar organization. FASEB J *15*, 1209-1211.

Lancrin, C., Sroczynska, P., Stephenson, C., Allen, T., Kouskoff, V., and Lacaud, G. (2009). The haemangioblast generates haematopoietic cells through a haemogenic endothelium stage. Nature *457*, 892-895.

McGrath, K.E., Frame, J.M., Fegan, K.H., Bowen, J.R., Conway, S.J., Catherman, S.C., Kingsley, P.D., Koniski, A.D., and Palis, J. (2015). Distinct Sources of Hematopoietic Progenitors Emerge before HSCs and Provide Functional Blood Cells in the Mammalian Embryo. Cell Rep *11*, 1892-1904.

McGrath, K.E., Frame, J.M., Fromm, G.J., Koniski, A.D., Kingsley, P.D., Little, J., Bulger, M., and Palis, J. (2011). A transient definitive erythroid lineage with unique regulation of the β-globin locus in the mammalian embryo. Blood *117*, 4600-4608.

McGrath, K.E., Koniski, A.D., Malik, J., and Palis, J. (2003). Circulation is established in a stepwise pattern in the mammalian embryo. Blood *101*, 1669-1676.

McKinney-Freeman, S.L., Naveiras, O., Yates, F., Loewer, S., Philitas, M., Curran, M., Park, P.J., and Daley, G.Q. (2009). Surface antigen phenotypes of hematopoietic stem cells from embryos and murine embryonic stem cells. Blood *114*, 268-278.

Medvinsky, A., and Dzierzak, E. (1996). Definitive hematopoiesis is autonomously initiated by the AGM region. Cell *86*, 897-906.

Mikkola, H.K., and Orkin, S.H. (2006). The journey of developing hematopoietic stem cells. Development *133*, 3733-3744.

Mikkola, H.K., Klintman, J., Yang, H., Hock, H., Schlaeger, T.M., Fujiwara, Y., and Orkin, S.H. (2003a). Haematopoietic stem cells retain long-term repopulating activity and multipotency in the absence of stem-cell leukaemia SCL/tal-1 gene. Nature *421*, 547-551.

Mikkola, H.K.A., Fujiwara, Y., Schlaeger, T.M., Traver, D., and Orkin, S.H. (2003b). Expression of CD41 marks the initiation of definitive hematopoiesis in the mouse embryo. Blood *101*, 508–516.

Moore, M.A., and Metcalf, D. (1970). Ontogeny of the haemopoietic system: yolk sac origin of in vivo and in vitro colony forming cells in the developing mouse embryo. Br. J. Haematol. *18*, 279–296.

Muller, A.M., Medvinsky, A., Strouboulis, J., Grosveld, F., and Dzierzak, E. (1994). Development of hematopoietic stem cell activity in the mouse embryo. Immunity *1*, 291-301.

Muzumdar, M.D., Tasic, B., Miyamichi, K., Li, L., and Luo, L. (2007). A global double-fluorescent Cre reporter mouse. Genesis *45*, 593-605.

North, T.E., Goessling, W., Peeters, M., Li, P., Ceol, C., Lord, A.M., Weber, G.J., Harris, J., Cutting, C.C., Huang, P., et al. (2009). Hematopoietic stem cell development is dependent on blood flow. Cell *137*, 736–748.

Org, T., Duan, D., Ferrari, R., Montel-Hagen, A., Van Handel, B., Kerényi, M.A., Sasidharan, R., Rubbi, L., Fujiwara, Y., Pellegrini, M.*, et al.* (2015). Scl binds to primed enhancers in mesoderm to regulate hematopoietic and cardiac fate divergence. EMBO J *34*, 759-777.

Palis, J. (2008). Ontogeny of erythropoiesis. Curr Opin Hematol *15*, 155-161.

Pang, W.W., Price, E.A., Sahoo, D., Beerman, I., Maloney, W.J., Rossi, D.J., Schrier, S.L., and Weissman, I.L. (2011). Human bone marrow hematopoietic stem cells are increased in frequency and myeloid-biased with age. Proc Natl Acad Sci U S A *108*, 20012-20017.

Pham, T.H.M., Baluk, P., Xu, Y., Grigorova, I., Bankovich, A.J., Pappu, R., Coughlin, S.R., McDonald, D.M., Schwab, S.R., and Cyster, J.G. (2010). Lymphatic endothelial cell sphingosine kinase activity is required for lymphocyte egress and lymphatic patterning. J. Exp. Med. *207*, 17–27.

Porcher, C., Swat, W., Rockwell, K., Fujiwara, Y., Alt, F.W., and Orkin, S.H. (1996). The T cell leukemia oncoprotein SCL/tal-1 is essential for development of all hematopoietic lineages. Cell *86*, 47-57.

Qiu, C., Olivier, E.N., Velho, M., and Bouhassira, E.E. (2008). Globin switches in yolk sac-like primitive and fetal-like definitive red blood cells produced from human embryonic stem cells. Blood *111*, 2400-2408.

Rhodes, K.E., Gekas, C., Wang, Y., Lux, C.T., Francis, C.S., Chan, D.N., Conway, S., Orkin, S.H., Yoder, M.C., and Mikkola, H.K. (2008). The emergence of hematopoietic stem cells is initiated in the placental vasculature in the absence of circulation. Cell Stem Cell *2*, 252-263.

Samokhvalov, I.M., Samokhvalova, N.I., and Nishikawa, S. (2007). Cell tracing shows the contribution of the yolk sac to adult haematopoiesis. Nature *446*, 1056-1061.

Schlaeger, T.M., Mikkola, H.K., Gekas, C., Helgadottir, H.B., and Orkin, S.H. (2005). Tie2Cre-mediated gene ablation defines the stem-cell leukemia gene (SCL/tal1)-dependent window during hematopoietic stem-cell development. Blood *105*, 3871-3874.

Schledzewski, K., Falkowski, M., Moldenhauer, G., Metharom, P., Kzhyshkowska, J., Ganss, R., Demory, A., Falkowska-Hansen, B., Kurzen, H., Ugurel, S., et al. (2006). Lymphatic endothelium-specific hyaluronan receptor LYVE-1 is expressed by stabilin-1+, F4/80+, CD11b+ macrophages in malignant tumours and wound healing tissue in vivo and in bone marrow cultures in vitro: implications for the assessment of lymphangiogenesis. J. Pathol. *209*, 67–77.

Shivdasani, R.A., Mayer, E.L., and Orkin, S.H. (1995). Absence of blood formation in mice lacking the T-cell leukaemia oncoprotein tal-1/SCL. Nature *373*, 432-434.

Sieburg, H.B., Cho, R.H., Dykstra, B., Uchida, N., Eaves, C.J., and Muller-Sieburg, C.E. (2006). The hematopoietic stem compartment consists of a limited number of discrete stem cell subsets. Blood *107*, 2311-2316.

Souroullas, G.P., Salmon, J.M., Sablitzky, F., Curtis, D.J., and Goodell, M.A. (2009). Adult hematopoietic stem and progenitor cells require either Lyl1 or Scl for survival. Cell Stem Cell *4*, 180-186.

Srinivas, S., Watanabe, T., Lin, C.S., William, C.M., Tanabe, Y., Jessell, T.M., and Costantini, F. (2001). Cre reporter strains produced by targeted insertion of EYFP and ECFP into the ROSA26 locus. BMC Dev Biol *1*, 4.

Van Handel, B., Montel-Hagen, A., Sasidharan, R., Nakano, H., Ferrari, R., Boogerd, C.J., Schredelseker, J., Wang, Y., Hunter, S., Org, T.*, et al.* (2012). Scl represses cardiomyogenesis in prospective hemogenic endothelium and endocardium. Cell *150*, 590-605.

Wang, Q., Stacy, T., Binder, M., Marin-Padilla, M., Sharpe, A.H., and Speck, N.A. (1996). Disruption of the Cbfa2 gene causes necrosis and hemorrhaging in the central nervous system and blocks definitive hematopoiesis. Proc. Natl. Acad. Sci. U. S. A. *93*, 3444–3449.

Weissman, I., Papaioannou, V., and Gardner, R. (1978). Fetal hematopoietic origins of the adult hematolymphoid system. In *Differentiation of Normal and Neoplastic Hematopoietic Cells*, B. Clarkson, P. Mark, and J. Till, eds. (Cold Spring Harbor Laboratory Press), pp. 33-47.

Weissman, I.L., Baird, S., Gardner, R.L., Papaioannou, V.E., and Raschke, W. (1977). Normal and neoplastic maturation of T-lineage lymphocytes. Cold Spring Harb Symp Quant Biol *41 Pt 1*, 9-21.

Yamamoto, R., Morita, Y., Ooehara, J., Hamanaka, S., Onodera, M., Rudolph, K.L., Ema, H., and Nakauchi, H. (2013). Clonal analysis unveils self-renewing lineage-restricted progenitors generated directly from hematopoietic stem cells. Cell *154*, 1112-1126.

Zeigler, B.M., Sugiyama, D., Chen, M., Guo, Y., Downs, K.M., and Speck, N.A. (2006). The allantois and chorion, when isolated before circulation or chorio-allantoic fusion, have hematopoietic potential. Development *133*, 4183-4192.

Zovein, A.C., Hofmann, J.J., Lynch, M., French, W.J., Turlo, K.A., Yang, Y., Becker, M.S., Zanetta, L., Dejana, E., Gasson, J.C.*, et al.* (2008). Fate tracing reveals the endothelial origin of hematopoietic stem cells. Cell Stem Cell *3*, 625-636.

CHAPTER TWO

LYVE1 Identifies a Population of Cells in the Embryo that Contributes to a Third of the Adult Definitive Hematopoietic Stem Cell Pool

Yasamine Ghorbanian[1], Shivashankar Othy[2], Ankita K. Shukla[1], Rocio Barahona[1], Shailey Patel[1], Andrew Pop[1], Fangyi Chen[2], Connie Chao[1], Alborz Karimzadeh[1], Ian Parker[3], Michael D. Cahalan[2], Hanna K.A. Mikkola[4] , Matthew A. Inlay[1]

[1]Sue and Bill Gross Stem Cell Research Center, Dept. of Molecular Biology & Biochemistry at UCI, [2]Dept. of Physiology and Biophysics at UCI, [3]Dept. of Neurobiology and Behavior at UCI, [4]Eli and Edythe Broad Center for Regenerative Medicine and Stem Cell Research, Dept. of Molecular, Cell & Developmental Biology at UCLA

Abstract

During embryogenesis, hematopoietic stem cells (HSCs) bud from hemogenic endothelium, a subset of endothelial cells with hematopoietic potential. Which tissue, or tissues, contains this source of HSCs is still being debated. It is fairly well agreed upon that the yolk sac (YS) is the source of early, primitive hematopoiesis. These primitive waves are characterized by the presence of nucleated erythrocytes that express fetal hemoglobins and are transient waves that fulfill the needs of the embryo at early stages of development. These waves of hematopoiesis are followed by the definitive waves, which ultimately give rise to the multipotent, self-renewing, engraftable HSCs that persist throughout adulthood. The YS, placenta, and aorta-gonad-mesonepheros (AGM) have all been implicated as sources of later definitive waves of hematopoiesis. We have previously found that LYVE1 marks definitive hemogenic endothelium, and labeling bypasses primitive hematopoiesis. Here we find that LYVE1-derived cells contribute to each definitive wave of hematopoiesis and that these cells persist to adulthood to constitute approximately a third of the adult HSC pool. These LYVE1-derived cells are first engraftable in conditioned neonatal recipients at E10.5 when found in the AGM, and at E11.5 from other tissues. LYVE1-derived cells from E14.5 fetal livers and adult bone marrow HSCs can engraft into conditioned adults demonstrating that these cells are true, functional HSCs. We propose that LYVE1 labels a subset of definitive hemogenic endothelium in both the YS and the AGM. The rare AGM labeled cells give rise to the first pre-HSCs while the LYVE1-derived cells from the YS require more time to mature. In our *ex vivo* embryo culturing system we see dynamic, actively dividing LYVE1-derived cells emerging from labeled endothelium in the YS of viable, intact embryos. This supports the idea that the YS is the tissue

in which the HSC precursor pool expands and that these cells then need to migrate to other tissues, such as the fetal liver or AGM, to mature.

Introduction

The ontogeny of hematopoietic stem cells (HSCs) has been a topic of research since the late 1960s (Moore and Owen 1967; Moore and Metcalf 1970). It is well accepted that all hematopoietic stem and precursor cells initially have a non-hematopoietic origin during embryonic development. The hemogenic endothelium is a specific subset of endothelial cells that has hematopoietic potential and gives rise to the embryonic hematopoietic stem and progenitor cells (Dieterlen-Lièvre 1998; Ottersbach and Dzierzak 2005). The tissue, or tissues, that contain the hemogenic endothelium that gives rise to definitive HSCs is still unclear.

It was first thought that all HSCs come from the extraembryonic yolk sac (YS) because it is the first site of hematopoiesis. At E7.5 developing blood islands are visualized on the surface of the YS (Moore and Metcalf 1970; Auerbach, Huang, and Lu 1996; Palis 2001; Lux et al. 2008). These early blood cells are large, nucleated erythrocytes that express fetal hemoglobins and they characterize the first “primitive” wave of hematopoiesis (Moore and Metcalf 1970; Auerbach, Huang, and Lu 1996; Lux et al. 2008). As the embryo develops and matures, so does the blood system. The hematopoietic needs of the growing embryo increase and there is a need for greater lineage potential from the HSC precursors.

Erythromyeloid progenitors (EMPs) constitute the first “definitive” wave of hematopoiesis, which begins around E8.5. In addition to small enucleated erythrocytes that

express adult hemoglobins, cells of the myeloid lineage—monocytes and granulocytes— are also produced during this stage of embryonic development (Lux et al. 2008).

Pre-HSCs are produced by E10. These HSC precursors have most of the defining properties of an HSC in that they are multipotent, self-renewing cells. They do not however have the potential to engraft into a conditioned adult. Instead, they are able to engraft into conditioned embryonic or neonatal recipients (Yoder, Hiatt, and Mukherjee 1997; Yoder and Hiatt 1998; Yoder et al. 1997). Cells from the fetal liver (FL) contain pre-HSC activity as well (Müller et al. 1994; A. Medvinsky and Dzierzak 1996) and the para-aortic splanchnopleura (PAS) exhibits multilineage potential (A. L. Medvinsky and Dzierzak 1998; Kumaravelu et al. 2002). Both of the intraembryonic tissues that possess pre-HSCs have important roles in hematopoiesis. The FL is colonized by pre-HSCs and definitive HSCs and by E12 becomes the embryonic hematopoietic niche (Johnson and Moore 1975; Palis 2001; Ghiaur et al. 2008). A portion of the PAS develops into the aorta-gonad-mesonephros (AGM), which is a tissue that is believed to give rise to definitive HSCs (A. L. Medvinsky et al. 1993; A. L. Medvinsky and Dzierzak 1998; Kumaravelu et al. 2002).

The final wave of hematopoiesis brings about the definitive HSCs that are not only mulitpotent and self-renewing, but much like their adult HSC counterparts, can engraft into conditioned adult recipients (Müller et al. 1994; A. Medvinsky and Dzierzak 1996). The first tissue that has this definitive HSC activity is the AGM, but it is still unclear as to whether those cells originate from the AGM or if they migrate there via circulation(Müller et al. 1994; A. L. Medvinsky and Dzierzak 1998). Because the YS is one of the first tissues to exhibit pre-HSC activity, it has been speculated that these pre-HSCs migrate and mature in the AGM (Yoder et

al. 1997; Yoder, Hiatt, and Mukherjee 1997; Yoder and Hiatt 1998). Additionally, hematopoietic stem and progenitor cells (HSPCs) are not seen within the embryo when circulation or migration of these cells is lost using $Ncx1^{-/-}$ or $Rac1^{-/-}$ respectively (Lux et al. 2008; Ghiaur et al. 2008). However, CFU-S and *in vitro* culturing assays demonstrate that the AGM can maintain and generate HSCs before the YS (A. L. Medvinsky et al. 1993; A. Medvinsky and Dzierzak 1996; Kumaravelu et al. 2002). Definitive HSC activity has been attributed to the placenta as well (Alvarez-Silva et al. 2003; Ottersbach and Dzierzak 2005; Gekas et al. 2005; Mikkola et al. 2005).

There have been many conflicting findings regarding the ontogeny of definitive HSCs because multipotency, self-renewal, and engraftability have all been demonstrated at different stages in the YS, AGM, and placenta. Whether these cells are generated *de novo*, or if they require generation in one tissue and then migration and maturation in another, or a combination of both is still unclear. It is important to understand the ontogeny of HSCs in order to better understand hematopoiesis and the hematopoietic system. If there is heterogeneity in that multiple tissues or microenvironments contribute to definitive hematopoiesis, what consequence does that have on the initiation, progression, and treatment of certain hematopoietic malignancies?

We have previously published that the lymphatic vessel hyaluronan receptor 1 (LYVE1) marks the divergence of definitive from primitive hemogenic endothelium (Lee et al. 2016). We now seek to determine whether these LYVE1-derived hematopoietic cells are true, functional HSCs. Our data suggests that LYVE1-derived cells do indeed give rise to functional HSCs, and that these HSCs mature at later stages during embryonic development as compared to their non-LYVE1-derived counterparts. There are two potential sources for these functional LYVE1-

labeled HSCs. The first is the YS, which contains LYVE1-derived hematopoietic cells that are highly dynamic, as seen by 2 photon imaging of *ex vivo* embryo cultures. We believe that these LYVE1-labeled cells in the YS may migrate to other intra-embryonic tissues to mature and become engraftable. The other potential source for these functional, LYVE1-derived HSCs is the AGM. LYVE1 labels a small percentage of endothelial cells in the AGM and these cells are potentially the hemogenic endothelium that gives rise to engraftable, LYVE1-derived HSCs. Although there is no way to distinguish between these two models, our data shows that LYVE1-derived HSCs make up a significant portion of the adult definitive HSC pool and that these cells may be important to understanding the heterogeneity of this population.

Results

Lyve1 expression is most abundant in the extra embryonic yolk sac

In order to determine what populations express LYVE1, we used the online microarray database Gene Expression Commons (Seita et al. 2012) to look at the expression of this gene in an unpublished dataset that examines embryonic endothelial cells and pre-HSCs, as well as in adult hematopoietic populations (**Figure 2.1A**). We found that LYVE1 is highly expressed in the YS endothelial cells and pre-HSCs and very lowly, or not expressed, in the other embryonic tissues or adult BM populations. To confirm this at the protein level, we then stained a wildtype E11.5 embryo using a LYVE1 antibody. The YS vasculature expressed LYVE1 as seen by positive antibody staining (**Figure 2.1B**). This confirmed the microarray results and we therefore decided to move forward using a Lyve1Cre lineage tracing model to survey the contribution of LYVE1-derived cells to definitive hematopoiesis.

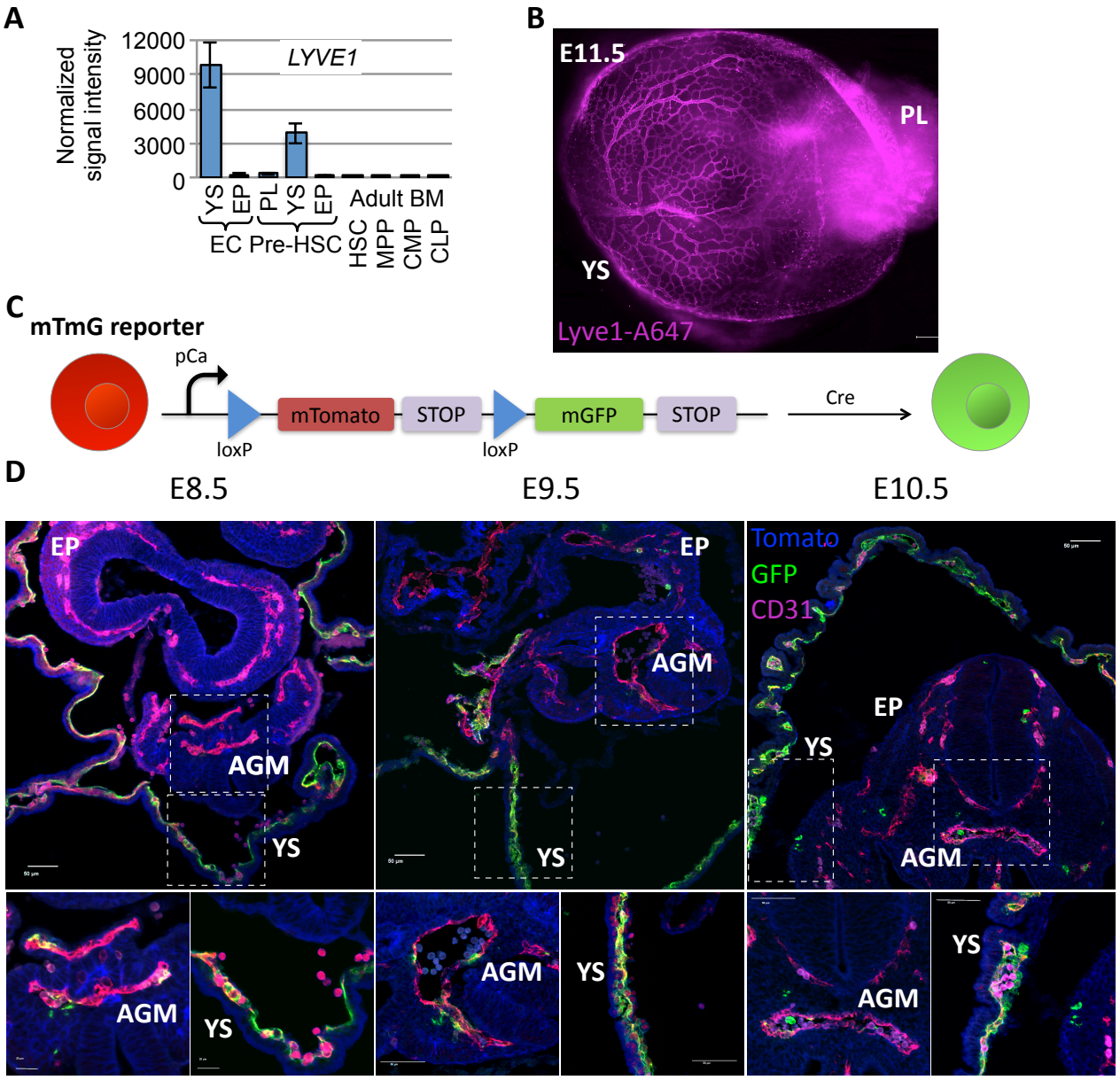

Figure 2.1 LYVE1 expression in embryonic tissues is most abundant in the extra embryonic yolk sac
(A) Microarray shows that LYVE1 is highly expressed in the YS EC and Pre HSC populations, but is not expressed in other embryonic populations or adult bone marrow populations.
(B) LYVE1 protein is detected in the YS vasculature by whole mount fluorescence microscopy in an E11.5 wildtype embryo.
(C) Diagram of the mTmG reporter system.
(D) IF staining of *Lyve1-Cre;mTmG* embryo sections shows GFP and CD31 co-localization in YS and AGM endothelium starting at E8.5. Representative images from independent experiments. Areas in the boxes correspond to the higher magnification images below.
Abbreviations: endothelial cells (EC), yolk sac (YS), embryo proper (EP), placenta (PL), hematopoietic stem cell (HSC), multipoint progenitor (MPP), common myeloid progenitor (CMP), common lymphoid progenitor (CLP), bone marrow (BM)

We crossed Lyve1-Cre mice (Pham et al. 2010) with mTmG reporter mice (MD et al. 2006) to yield Lyve1-Cre;mTmG embryos. In this system, all the cells are initially Tomato+. When Cre is expressed, which in this case is when LYVE1 is expressed, the Tomato is floxed out and a downstream GFP is expressed instead (**Figure 2.1C**). In this way, all LYVE1-expressing cells and their progeny are marked by GFP expression. In the initial paper describing the Lyve1Cre mice, the authors noted that a portion of the blood endothelial cells in the embryo and CD45+ hematopoietic cells in the adult mice were labeled when Lyve1Cre mice were crossed with a YFP reporter strain (Pham et al. 2010). This provided further preliminary evidence that LYVE1-derived cells contribute to definitive hematopoiesis.

As we and others have previously seen (Lee et al. 2016; Ganuza et al. 2018), LYVE1 labeling begins at E8.5 in Lyve1-Cre;mTmG embryos (**Figures S2.1 and 2.1D**). At this time point, there is abundant LYVE1 labeling of CD31+ endothelial cells in the YS and a small number in the AGM (**Figure 2.1D**). This co-localization of CD31 and GFP continues to be seen in these important hematopoietic tissues in E9.5 and E10.5 Lyve1-Cre;mTmG embryos as well. Because LYVE1 labels definitive HSPCs but bypasses the primitive wave of hematopoiesis, we concluded that LYVE1 is marking a subset of definitive hemogenic endothelium (Lee et al. 2016) and this is confirmed by our findings here. Moreover, these results highlight the differences in LYVE1 endothelial labeling. The YS endothelium is more abundantly labeled than that of the AGM, but it is unlikely that all of the labeled YS is hemogenic. Conversely, labeling in the AGM is infrequent and it is possible LYVE1 reveals a rare hemogenic endothelial population in this tissue.

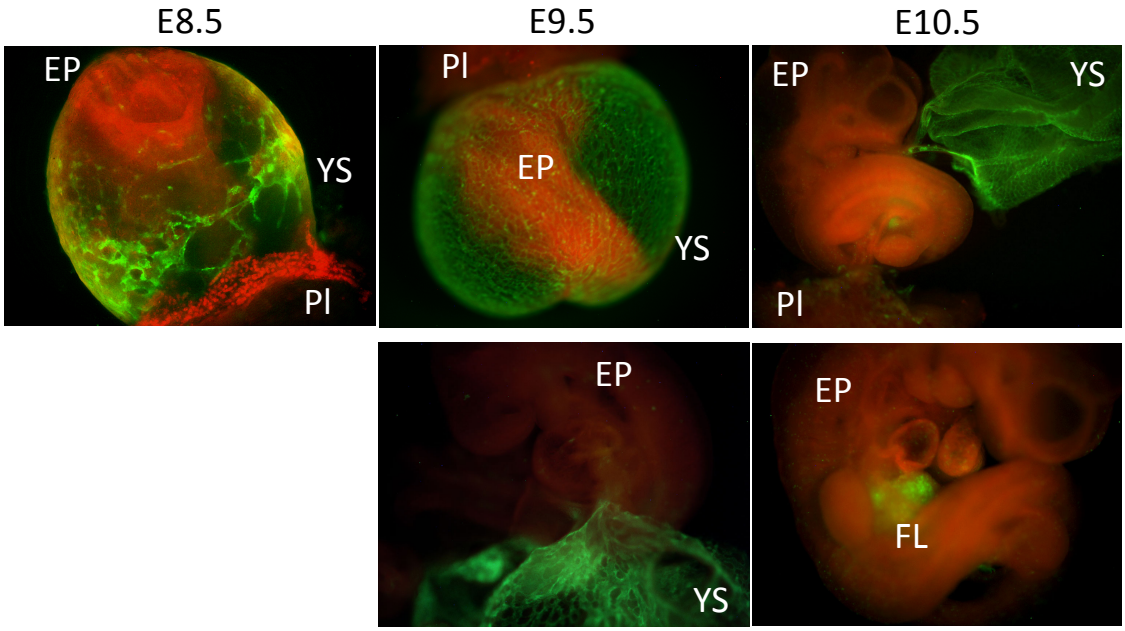

Supplemental Figure 2.1 LYVE1 labeling begins at e8.5 in the yolk sac
Whole mount fluorescence microscopy images of *Lyve1-Cre;mTmG* embryos show that LYVE1 labeling begins in the YS vasculature at E8.5.
Abbreviations: yolk sac (YS), embryo proper (EP), placenta (PL), fetal liver (FL)

LYVE1-derived cells contribute to definitive hematopoiesis

We next wanted to determine which waves of hematopoiesis have contributions from LYVE1-derived cells (**Figure 2.2A**). We previously established that LYVE1-labeling bypasses the primitive wave of hematopoiesis (Lee et al. 2016). We therefore surveyed LYVE1-labeling of the following wave of hematopoiesis by analyzing erythromyeloid progenitors (EMPs). GFP+ EMPs were found at comparable levels in every tissue in E10.5 Lyve1-Cre;mTmG embryos (**Figure 2.2B**). This indicates that the LYVE1-derived hematopoietic cells have mulitlineage potential, a characteristic of more definitive hematopoiesis.

We subsequently examined the labeling of CD11a- KLS cells, which our lab has identified as containing a pre-HSC population (Inlay et al. 2014). In wildtype embryos, this population is most abundant in the YS at E9.5, with increasing presence of these cells in other tissues as the embryo matures (**Figure 2.2C**). GFP labeling of CD11a- KLS cells is also the most abundant in the YS, by both percentage and absolute cell number, at E9.5. By E10.5, once circulation has been established, there is an increased distribution of these LYVE1-labeled cells in the other embryonic tissues. These findings suggest that not only is the YS the most abundant source of CD11a- KLS cells, but that this population also has the most LYVE1 contribution. These cells either bud directly from the abundant LYVE1-labeled endothelial cells in the YS, or they come from LYVE1-derived hematopoietic precursors that mature into CD11a- KLS cells.

In order to determine if these LYVE1-labeled hematopoietic cells persist to adulthood, we bled and harvested bone marrow from a cohort of adult Lyve1-Cre;mTmG mice. LYVE1-derived cells make up about 22% of the adult HSC pool and these cells contribute to all of the

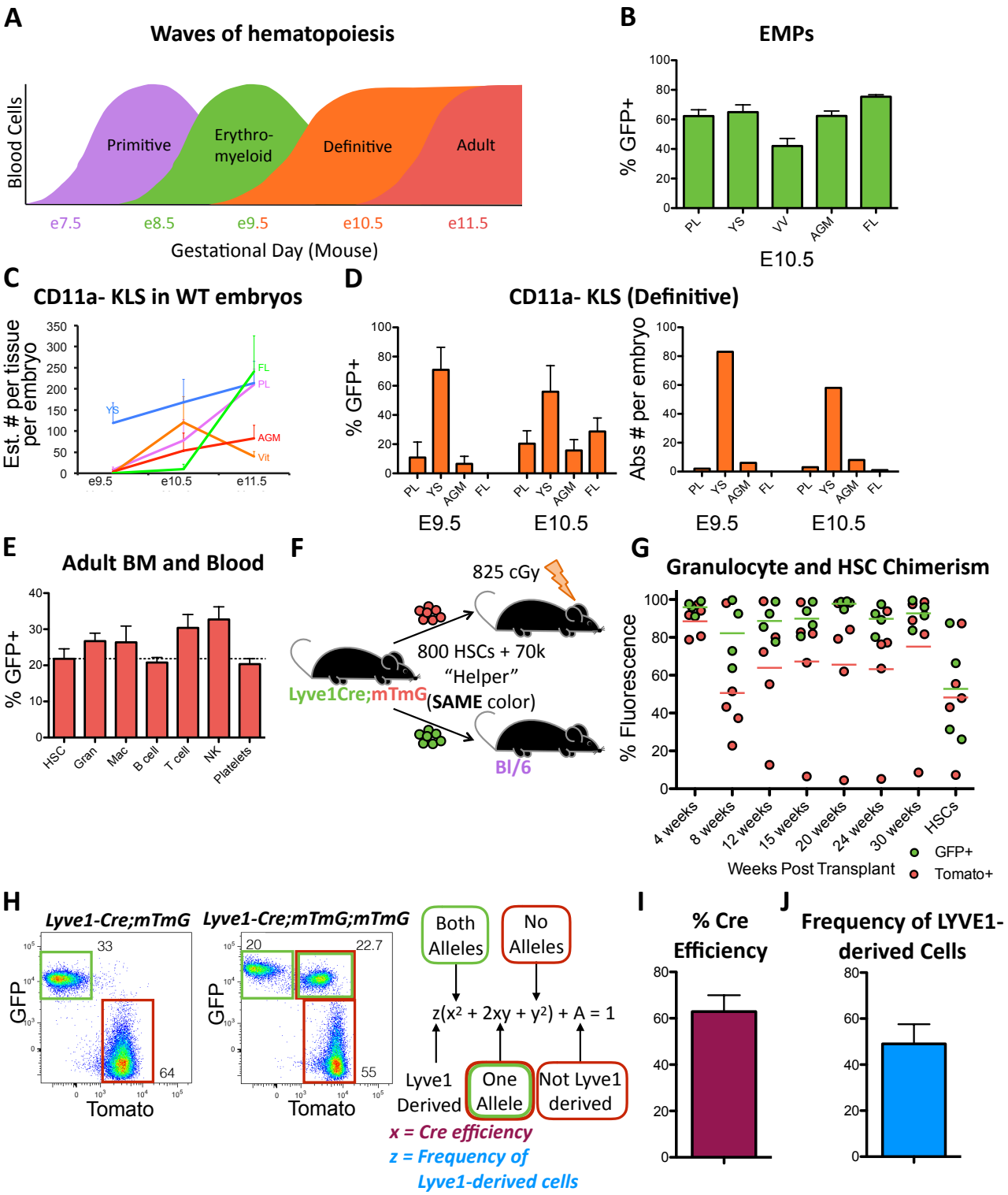
A
Waves of hematopoiesis
Blood Cells
Primitive
Erythro-myeloid
Definitive
Adult
e7.5
e8.5
e9.5
e10.5
e11.5
Gestational Day (Mouse)
B
EMPs
% GFP+
PL
YS
VV
AGM
FL
E10.5
C
CD11a- KLS in WT embryos
Est. # per tissue per embryo
YS
PL
FL
AGM
Vit
e9.5
e10.5
e11.5
D
CD11a- KLS (Definitive)
% GFP+
Abs # per embryo
E9.5
E10.5
E9.5
E10.5
E
Adult BM and Blood
% GFP+
HSC
Gran
Mac
B cell
T cell
NK
Platelets
F
825 cGy
800 HSCs + 70k
"Helper"
(SAME color)
Lyve1Cre;mTmG
Bl/6
G
Granulocyte and HSC Chimerism
% Fluorescence
4 weeks
8 weeks
12 weeks
15 weeks
20 weeks
24 weeks
30 weeks
HSCs
Weeks Post Transplant
GFP+
Tomato+
H
Lyve1-Cre;mTmG
Lyve1-Cre;mTmG;mTmG
GFP
Tomato
33
64
20
22.7
55
Both Alleles
No Alleles
z(x² + 2xy + y²) + A = 1
Lyve1 Derived
One Allele
Not Lyve1 derived
x = Cre efficiency
z = Frequency of Lyve1-derived cells
I
% Cre Efficiency
J
Frequency of LYVE1-derived Cells

Figure 2.2 LYVE1-derived cells contribute to all definitive waves of hematopoiesis during embryonic development and to functional HSCs in the adult
(A) Schematic of the waves of hematopoiesis during embryonic development.
(B) GFP+ EMPs (Ter119- CD41+ ckit+ FcyR+) are found in all *Lyve1-Cre;mTmG* embryonic tissues at E10.5 by flow cytometry analysis. n=3 litters
(C) The YS is the highest source of CD11a- KLS cells in WT embryos at E9.5. The number of CD11a- KLS cells present in the other tissues increases with age. n=6-8 litters per time point
(D) The YS has the highest percentage and absolute cell number of GFP+ CD11a- KLS (Ter119- CD41+ CD11a- ckit+ lin- Sca+) cells at E9.5. The percentage and absolute cell numbers of GFP+ CD11a- KLS cells in other tissues increases from E9.5 to E10.5 as determined by flow cytometry analysis of *Lyve1-Cre;mTmG* embryos. n=7 litters
(E) Flow cytometry analysis of *Lyve1-Cre;mTmG* adult blood and bone marrow populations shows that labeled cells are found in all major blood lineages. The line indicates the mean of HSC labeling. n=4-5 mice
(F) Diagram of the transplantation experiment setup. HSCs were sorted on Ter119- CD27+ ckit+ Sca+ CD34- Slam+ cells. “Helper” cells were sorted on the Ter119- ckit+ Sca- population. The HSCs and “helper” were then sorted by GFP+ or Tomato+. Donors and recipients were age and gender matched (17-19 weeks old).
(G) Flow cytometry analysis of granulocyte (CD45+ NK1.1- CD11b+ Gr1+) and HSC (Ter119- CD27+ ckit+ Sca+ CD34- Slam+) chimerism. Each point represents one recipient mouse. n=9
(H) Representative flow plots gated on total CD45+ cells from *Lyve1-Cre;mTmG* and *Lyve1-Cre;mTmG;mTmG* peripheral blood.
(I and J) Calculations for percent Cre efficiency and frequency of LYVE1-derived cells from *Lyve1-Cre;mTmG;mTmG* mice. n=7
Abbreviations: erythromyeloid progenitors (EMP), placenta (PL), yolk sac (YS), vitelline vessels (VV), fetal liver (FL), granulocytes (Gran), natural killer cells (NK), hematopoietic stem cells (HSCs), wild type (WT)

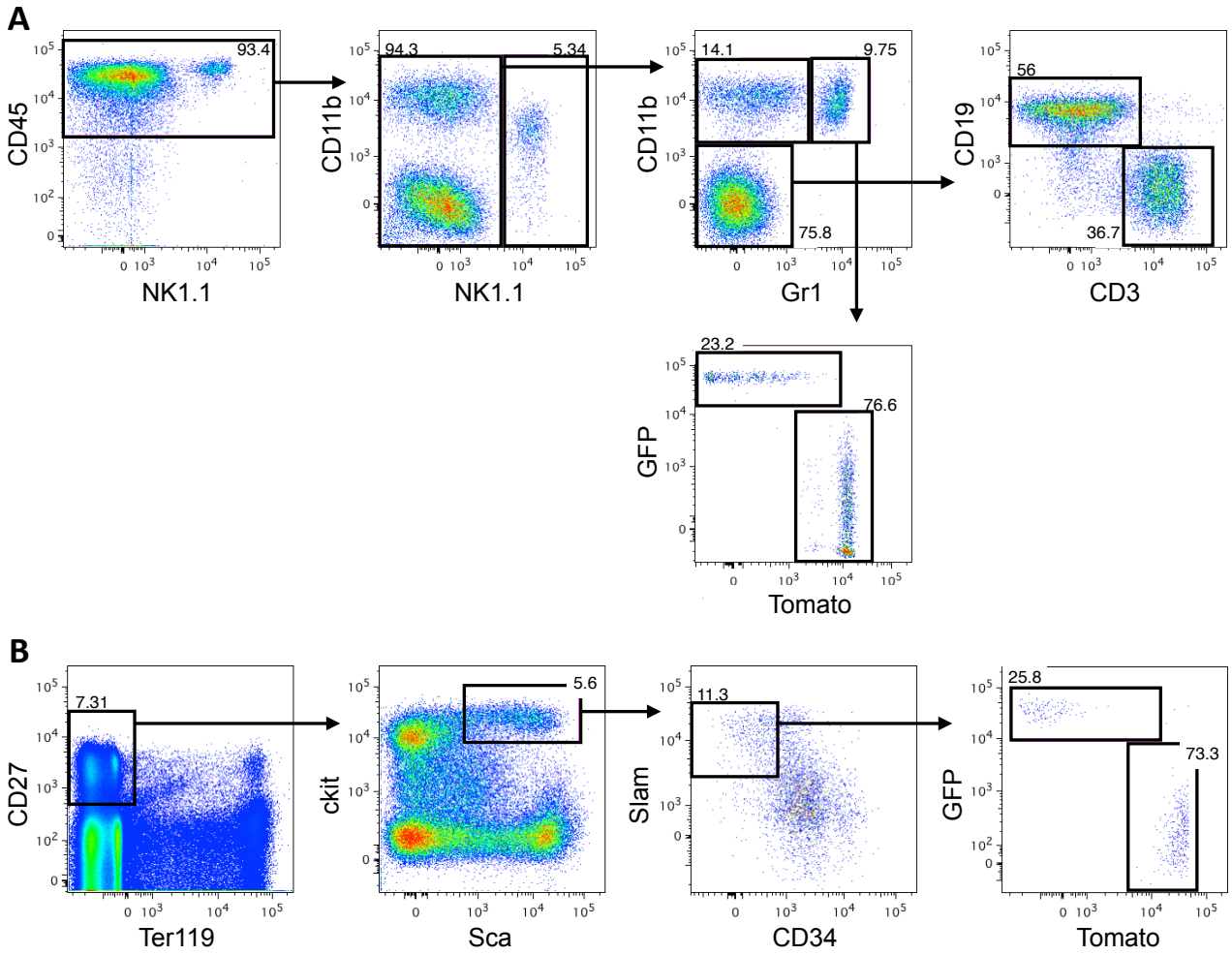

Supplemental Figure 2.2 Representative flow cytometry plots
(A) Lineage stain on peripheral blood from a Lyve1-Cre;mTmG mouse (gated on live, single cells).
(B) HSC stain on bone marrow from a Lyve1-Cre;mTmG mouse (gated on live, single cells).

major hematopoietic lineages (**Figure 2.2E**). Thus, LYVE1-derived cells to contribute to definitive adult hematopoiesis and like true definitive HSCs, exhibit multilineage potential.

Transplantation of Lyve1-derived (GFP+) and non-LYVE1-derived (Tomato+) cells was then performed to establish whether or not these cells are functional HSCs. GFP+ and Tomato+ HSCs from Lyve1Cre;mTmG adults were sorted and transplanted into lethally irradiated Bl/6 mice. Sorted "helper" BM, which contains progenitor populations to provide short-term hematopoietic reconstitution until the HSCs engraft and differentiate, was also included in the transplanted population. In order to avoid any potential contamination or signals from LYVE1-derived cells onto non-LYVE1-derived cells or vice versa, the "helper" population of the same color as the HSC population was used for each transplant (**Figure 2.2F**). Both GFP+ and Tomato+ HSCs exhibited successful engraftment at comparable levels (**Figure 2.2G**). This reveals that the LYVE1-derived HSCs are true, definitive HSCs in that the exhibit multipoteny, self-renewal capacity, and are engraftable. Neither the LYVE1-derived, nor the non-LYVE1-derived, HSCs demonstrated any statistical advantage in engraftment over the other indicating that these populations do not differ in this regard.

The level of labeling in any Cre system is dependent on the efficiency of the Cre itself. Because of this, the level of GFP labeling may not reflect the true number of LYVE1-derived cells (i.e. % GFP is lower than % LYVE1-derived) because the Cre was not efficient enough to recombine in all LYVE1-expressing cells. In order to evaluate this in our lineage tracing system we took advantage of the fact that the mTmG is a two-colored reporter. We bred Lyve1-Cre;mTmG;mTmG mice so that recombination levels of each allele can be determined. If one allele recombines, that results in a GFP+ Tomato+ population; whereas, if neither allele

recombines, or if both alleles recombine, that results in a Tomato+ or GFP+ population respectively (**Figure 2.2H**). Then, using a probability equation (**Figure 2.2H**) and the percent labeling of peripheral blood cells (CD45+), we calculated the Cre to be 63% efficient at labeling Lyve1-expressing cells (**Figure 2.2I**). This then allowed us to calculate that the true frequency of LYVE1-derived CD45+ cells to be about 49% (**Figure 2.2J**). Therefore, nearly half of all adult HSCs are likely derived from LYVE1+ precursors.

Embryonic LYVE1-derived pre-HSC and HSC populations are engraftable

We next sought to determine if the LYVE1-derived pre-HSCs we found in the embryo were able to engraft into a conditioned neonatal recipient, and if so, what tissue(s) these cells are found in. E10.5, E11.5 and E14.5 embryos were dissected into their different tissue populations (P+U, YS, VV, AGM, FL+Hrt) and transplanted into lethally irradiated neonatal NSGs along with CFP+ helper whole bone marrow (WBM) (**Figure 2.3A**). At E10.5, only non-LYVE1-derived pre-HSCs were capable of successfully engrafting into the neonatal host as indicated by the presence of Tomato+ donor HSCs in the recipients. The exception to this was only seen in AGM donors where some LYVE1-derived (GFP+) HSCs were found in the recipients (**Figure 2.3B**). By E11.5. LYVE1-derived cells found in all transplanted tissues, excluding the VV, were capable of engraftment (**Figure 2.3B**). LYVE1-derived cells transplanted from E14.5 FLs were all fully capable of engraftment as shown by the presence of GFP+ HSCs in all of the recipients (**Figure 2.3B**). Since HSCs are known to be present in the embryo by E14.5, we wanted to determine the contribution of LYVE1-derived cells to this population. The percent of LYVE1 labeling of HSCs in the E14.5 FL population is similar to that of the adult BM HSC population

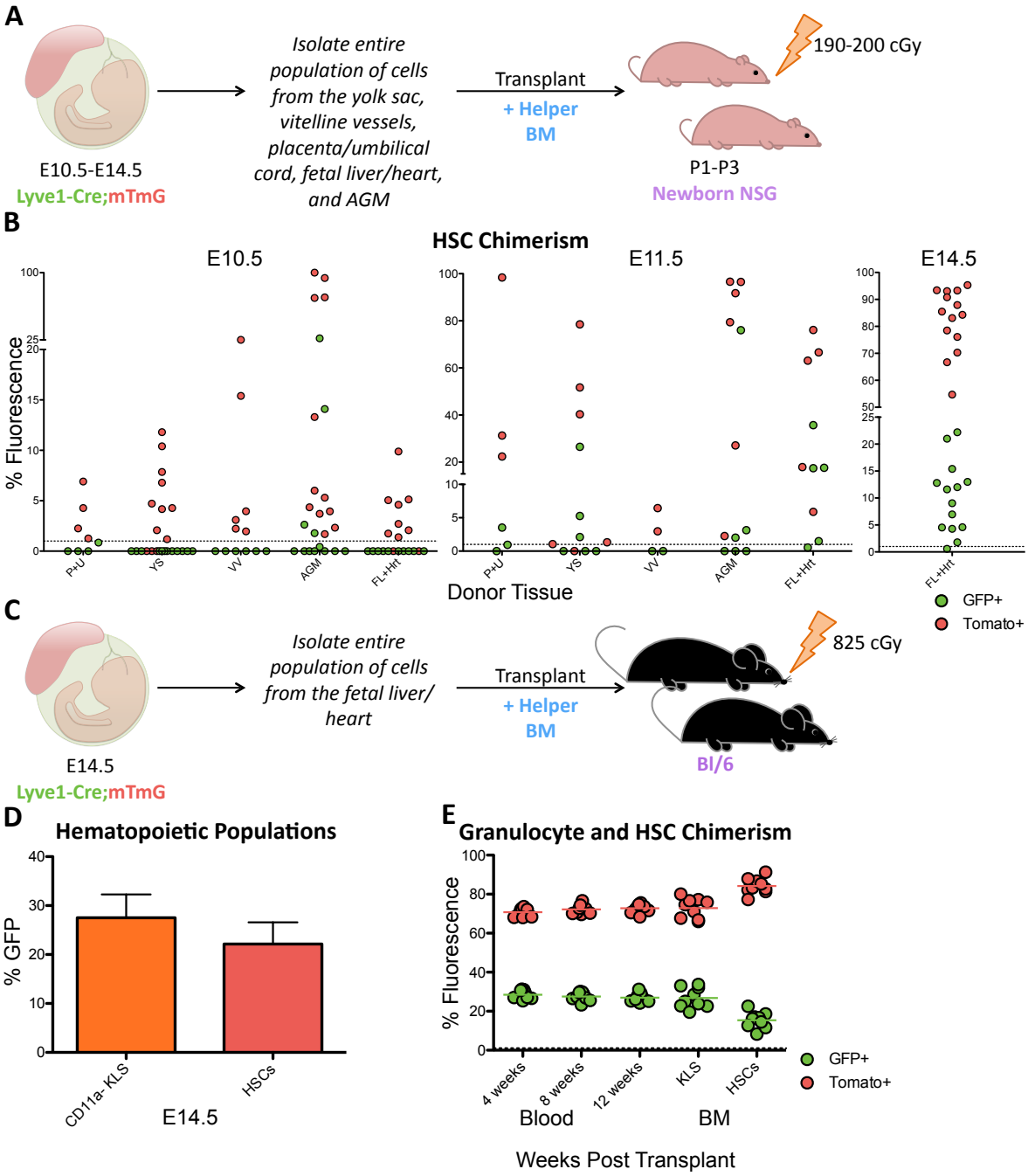
A
E10.5-E14.5
Lyve1-Cre;mTmG
Isolate entire population of cells from the yolk sac, vitelline vessels, placenta/umbilical cord, fetal liver/heart, and AGM
Transplant
+ Helper BM
190-200 cGy
P1-P3
Newborn NSG
B
HSC Chimerism
E10.5
E11.5
E14.5
% Fluorescence
P+U
YS
VV
AGM
FL+Hrt
Donor Tissue
GFP+
Tomato+
C
E14.5
Lyve1-Cre;mTmG
Isolate entire population of cells from the fetal liver/ heart
Transplant
+ Helper BM
825 cGy
Bl/6
D
Hematopoietic Populations
% GFP
CD11a- KLS
HSCs
E14.5
E
Granulocyte and HSC Chimerism
% Fluorescence
4 weeks
8 weeks
12 weeks
KLS
HSCs
Blood
BM
GFP+
Tomato+
Weeks Post Transplant

Figure 2.3 LYVE1-derived pre-HSCs and HSCs are functional and exhibit the most robust engraftment in later stage embryos
(A) Diagram of the neonatal transplantation experiment setup.
(B) HSC chimerism (Ter119- CD27+ ckit+ Sca+ CD34- Slam+) determined by flow cytometry analysis 12 weeks post transplantation. Line at 1% HSC donor chimerism. Each donor is represented by 1 Tomato+ and 1 GFP+ point. Data compiled from 16 (e10.5), 7 (e11.5), and 3 (e14.5) independent experiments.
(C) Diagram of the adult transplantation setup.
(D) Flow cytometry analysis of *Lyve1-Cre;mTmG* E14.5 fetal liver/heart populations. Percent of labeling was determined for CD11a- KLS (Ter- CD41+ ckit+ Sca- CD43+ CD11a-) and HSC (CD27+ Ter- CD45+ ckit+ Sca+ Slam+ CD48- EPCR+) populations. n= 12 from 4 litters and 2 independent experiments.
(E) Granulocyte (CD45+ NK1.1- CD11b+ Gr1+) and HSC chimerism (Ter119- CD27+ ckit+ Sca+ CD34- Slam+) determined by flow cytometry analysis 12 weeks post transplantation of E14.5 *Lyve1-Cre;mTmG* fetal liver/heart cells into Bl/6 adults. Line at 1% HSC donor chimerism. Each donor is represented by 1 Tomato+ and 1 GFP+ point. n=9

(**Figure 2.3D**). We next wanted to assess if the engraftment by E14.5 donor cells is due to the presence of these LYVE1-derived HSCs. To test this, E14.5 FL+Hrt populations with CFP+ helper WBM were transplanted into lethally irradiated Bl/6 adults (**Figure 2.3C**). Only HSCs, and not pre-HSCs can engraft in this system. Both the LYVE1-derived and non-LYVE1-derived cells were capable of engraftment when transplanted into adult Bl/6 mice and the level of chimerism is slightly lower, but reflective of the levels of labeling found in adult Lyve1-Cre;mTmG mice (**Figure 2.3E**). Based on these results, we can conclude that LYVE1-derived pre-HSCs are only capable of engraftment at E10.5 when found in the AGM, and in most other hematopoietic tissues at E11.5. By E14.5 the FL contains LYVE1-derived HSCs that are capable of engrafting into conditioned adult recipients and are therefore true, definitive HSCs. The levels of labeling seen in the FL HSCs is similar to that seen in the adult HSC pool in the BM indicating that these levels are established early on in development in the FL HSC niche and are maintained in the adult BM niche.

Ex vivo culturing of Lyve1-Cre;mTmG embryos reveals dynamic nature of hematopoietic cells

The emergence and behaviors of live, *in vivo*, HSPCs has only been observed intact in zebra fish embryos(Bertrand et al. 2010). We therefore sought to do similar studies looking at the characteristics of hematopoietic cell motility, interactions, and emergence in murine embryos. In these studies, we focused on the YS because it the only murine hematopoietic tissue that can be studied while keeping entire embryo intact. Lyve1-Cre;mTmG embryos were carefully harvested to ensure that they remained intact and that there were no punctures in the yolk sac. These embryos were incubated for at least one hour to evaluate the viability and

health of each embryo and those with a robust heart beat and intact circulation were then used for 2 photon imaging (**Figures 2.4A and SM2.1**). The advantage of this imaging system is that it is an inherently confocal and highly sensitive method to image biological samples with much less photobleaching as compared to confocal imaging. This is ideal for our *ex vivo* embryo cultures because they are imaged for long periods of time.

First, the organization of LYVE1-derived cells in the yolk sac was observed using this *ex vivo* culturing system (**Figures 2.4B and SM2.2**). At E8.5, the blood vessels are labeled and appear to be wide and are not very complex in their branching. There are not very many labeled hematopoietic cells seen within these vessels. This is expected as the LYVE1 system bypasses labeling of primitive hematopoiesis, the predominant wave at this stage of embryonic development. By E9.5 there are noticeably more labeled hematopoietic cells within the blood vessels. The vasculature itself is more complex as the vessels are thinner and more intricately branched. There appear to be regions in the YS that are more densely populated with LYVE1-derived hematopoietic cells and we propose that these might be “hematopoiesis hot spots”. At E10.5 the vasculature becomes even more complex in its architecture and there is an abundance of labeled cells seen throughout the entire YS. Circulation is robust by this stage and is most likely responsible for dispersing the cells that were seen in the E9.5 “hot spots”. Therefore, using the *ex vivo* culturing system we were able to see the vascular remodeling that is occurring between E8.5 and E10.5. This increase in complexity of vasculature branching and architecture is accompanied by an increase in the number of LYVE1-derived hematopoietic cells seen in these vessels. At E9.5 there seem to be distinct sites that have a higher density of

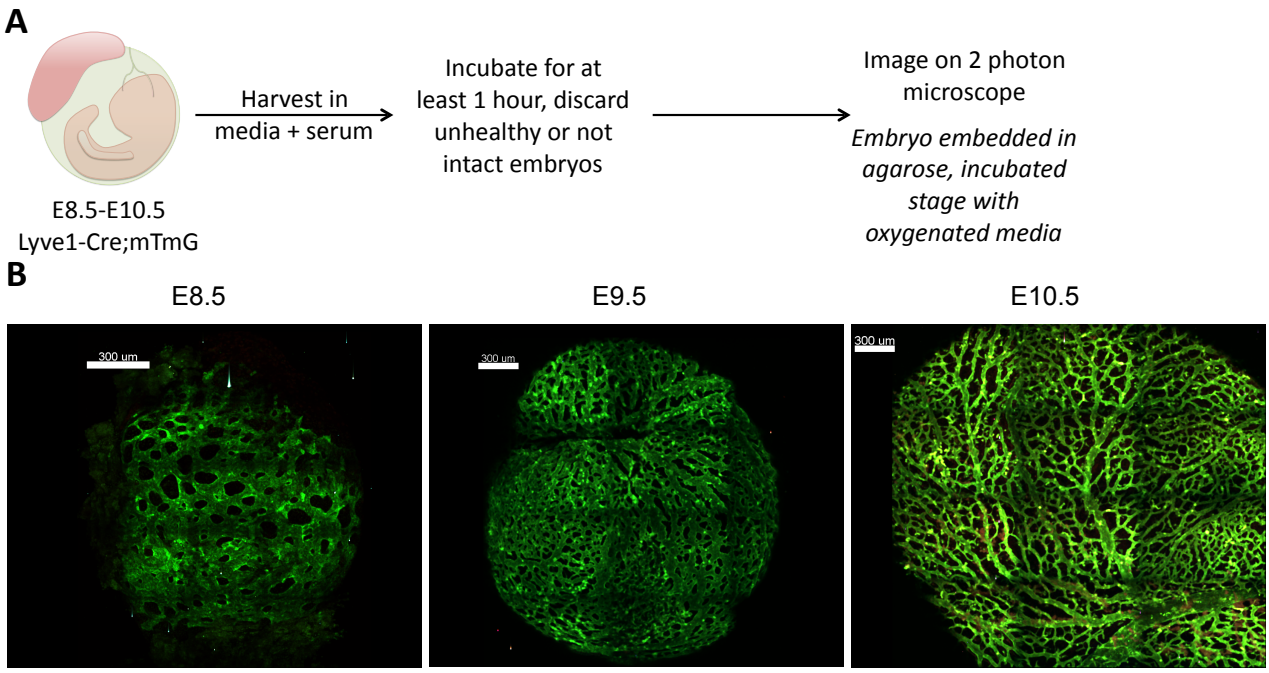

Figure 2.4 Organization of LYVE1-derived cells in the yolk sac
(A) Diagram of *ex vivo* embryo culture system for two photon imaging.
(B) 3D reconstruction of 2-photon-microscopy-derived montage image of E8.5, E9.5, and E10.5 yolk sacs from Lyve1-Cre;mTmG embryos shows the hierarchical network of vasculature (green fluorescence) and organization of LYVE1-derived cells (bright green) within the vessels; scale bar = 200 µm. Magnified areas showing boxed regions, highlighting hematopoietic clusters (1 & 2) and isolated cells (3 & 4); scale bar = 20 µm.

labeled hematopoietic cells, but by E10.5 these are all distributed throughout the YS vasculature.

Embryos were imaged overnight during the *ex vivo* culturing and the videos were analyzed to look at cell behaviors for the duration of time that the embryos remained viable. It is important to note that there are many hematopoietic cells in circulation that are traveling too fast to be captured by 2 photon imaging and that we are only looking at definitive hematopoietic cells as LYVE1 labeling bypasses primitive hematopoiesis. The LYVE1-derived hematopoietic cells in the YS vasculature are highly motile and very few remain in one place. Although most do not move very fast (as measured by the instantaneous velocity and mean track speed), they are constantly surveying the environment by coming into contact with endothelial cells and other hematopoietic cells (**Figures 2.5A and SM2.3**). Despite the fact that most of these cells are constantly moving, and perhaps because of the extensive evaluation of their environment, these cells do not move very far from where they are found (as measured by their displacement, **Figure 2.5A**). Hematopoietic cells in the E10.5 embryos move faster and farther than those in E9.5 embryos.

Emergence, or budding, of hematopoietic cells from endothelial cells has been visualized in the AGM region of zebra fish embryos(Bertrand et al. 2010), but these events have yet to be seen in live, intact murine embryos. Using this novel *ex vivo* culturing system, we were able to visualize the emergence and budding of LYVE1-labeled hematopoietic cells from labeled endothelial cells in the YS of intact Lyve1-Cre;mTmG embryos (**Figures 2.5B, 2.5D, and SM2.4**). These emergence events were confirmed and quantified by measuring the amount of fluorescence at a given area where a budding or emergence event was observed (**Figure 2.5C**).

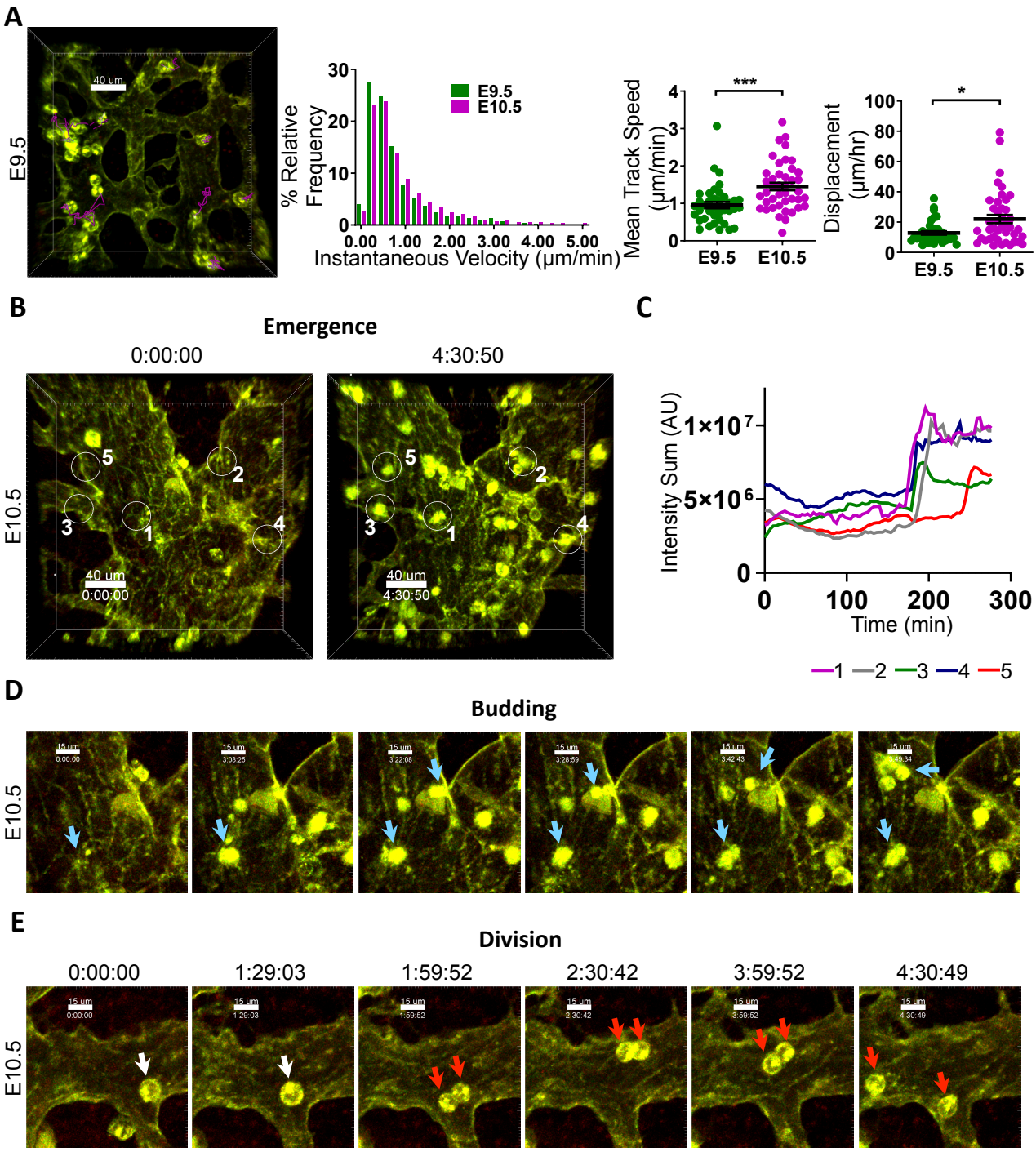
A
E9.5
40 um
% Relative Frequency
E9.5
E10.5
Instantaneous Velocity (µm/min)
Mean Track Speed (µm/min)
***
Displacement (µm/hr)
*
B
Emergence
0:00:00
4:30:50
E10.5
40 um
C
Intensity Sum (AU)
Time (min)
1 2 3 4 5
D
Budding
E10.5
E
Division
0:00:00
1:29:03
1:59:52
2:30:42
3:59:52
4:30:49
E10.5

Figure 2.5 *Ex vivo* culture of Lyve1Cre;mTmG embryos reveals that labeled hematopoietic cells exhibit dynamic behaviors in the yolk sac vasculature

Lyve1Cre;mTmG embryos are carefully removed and mounted in low-melt agarose for 2 photon-imaging at E9.5-10.5. (A) Representative image showing round LYVE1-labeled cells (green) and their tracks (magenta) within the vessels from live embryo imaging. Scale bar = 40 µm. Data from 4 imaging sessions are pooled, green symbols for E9.5 and magenta symbols for E10.5. Instantaneous 3D velocity histograms at E9.5 and E10.5, arrows point to median values (mean ± SEM, 0.81 ± 0.01 vs 1.04 ± 0.02 µm/min, for E9.5 and E10.5 respectively, $p < 0.0001$, Mann Whitney test, $n > 1967$ velocity measurements). Scatter plot showing mean track speed, black bars indicate mean ± SEM (0.95 ± 0.08 and 1.45 ± 0.09 µm/min, for E9.5 and E10.5 respectively, $p = 0.02$, Mann Whitney test, $n > 38$ tracks). Net displacement in one hour, black bars indicate mean ± SEM (12.83 ± 1.15 and 22.03 ± 2.70 µm/hour, for E9.5 and E10.5 respectively, $p = 0.02$, Mann Whitney test, $n > 38$ tracks).

(B) Images of the yolk sac at the beginning and 4h30min after 2 photon imaging. White circles mark regions of emergence of a LYVE1-derived cells from the endothelium; Scale bar = 40 µm, time is shown in h:min:sec. Quantification of florescence intensity in cuboid ROI (24.4 µm x 24.4 µm x 80 µm) over time for five emergence areas in E.

(C) Examples of LYVE1-derived cells budding from LYVE1-labeled endothelium, close-up sequences over 3h49min, blue arrows point to LYVE1-derived cells that bud off from labeled endothelium.

(D) Example of in intravascular division of LYVE1-labeled cells, close-up sequences over 4h30 min; white arrows point to a rounded, enlarged LYVE1-labeled cell undergoing mitosis, red arrows point to daughter cells.

An emergence event corresponds to a sharp increase in fluorescence intensity, or rise time, and this increase is maintained for a longer duration of time as compared to a cell that is passing through in that particular field of view. This rise time is also seen to be the same for all of the emergence events that we quantified in this way, confirming that these are true emergence events; however, we cannot determine whether these emerging cells are pre-HSCs, progenitors, or some other type of hematopoietic cell.

The labeled hematopoietic cells also contribute to establishing the number of hematopoietic cells in the developing embryo as these cells were also seen to be dividing rapidly (**Figures 2.5E and SM2.5**). The number of divisions is fairly high as the evidence by the noticeable increase in the number of cells in a field of view when comparing the beginning of an imaging session to the end (**Figure 2.5B**). This is a strong indication that they YS compartment is filled by cells that have derived from other hematopoietic cells as opposed to unique emergence events.

Discussion

The origin of hematopoietic cells during embryonic development is an active area of investigation in the hematopoiesis field. Hemogenic endothelium is a consensus source of these cells and here we have shown that a specialized subset of hemogenic endothelium that is labeled by LYVE1 gives rise to about a third of the definitive HSC pool.

LYVE1-derived cells are seen to contribute to each definitive wave of hematopoiesis in the embryo and to the adult HSC pool. These adult cells are functional HSCs in that they exhibit robust engraftment when transplanted into lethally irradiated recipients. This is true of the

embryonic LYVE1-derived populations as well. When transplanted at the native LYVE1-derived to non-LYVE1-derived ratios, HSCs found at E14.5 are able to reconstitute the recipient blood system and reach a level of HSC homeostasis that has the same percentages of LYVE1-derived and non-LYVE1-derived HSCs as the adult Lyve1Cre;mTmG BM. This shows that when these two different populations of HSCs are in direct competition with one another, there is a cell or system intrinsic ratio that governs the amount of each cell type that constitutes the whole population. Although this could also be stochastic, it is more likely that there is some stability inherent to the system.

The two populations of pre-HSCs in the embryo, LYVE1-derived and not, appear different in terms of their maturation kinetics. The non-LYVE1-derived cells seem to mature faster as evident by their engraftment capabilities at E10.5 regardless of what tissue they are found in. In contrast, the LYVE1-derived cells are only capable of engraftment at E10.5 if they are found in the AGM. This leads us to believe the majority of these cells take longer to mature as they are capable of engraftment from almost any tissue by E11.5. Our data implies that these cells may need to receive signals from the intra-embryonic environment in order to fully mature and become capable of engraftment. This may be particularly true for the LYVE1-derived cells found in the YS. This tissue has the highest abundance of LYVE1-derived phenotypic pre-HSCs and LYVE1-labeled endothelium; however, because the cells found here are not capable of engraftment at E10.5 it leads us to speculate that these cells need to enter circulation and migrate into the embryo, most likely to the FL or AGM, to receive maturation signals to become functional. It is possible that the cells in the AGM have already migrated there from other tissues, but our embryo culture experiments seem to suggest that a lot of these cells stay within

their tissue of origin. Additionally, these transplanted cells were not sorted, so the identity of the engrafting cell type is not known. However, we recently published that all pre-HSC activity comes from the CD11a- KLS population and so it is reasonable to assume that this is the cell type that is engrafting.

We were able to observe the behavior of these LYVE1-labeled cells in the YS utilizing our novel *ex vivo* embryo culture system. This is the first time that this has been done in an intact and living murine embryo. The labeled cells are non-meandering and dynamic, but with a confined motility. The movement of these cells is systematic. If they were randomly migrating then their displacement would be at a rate of about 60 μm per hour, but it is much lower than that indicating that they don't move far from where they originated. Instead, the LYVE1-derived cells that we observed were seen to be continuously interacting with the endothelial cells from which they came. Hematopoietic cells in the E10.5 embryos move faster, with a 50% increase in mean velocity from E9.5 to E10.5, and farther than E9.5 embryos. This is likely because circulation is more robust and environmental signals promote migration and subsequent maturation of these cells. At E9.5 the LYVE1-derived cells are still emerging and they are actively surveying the environment as suggested by their constant movement. These cells are perhaps aiding in signaling for vasculature remodeling and emergence of additional hematopoietic cells. Alternatively, they could be stuck to there due their VE-Cadherin expression and need to downregulate that before they can be released into circulation. E10.5 cells are also actively dividing in order to expand the hematopoietic pool and fulfill the needs of the growing embryo. It is important to note that we are only looking at GFP+ cells and that the

non-LYVE1-derived, Tomato+ cells may behave differently. This would not be surprising given that the Tomato+ cells contain the engraftable pre-HSC population at this stage.

These observations were made with minimal manipulation to the intact and developing embryo and are therefore a reliable reflection of what occurs *in utero*. Serum is added the media during the initial embryo harvesting and incubation and only oxygenated media (no serum) is used during imaging. This is the most natural way to look at hematopoiesis during embryonic development because there is no artificial addition of growth factors or cytokines. For future studies, it would be important to add factors to either promote or inhibit hematopoiesis. In this way we could determine if these cells can be manipulated this *ex vivo* culture system. This would allow us to mature or direct hematopoiesis in a certain way in hopes of improving transplantation. These studies may have implications on the use of cord blood as a source for blood and marrow transplants as they may lead to insights on how to mature and expand these cells to increase the efficiency and effectiveness of this donor cell source.

The findings in this study and our previous studies suggest that LYVE1 identifies a population of hemogenic endothelial cells that give rise to definitive HSCs. There is a large population of LYVE1-labeled endothelium and pre-HSCs in the YS; however, these cells need to migrate to other tissues to mature. There is also a rare population of LYVE1-labeled endothelium in the AGM. The cells found in this tissue are the first of this subset of pre-HSCs that appear capable of engraftment. Because LYVE1 labels endothelial cells in both the AGM and the YS it is not possible to determine if one or both of these tissues is the source of the LYVE1-derived HSCs. The findings of a recent study using the Lyve1-Cre system would suggest that the cells in the AGM are the source of LYVE1-derived HSCs, but that these cells need to be

matured (as demonstrated *in vitro*). If this is true, then the rarity of the LYVE1 labeled endothelial cells in the AGM would suggest that these GFP+ cells are highly enriched for hemogenic endothelium.

In this study, we have identified a particular subset of the HSC pool and future studies can be done to determine if, and how, LYVE1-derived HSCs differ from the rest of the HSC population. Insights into this question may help to inform about the heterogeneity of the HSC pool. If one population is more resilient or more prone to certain disease states, that would have a substantial impact on the clinical therapies. It would allow for a more targeted approach for treatment by identifying helpful or harmful HSC subsets. It could also be informative for blood and marrow transplantation if depletion of a certain subset of cells would increase engraftment, enhance graft versus leukemia, or prevent graft versus host disease. Our data suggests that both LYVE1-derived and non-LYVE1-derived cells have equal engraftment potential, but the other avenues would be an interesting area of future studies. The presence of certain subsets of HSCs and the contribution of LYVE1-derived endothelium to these cells can also impact the study of how to differentiate HSCs from iPSCs. These findings provide further evidence that there are multiple sources of HSCs and that these cells have different origins. Whether we want to move forward and recapitulate the heterogeneity of the HSC pool by deriving the different subsets of HSCs, or if there should be a focus on the derivation of just one particular subset, is something that still needs to be investigated and will have a significant impact on the field.

Materials and Methods

Mouse models

All mice were obtained from Jackson Laboratories unless otherwise noted. Animals were housed in 12 hour light and dark cycles in the Gross Hall and Medical Sciences A vivarium facilities at the University of California, Irvine. All mice were given open access to food and water. The International Animal Care and Use Committee (IACUC) and the University Laboratory Animal Resources (ULAR) of the University of California, Irvine approved all animal procedures. The strains of mice that were used in this study were Lyve1-Cre (012601), mTmG (007576), C57 Bl/6 (00664), NSG (005557), and TM5 ($Rosa^{CFP/CFP}$, donated by Dr. Irving Weissman).

Immunofluorescence

Whole mount embryo images were taken with a Nikon SMZ1500 Dissecting Microscope and embryo sections were imaged using the Olympus FV3000 Confocal Scanning Microscope.

Antibody staining

See table 2.1 for the antibodies used in flow cytometry and immunofluorescence.

Cell processing

Briefly, embryos were dissected into their different tissues of interest and single cell suspensions were created by incubating the tissues in collagenase IV (1 mg/mL in DMEM) for 45 minutes at 38°C . The cells were then washed with a solution of PBS and 2% FBS to remove

any residual collagenase. The cells were then ready for transplantation or staining for flow cytometry analysis/FACS.

Bone marrow was harvested via flushing or crushing of the femur and tibia. Peripheral blood was collected into EDTA via the tail vein. Red blood cells were lysed using 1X ACK Lysis Buffer and then washed with a solution of PBS and 2% FBS to remove any residual lysis buffer. The cells were then ready for transplantation or staining for flow cytometry analysis/FACS.

Adult and neonatal transplantation

Recipient mice were irradiated at 190-200 cGy for NSG neonates and 825 cGy for C57 Bl/6 adults using a cabinet irradiator. Donor cells were delivered via facial vein injection for neonatal recipients or retro orbital injection for adult reciepients. Recipeient mice were bled to check for granulocyte chimerism and bone marrow was harvested to determine HSC chimerism by flow cytometry analysis.

Flow cytometry

Flow cytometry analysis was done on the BD LSR II or BD Fortessa X20 and data was analyzed using FlowJo. Sorting was done on the BD FACS Aria II.

Ex vivo embryo culture

Embryos were dissected in warm media (DMEM/F12 +L Glutamine + 15mM HEPES, Gibco 11330-032, containing Pen/Strep, Sodium Pyruvate, and 10% FBS) taking care not to puncture

the YS. The embryos were incubated for at least one hour and then checked for viability (robust heart beat and circulation, no tears in the YS).

2 photon microscopy

Images were acquired using a custom-built two-photon microscope based on an Olympus BX51 upright microscope frame, fitted with a motorized Z-Deck stage (Prior) and a Nikon 25x objective (CFI75 Apo L, water-immersion, NA = 1.1, WD = 2.0 mm). A tunable femtosecond laser (Chameleon Ultra-II or Vision-II, Coherent) set to 920 nm to excite mGFP and mTomato. Dichroic filters (495 nm and 538 nm) were arranged in series to collect signal in blue (SHG), green (mGFP), and red (mTomato) photomultiplier channels as described in previously (Matheu et al. 2015). Embryos were carefully harvested and embedded in 2.5% low gelling temperature agarose in PBS (Sigma A9414). For *montage imaging*, several 3D image stacks (350 µm X 350 µm X 500 µm) were collected with XYZ voxel size of 0.68 µm x 0.68 µm x 5 µm using image acquisition software (Slidebook, Intelligent Imaging Innovations). 3D Image blocks were stitched using Slidebook montage module. Imaris version 9.2.1 (Bitplane) was used for rendering and visualization, final image size is 2 mm X 2 mm X 0.5 mm. For *live imaging,* agarose embedded embryo were immediately placed in a custom-built heated and oxygenated imaging chamber maintained at 37˚ ± 0.5˚C using a thermocouple-based temperature sensor placed next to the tissue. A peristaltic heating system (Warner Instruments) provided continuous superfusion of warm medium (DMEM/F12 +L Glutamine + 15mM HEPES, Gibco 11330-032, containing Pen/Strep and Sodium Pyruvate) bubbled with medical grade Carbogen gas (Airgas, 95% O2 / 5% CO2). 3D image stacks of X=250 µm, Y=250 µm, and Z=80 µm (voxel size 0.24 µm x 0.24 µm

x 4 μm) were sequentially acquired at 3.5 min intervals for cell tracking. Embryos were oriented with the yolk sac facing the media dipping objective.

All 2P-derived images displayed in the manuscript are maximum intensity projections through the Z-axis. Median filtered and histogram adjusted 4D data sets enabled detection and tracking of LYVE1^{+} cells using Imaris (Bitplane USA, Concord, MA). A combination of manual and automatic tracking was used to generate cell tracks; accuracy was confirmed by careful visual inspection of 3D-rotated images. X, Y, and Z coordinates of the tracks were used to calculate instantaneous 3D velocity, mean track speed, and 1hr displacement. Imaris Animation and Vantage modules were used to generate time-lapse movies. Cuboid regions of interest (ROI, 24.4 μm x 24.4 μm x 80 μm) of 47,628.8 μm^3 were drawn using Imaris Surfaces module and intensity sum over time is plotted in to analyses emergence events.

Author Contributions

Conceptualization, M.A.I. and Y.G.; Methodology, M.A.I., Y.G., S.O, A.K.S, A.K., I.P., M.D.C; Investigation, Y.G., S.O., R.B., S.P., A.P., F.C.; Writing – Original draft, Y.G. and M.A.I. Writing – Review and Editing, S.O., M.D.C., H.K.A.M Visualization, Y.G., S.O., M.A.I.

Antibody	Fluorochrome	Clone	Dilution	Manufacturer	Catalog
CD11a	PE	M17/4	1:200	BioLegend	101107
CD11a	Biotin	M17/4	1:200	BioLegend	101103
CD11b	APC	M1/70	1:200	BioLegend	101212
CD11b	APC-eFluor 780	M1/70	1:200	eBioscience	47-0112-82
CD16/32 (FcyR)	PE	93	1:200	BioLegend	101307
CD19	PerCP-Cyanine 5.5	eBio1D3	1:200	eBioscience	45-0193-82
CD27	APC	LG.7F9	1:200	eBioscience	17-0271-82
CD27	APC/Cy7	LG.3A10	1:100	BioLegend	124226
CD3	PE/Cy7	17A2	1:100	BioLegend	100220
CD31	PerCP-eFluor 710	390	1:200	eBioscience	46-0311-80
CD31	Alexa Fluor 647	MEC13.3	1:200	BioLegend	102516
CD34	eFluor660	RAM34	1:50	Invitrogen	50-0341-82
CD41	APC-eFluor 780	MWReg30	1:400	eBioscience	47-0411-82
CD43	APC	S7	1:200	BD Biosciences	560663
CD45	APC/Cy7	30-F11	1:200	BioLegend	103116
CD45	Alexa Fluor 700	30-F11	1:200	BioLegend	103128
CD48	Brilliant Violet 421	HM48-1	1:200	BioLegend	103427
ckit	APC-eFluor 780	2B8	1:200	eBioscience	47-1171-82
ckit	Brilliant Violet 421	2B8	1:200	BioLegend	105827
ckit	PE/Cy7	2B8	1:200	BioLegend	105814
ckit	APC	ACK2	1:200	BioLegend	135108
EPCR	PerCP-eFluor 710	eBio1560	1:200	eBioscience	46-2012-82
GFP	Rabbit	—	1:2000	Abcam	ab6556
Gr1	Alexa Fluor 700	RB6-8C5	1:200	BioLegend	108422
Gr1	PE	RB6-8C5	1:200	Tonbo	50-5931-UO25
LYVE1	eFluor660	ALY7	1:50	Invitrogen	50-0443-80

NK1.1	PE	PK136	1:200	BioLegend	108708
NK1.1	APC	PK136	1:200	BioLegend	108710
Sca	PE/Cy7	E13-161.7	1:100	BioLegend	122514
SLAM	PE	TC15-12F12.2	1:100	BioLegend	115904
Streptavidin	Qdot605	—	1:200	Invitrogen	Q10103MP
Ter119	PE/Cy5	TER-119	1:200	BioLegend	116210
VE Cadherin	Biotin	BV13	1:200	BioLegend	138008

Table 2.1 Antibodies

References

Alvarez-Silva, M., P. Belo-Diabangouaya, J. Salaun, and F. Dieterlen-Lievre. 2003. “Mouse Placenta Is a Major Hematopoietic Organ.” *Development* 130: 5437–44.

Auerbach, Robert, Hua Huang, and Lisheng Lu. 1996. “Hematopoietic Stem Cells in the Mouse Embryonic Yolk Sac.” *Stem Cells* 14 (3): 269–80. https://doi.org/10.1002/stem.140269.

Batsivari, Antoniana, Stanislav Rybtsov, Celine Souilhol, Anahi Binagui-Casas, David Hills, Suling Zhao, Paul Travers, and Alexander Medvinsky. 2017. “Understanding Hematopoietic Stem Cell Development through Functional Correlation of Their Proliferative Status with the Intra-Aortic Cluster Architecture.” *Stem Cell Reports* 8 (6): 1549–62. https://doi.org/10.1016/j.stemcr.2017.04.003.

Bertrand, Julien Y., Neil C. Chi, Buyung Santoso, Shutian Teng, Didier Y R Stainier, and David Traver. 2010. “Haematopoietic Stem Cells Derive Directly from Aortic Endothelium during Development.” *Nature* 464 (7285): 108–11. https://doi.org/10.1038/nature08738.

Dieterlen-Lièvre, Françoise. 1998. “Hematopoiesis: Progenitors and Their Genetic Program.” *Current Biology* 8 (20): 727–30. https://doi.org/10.1016/s0960-9822(98)70460-9.

Ganuza, Miguel, Ashley Chabot, Xing Tang, Wenjian Bi, Sivaraman Natarajan, Robert Carter, Charles Gawad, Guolian Kang, Yong Cheng, and Shannon McKinney-Freeman. 2018. “Murine Hematopoietic Stem Cell Activity Is Derived from Pre-Circulation Embryos but Not Yolk Sacs.” *Nature Communications* 9 (1). https://doi.org/10.1038/s41467-018-07769-8.

Gekas, Christos, Francoise Dieterlen-Lièvre, Stuart H. Orkin, and Hanna K.A. Mikkola. 2005. “The Placenta Is a Niche for Hematopoietic Stem Cells.” *Developmental Cell* 8 (3): 365–75. https://doi.org/10.1016/j.devcel.2004.12.016.

Ghiaur, Gabriel, Michael J. Ferkowicz, Michael D. Milsom, Jeff Bailey, David Witte, Jose A. Cancelas, Mervin C. Yoder, and David A. Williams. 2008. “Rac1 Is Essential for Intraembryonic Hematopoiesis and for the Initial Seeding of Fetal Liver with Definitive Hematopoietic Progenitor Cells.” *Blood* 111 (7): 3322–30. https://doi.org/10.1182/blood-2007-09-078162.

Inlay, Matthew A., Thomas Serwold, Adriane Mosley, John W. Fathman, Ivan K. Dimov, Jun Seita, and Irving L. Weissman. 2014. “Identification of Multipotent Progenitors That Emerge Prior to Hematopoietic Stem Cells in Embryonic Development.” *Stem Cell Reports* 2 (4): 457–72. https://doi.org/10.1016/j.stemcr.2014.02.001.

Johnson, G. R., and M. A.S. Moore. 1975. “Role of Stem Cell Migration in Initiation of Mouse Foetal Liver Haemopoiesis.” *Nature* 258 (5537): 726–28. https://doi.org/10.1038/258726a0.

Kumaravelu, Parasakthy, Lilian Hook, Aline M. Morrison, Jan Ure, Suling Zhao, Sergie Zuyev, John Ansell, and Alexander Medvinsky. 2002. “Quantitative Developmental Anatomy of Definite Haematopoietic Stem Cells/Long-Term Repopulating Units (HSC/RUs): Role of the Aorta-Gonad-Mesonephros (AGM) Region and the Yolk Sac in Colonisation of the Mouse Embryonic Liver.” *Development* 129 (21): 4891–99.

Lee, Lydia K., Yasamine Ghorbanian, Wenyuan Wang, Yanling Wang, Yeon Joo Kim, Irving L. Weissman, Matthew A. Inlay, and Hanna K.A. Mikkola. 2016. “LYVE1 Marks the Divergence of Yolk Sac Definitive Hemogenic Endothelium from the Primitive Erythroid Lineage.” *Cell Reports* 17 (9): 2286–98. https://doi.org/10.1016/j.celrep.2016.10.080.

Lux, Christopher T., Momoko Yoshimoto, Kathleen McGrath, Simon J. Conway, James Palis, and Mervin C. Yoder. 2008. “All Primitive and Definitive Hematopoietic Progenitor Cells Emerging before E10 in the Mouse Embryo Are Products of the Yolk Sac.” *Blood* 111 (7): 3435–38. https://doi.org/10.1182/blood-2007-08-107086.

Matheu, Melanie P., Shivashankar Othy, Milton L. Greenberg, Tobias X. Dong, Martijn Schuijs, Kim Deswarte, Hamida Hammad, Bart N. Lambrecht, Ian Parker, and Michael D. Cahalan. 2015. “Imaging Regulatory T Cell Dynamics and Suppression of T Cell Priming Mediated by CTLA4.” *Nature Communications* 6: 6219. https://doi.org/10.1111/mec.13536.Application.

McGrath, Kathleen, and James Palis. 2005. “Hematopoiesis in the Yolk Sac: More than Meets the Eye.” *Experimental Hematology* 33 (9): 1021–28. https://doi.org/10.1016/j.exphem.2005.06.012.

MD, Muzumdar, Tasic B, Miyamichi K, Li L, and Luo L. 2006. “A Global Double-Fluorescent Cre Reporter Mouse.” *Genesis* 224 (September): 219–24. https://doi.org/10.1002/dvg.

Medvinsky, Alexander, and Elaine Dzierzak. 1996. “Definitive Hematopoiesis Is Autonomously Initiated by the AGM Region.” *Cell* 86 (6): 897–906. https://doi.org/10.1016/S0092-8674(00)80165-8.

Medvinsky, Alexander L., and Elaine A. Dzierzak. 1998. “Development of the Definitive Hematopoietic Hierarchy in the Mouse.” *Developmental & Comparative Immunology* 22 (3): 289–301. https://doi.org/10.1016/S0145-305X(98)00007-X.

Medvinsky, Alexander L., Nina L. Samoylina, Albrecht M. Müller, and Elaine A. Dzierzak. 1993. “An Early Pre-Liver Intraembryonic Source of CFU-S in the Developing Mouse.” *Nature* 364 (6432): 64–67. https://doi.org/10.1038/364064a0.

Mikkola, H.K.A., C. Gekas, S. Orkin, and F. Dieterlen-Lievre. 2005. “Placenta as a Site for Hematopoietic Stem Cell Development.” *Experimental Hematology* 33 (9): 1048–54. https://doi.org/10.1016/j.exphem.2005.06.011.

Moore, Malcolm A.S., and Donald Metcalf. 1970. “Ontogeny of the Haemopoietic System: Yolk Sac Origin of In Vivo and In Vitro Colony Forming Cells in the Developing Mouse Embryo.” *British Journal of Haematology* 18 (3): 279–96. https://doi.org/10.1111/j.1365-2141.1970.tb01443.x.

Moore, Malcolm A.S., and J Owen. 1967. “Stem-Cell Migration in Developing Myeloid and Lymphoid Systems.” *Lancet* 11: 658–59.

Müller, Albrecht M., Alexander Medvinsky, John Strouboulis, Frank Grosveld, and Elaine Dzierzakt. 1994. “Development of Hematopoietic Stem Cell Activity in the Mouse Embryo.” *Immunity* 1 (4): 291–301. https://doi.org/10.1016/1074-7613(94)90081-7.

Ottersbach, Katrin, and Elaine Dzierzak. 2005. “The Murine Placenta Contains Hematopoietic Stem Cells within the Vascular Labyrinth Region.” *Developmental Cell* 8 (3): 377–87. https://doi.org/10.1016/j.devcel.2005.02.001.

Palis, J. 2001. “Yolk-Sac Hematopoiesis The First Blood Cells of Mouse and Man.” *Experimental Hematology* 29 (8): 927–36. https://doi.org/10.1016/S0301-472X(01)00669-5.

Pham, Trung H.M., Peter Baluk, Ying Xu, Irina Grigorova, Alex J. Bankovich, Rajita Pappu, Shaun R. Coughlin, Donald M. McDonald, Susan R. Schwab, and Jason G. Cyster. 2010. “Lymphatic Endothelial Cell Sphingosine Kinase Activity Is Required for Lymphocyte Egress and Lymphatic Patterning.” *Journal of Experimental Medicine* 207 (1): 17–27. https://doi.org/10.1084/jem.20091619.

Seita, Jun, Debashis Sahoo, Derrick J. Rossi, Deepta Bhattacharya, Thomas Serwold, Matthew A. Inlay, Lauren I.R. Ehrlich, John W. Fathman, David L. Dill, and Irving L. Weissman. 2012. "Gene Expression Commons: An Open Platform for Absolute Gene Expression Profiling." *PLoS ONE* 7 (7): 1–11. https://doi.org/10.1371/journal.pone.0040321.

Yoder, Mervin C., and Kelly Hiatt. 1998. "Engraftment of Embryonichemato- Poietic Cells in Conditioned Newborn Recipients." *Blood* 89: 2176–83.

Yoder, Mervin C., Kelly Hiatt, Parmesh Dutt, Pinku Mukherjee, David M. Bodine, and Donald Orlic. 1997. "Characterization of Definitive Lymphohematopoietic Stem Cells in the Day 9 Murine Yolk Sac." *Immunity* 7 (3): 335–44. https://doi.org/10.1016/S1074-7613(00)80355-6.

Yoder, Mervin C., Kelly Hiatt, and Pinku Mukherjee. 1997. "In Vivo Repopulating Hematopoietic Stem Cells Are Present in the Murine Yolk Sac at Day 9.0 Postcoitus." *Proc. Natl. Acad. Sci.* 94: 6776–80.

CHAPTER THREE

Lineage Bias Seen in the Lyve1Cre Model is Specific to the Reporter System Used

Yasamine Ghorbanian, Shailey Patel, Angela Nguyen, Rocio Barahona, Matthew A. Inlay

Sue and Bill Gross Stem Cell Research Center, Dept. of Molecular Biology & Biochemistry at UCI

Abstract

Lineage tracing using Cre-LoxP recombination is a common technique used in developmental biology to study cell ontogeny. Here we have found that phenotypes that are uncovered using this method are dependent on the reporter line used. A T cell bias is revealed using the mTmG reporter system when studying the lineage output of LYVE1-labeled hematopoietic stem cells. This bias, which is not developmentally derived, remains after exposure to irradiation stress indicating that it is intrinsic and homeostatically maintained. However, different biases are seen when using Confetti or Ai14 reporter systems. These findings emphasize the necessity to validate observed phenotypes in multiple reporter systems to ensure reproducibility.

Introduction

Cre-LoxP recombination is a widely used technique to address many different scientific questions. It is often utilized to generate conditional knockouts that may otherwise prove to be lethal if done constitutively. Lineage tracing studies make use of this technique as well. In these studies, a reporter mouse strain that contains loxP sites governing the expression of a colorimetric marker (ie LacZ or fluorescent protein expression) is bred to a mouse with a specific gene driven Cre. The resulting offspring will have labeled the cells that express(ed) that specific gene or are the progeny of such cells. In this way, specific populations of cells can be labeled and tracked.

We have previously identified a subset of hematopoietic stem cells (HSCs) that are LYVE1-derived (Lee et al. 2016). In this study we sought to determine if there are any biases in

the lineage output of these LYVE1-derived HSCs. We found that different reporter lines revealed different biases in this lineage tracing system. These biases were cell intrinsic and were not developmentally derived. This study highlights the importance of the use of different reporter strains in order to validate the occurrence of observed phenotypes.

Results

A T cell bias is revealed in the mTmG system

In order to determine if there is a bias in the lineage output of LYVE1-derived cells, we utilized the Lyve1-Cre;mTmG lineage tracing system that was used in our previous studies (Lee et al. 2016; Pham et al. 2010; MD et al. 2006). In this system, all cells are initially Tomato+. LYVE1-expressing cells and their progeny become GFP+ as a result of Cre activation and subsequent excision of the Tomato cassette. We bled a cohort of Lyve1-Cre;mTmG mice over a period of more than 2 years and analyzed the lineage distribution of the blood system by flow cytometry. There is no change in the contribution of the LYVE1-derived HSCs to the overall blood system as measured by the level of labeling of total CD45 cells (**Figure 3.1Ai**). It has been found that the blood system develops a myeloid bias with age, but this was not reflected in the LYVE1-derived HSCs, as the contribution towards each of these branches is unchanged over time (**Figure 3.1Aii**). However, there was a bias seen within the lymphoid branch. We observed a higher percentage of GFP+ T cells compared to GFP+ B cells (**Figure 3.1Aiii**). It is important to note that there is no defect in the overall lineage distribution in these mice compared to wild type mice, only the distribution of GFP+ lineages was skewed towards T cells. Thus, the LYVE1-derived HSCs appear favorably biased towards the production of T cells at the expense of B

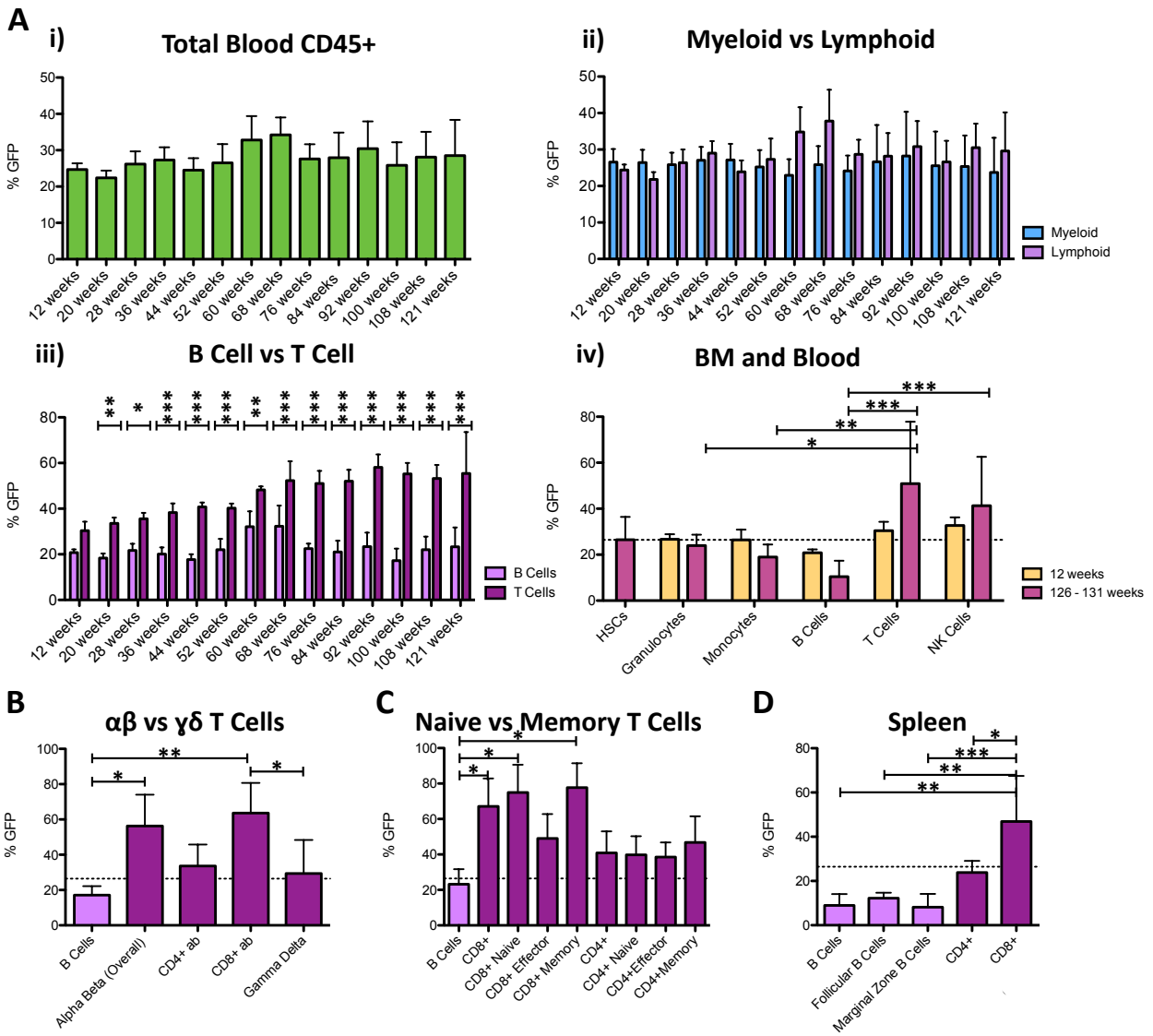

Figure 3.1 LYVE1-derived cells are biased towards the production of cytotoxic T cells in the in the mTmG reporter system
(A) Flow cytometry analysis of GFP labeling of peripheral blood from *Lyve1-Cre;mTmG* mice gated on (i) total CD45+ cells (ii) myeloid (CD45+ CD11b+ NK1.1-) and lymphoid (CD45+ NK1.1- CD11b- Gr1-) populations (iii) B cells (CD45+ NK1.1- CD11b- Gr1- CD3- CD19+) and T cells (CD45+ NK1.1- CD11b- Gr1- CD3+ CD19-) (iv) granulocytes (CD45+ NK1.1- CD11b+ Gr1+), monocytes (CD45+ NK1.1- CD11b+ Gr1-), B cells (CD45+ NK1.1- CD11b- Gr1- CD3- CD19+), T cells (CD45+ NK1.1- CD11b- Gr1- CD3+ CD19-), NK cells (CD45+ NK1.1+), and bone marrow HSCs (Ter119- CD27+ ckit+ Sca+ Slam+ CD34-). Line at mean of HSC labeling. n=5
(B) Analysis of T cell subsets in *Lyve1-Cre;mTmG* peripheral blood at 121 weeks of age by flow cytometry. B cells (CD19+), alpha beta T cells (CD19- TCRαβ+ TCRɣδ-), helper T cells (CD19- TCRαβ+ TCRɣδ- CD4+ CD8-), cytotoxic T cells (CD19- TCRαβ+ TCRɣδ- CD4- CD8+), and gamma delta T cells (CD19- TCRαβ- TCRɣδ+) were analyzed for GFP labeling. Line at mean of HSC labeling. n=4
(C) *Lyve1-Cre;mTmG* peripheral blood analyzed by flow cytometry at 121 weeks. GFP labeling of T cell subsets was determined by gating on B cells (CD19+), and CD4+ or CD8+ naive (CD19- CD44+ CD62L+), effector (CD19- CD44mid CD62L-), or memory T (CD19- CD44high CD62L-) cells. Line at mean of HSC labeling. n=4
(D) Flow cytometry analysis of GFP labeling of *Lyve1-Cre;mTmG* immune populations in the spleen. B cells (CD19+), follicular B cells (CD19+ IgD+ IgM+ CD21+ CD23+), marginal zone B cells (IgD- IgM+ CD21+ CD23-), helper T cells (CD19- CD3+ CD4+ CD8-), and cytotoxic T cells (CD19- CD3+ CD4- CD8+). Line at mean of HSC labeling. n=4
Statistical analysis: (A iv) 2 way ANOVA, (B-D) 1 way ANOVA. *p<0.5, **p<0.01, ***p<0.001

A

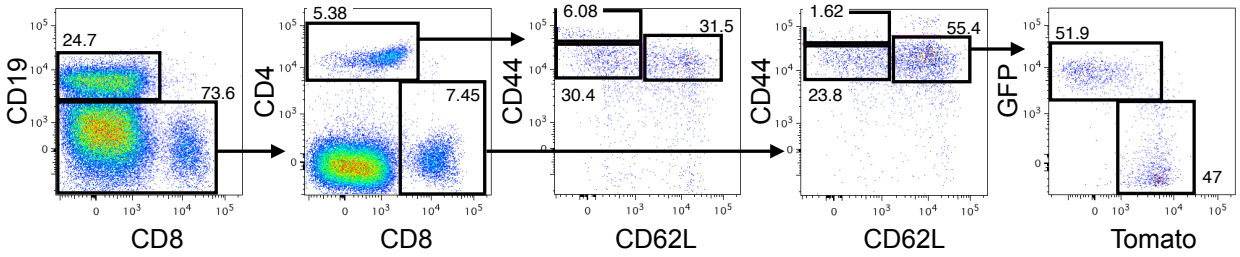

Supplemental Figure 3.1 Representative flow cytometry plots
(A) T cell subset stain on peripheral blood from a Lyve1-Cre;mTmG mouse.

cells. This is also seen when looking at the level of HSC labeling in these mice and comparing that to the level of labeling of the major blood lineages (**Figure 3.1Aiv**). In an unbiased system, the percentage of GFP+ cells of each blood cell type should be identical to the GFP+ percentage of HSCs. This is seen for most cells in the Lyve1-Cre;mTmG system with the exception of the T and B cells (**Figure 3.1Aiv**).

We wanted to know if there was a certain subset of T cells that specifically contributed to the bias. In the peripheral blood, the CD8+ cytotoxic T cells have significantly higher labeling as compared to the B cells and there is no bias seen in the CD4+ helper T cells or the gamma-delta T cells (**Figure 3.1B**). The bias is reflected in both naïve and memory CD8+ T cells (**Figure 3.1C and S3.1**) and it is seen in other lymphoid organs such as the spleen (**Figure 3.1D**).

LYVE1-derived T cell bias does not occur during development

Because B and T cells have a common progenitor, called the common lymphoid progenitor (CLP), we wanted to know at what point in their development they diverge from one another in their expression of LYVE1 (and subsequent GFP labeling). In order to address this, we analyzed labeling of B cells and T cells at their different developmental stages in the bone marrow and thymus respectively. If the bias occurred at some point during development, we would expect a divergence in levels of labeling after the CLP stage as this is when the B and T cell fates are specified. The B cell progenitors remain in the bone marrow for further differentiation, while the T cell progenitors migrate to the thymus to complete their development. Our data suggests that this bias in LYVE1 contribution towards T cell production in the Lyve1-Cre;mTmG system is not a developmental phenomenon as the levels of B and T cell

labeling do not change significantly from the HSCs from which they differentiate until these cells have completed development and have entered the peripheral blood stream (**Figure 3.2A and 3.2B**).

In order to verify that the increase in LYVE1-labeling that is seen in T cells is not due to the re-expression of this gene, we looked at LYVE1 cell surface protein levels by flow cytometry. When compared to a FMO control, there is a shift in the histogram peak for B cells and a small positive bump at the corresponding LYVE1 fluorescence intensity in T cells (**Figure 3.2C**). Given this data, one might conclude that their similar shifts are background and that this would negate any changes in LYVE1-labeling since they are comparable. Another possibility is that since there is a shift as opposed to a small bump in the B cells that this would have a greater impact on LYVE1 labeling by Cre, but this is not what is seen when using the mTmG reporter system.

The bias is not due to an accumulation of a particular subset of T cells with age

Due to the increase in severity of the bias with age, we hypothesized that the bias may be due to the accumulation of GFP+ naïve or memory T cells. We examined the different subsets of T cells by flow cytometry in Lyve1-Cre;mTmG mice at different ages. Specifically, CD4+ or CD8+ naïve/effector/memory populations were examined (**Figure S3.1**) and found that there is no significant accumulation of GFP+ cells within any T cell subset with age (**Figure 3.2D**).

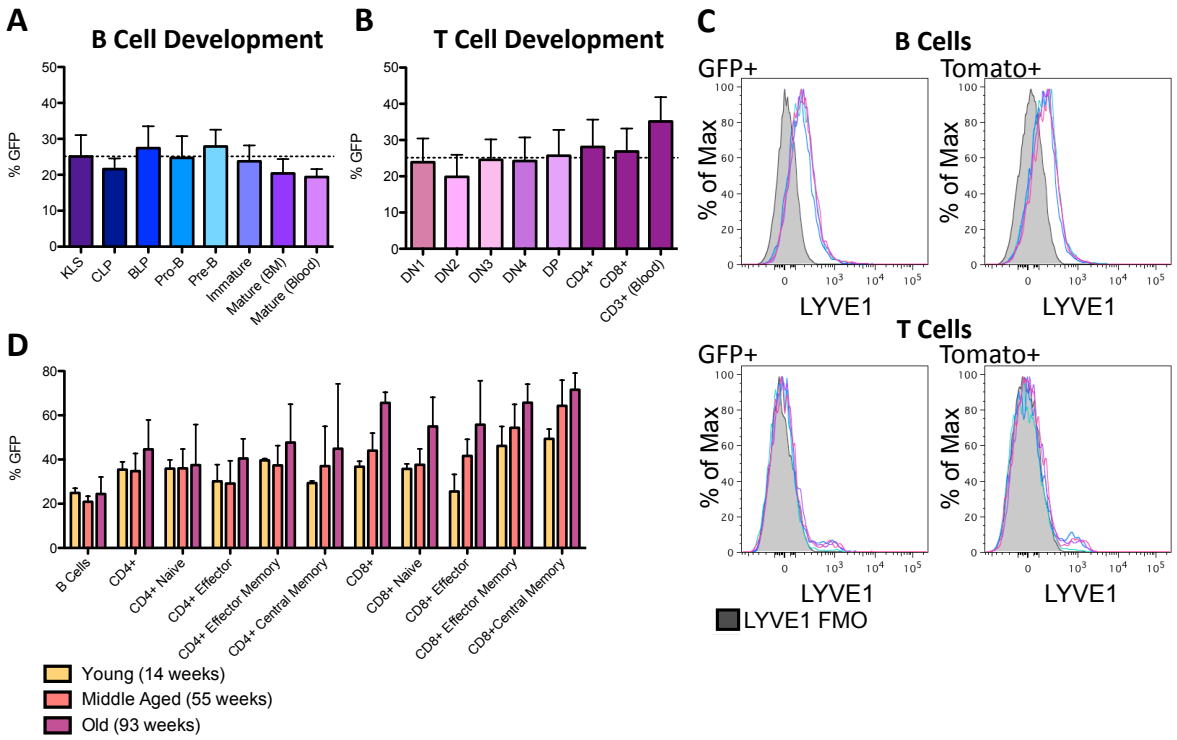

Figure 3.2 LYVE1-derived T cell bias does not occur during development nor is is due to the accumulation of a particular T cell subset in the periphery

(A and B) Flow cytometry on *Lyve1-Cre;mTmG* adults was used to determine the LYVE1 labeling of B cell progenitors in the bone marrow and T cell progenitors in the thymus. The line indicates the mean GFP labeling of HSCs (Ter119- CD27+ ckit+ Sca+ Slam+ CD34-) in these mice. n=5

(C) Cell surface expression of LYVE1 as determined by flow cytometry analysis. The level of LYVE1 expression in B (CD45+ NK1.1- CD11b- Gr1- CD19+ CD3-) and T cells (CD45+ NK1.1- CD11b- Gr1- CD19 CD3+) was compared to a LYVE1 FMO control. n=4

(D) Naive, effector, and memory T cell subsets were assessed by flow cytomtery analysis of different aged *Lyve1-Cre;mTmG* adults. n=3-6 mice per age group

Statistical analysis: (A and B) 1 way ANOVA, (D) 2 way ANOVA

LYVE1-labeled T cell bias is not affected by stress

In order to determine if the T cell bias is homeostatically intrinsic, we stressed the system and evaluated its effects on the GFP+ T and B cell levels. Irradiation results in hematopoietic stress by killing dividing cells. As a result, the surviving HSCs have to reconstitute the blood system and this essentially results in a system reset. We experimentally determined a sublethal dose of irradiation that would cause the most stress (greatest drop in peripheral blood cells) without the need for a BM transplant as a rescue. We then collected 50 µL of blood every week for 5 weeks following the irradiation-induced stress (**Figure 3.3A**). The number of total CD45 cells was quantified to evaluate hematopoietic reconstitution following irradiation stress (**Figure 3.3B**). Total CD45 levels drop significantly in the first two weeks following irradiation compared to baseline, but the system begins to restore itself at three weeks post irradiation. This confirms that the irradiation did eliminate a significant number of peripheral blood cells and as a result, the HSCs differentiated to reconstitute the blood system. When looking at the LYVE1-derived HSC contribution to the T and B cell pools, resetting the system via irradiation stress does not change the ratio of GFP+ T to B cells (**Figure 3.3C**). In fact, in a couple of mice there is an increase in the GFP+ T to B cell ratio indicating exacerbation of the bias. This data suggests that the propensity of these LYVE1-derived HSCs to produce T cells at greater levels than B cells in the Lyve1Cre;mTmG system is innate to the overall hematopoietic compartment.

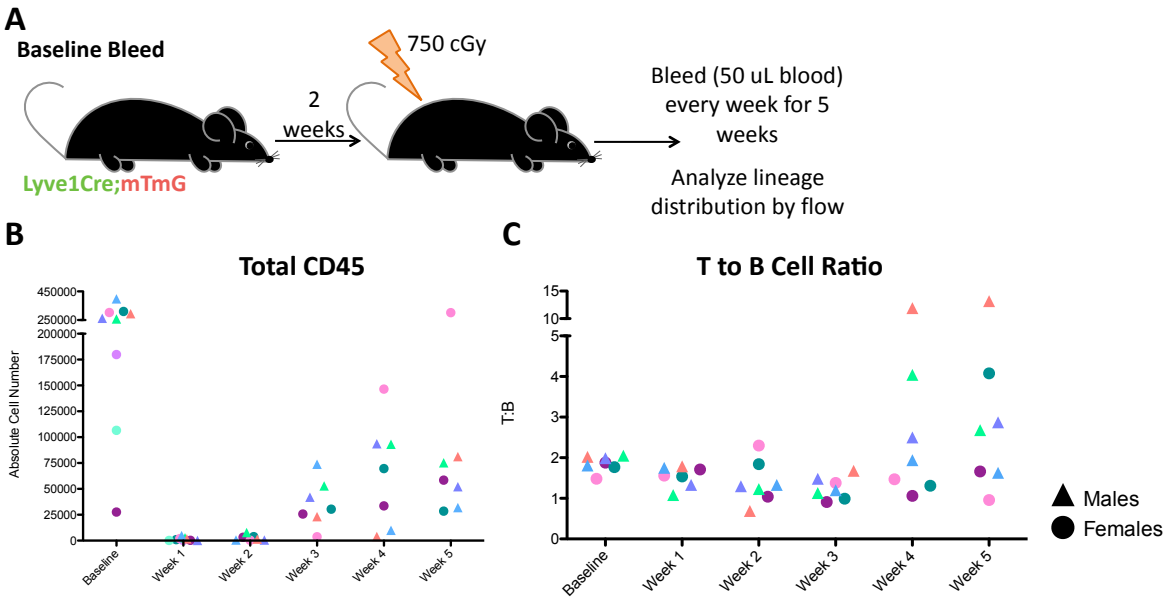

Figure 3.3 Bias is not significantly affected by stress
(A) Experimental setup of hematopoietic stress test via irradiation.
(B) Flow cytometry analysis of total CD45+ hematopoietic cells in *Lyve1-Cre;mTmG* adults that underwent the irradiation stress test. Count bright beads were used to calculate the absolute cell number. n=7
(C) Ratio of GFP+ T (CD45+ NK1.1- CD11b- Gr1- CD19- CD3+) to GFP+ B cells (CD45+ NK1.1- CD11b- Gr1- CD19+ CD3-) in the *Lyve1-Cre;mTmG* adults that underwent the irradiation stress test. n=7
Statistical Analysis: (B and C) 1 and 2 way ANOVA

Other reporter systems do not reveal a T cell bias

To confirm the T cell bias phenotype that is seen in the Lyve1-Cre;mTmG system is not reporter specific, we crossed the Lyve1-Cre mice with two other reporter mouse strains. The first is the Ai14 reporter strain in which all cells are constitutively unmarked, but upon Cre expression become tdTomato+ (**Figure 3.4Ai**). The second is the Confetti reporter system, which is also unmarked prior to Cre expression. Once Cre is expressed, there is a random recombination event that results in nGFP, YFP, mCFP, or RFP expression in each cell and that specific recombination event is permanent and inherited by that cell's progeny (**Figure 3.4Aii**). If the bias is not specific to the mTmG reporter, then we expect the same degree of bias to hold when Lyve1-Cre is crossed to the other reporter strains. However, the overall level of labeling seen in the three systems varied. The Ai14 displayed the most (**Figure 3.4Bi**) and the Confetti has the least labeled CD45+ cells (**Figure 3.4Bii**). The biases seen in both these reporter systems were similar to one another, but were different than what was revealed in the mTmG background. Both systems showed a significant myeloid bias and had a slight B cell over T cell bias within the lymphoid branch (**Figures 3.4Bi and 3.4Bii**). Unlike the mTmG system, the level of labeling of the HSCs in the other reporter was not always a reliable indicator of labeling levels in peripheral cell populations. The peripheral cell labeling was much higher than HSCs in the Ai14 reporter system (**Figure 3.4C**). In the Confetti reporter system, the lymphocyte labeling seems to be similar to HSCs, but there is great variation in labeling levels of other peripheral cells (**Figure 3.4**). This variation is most likely due to the low recombination rate in the Confetti system.

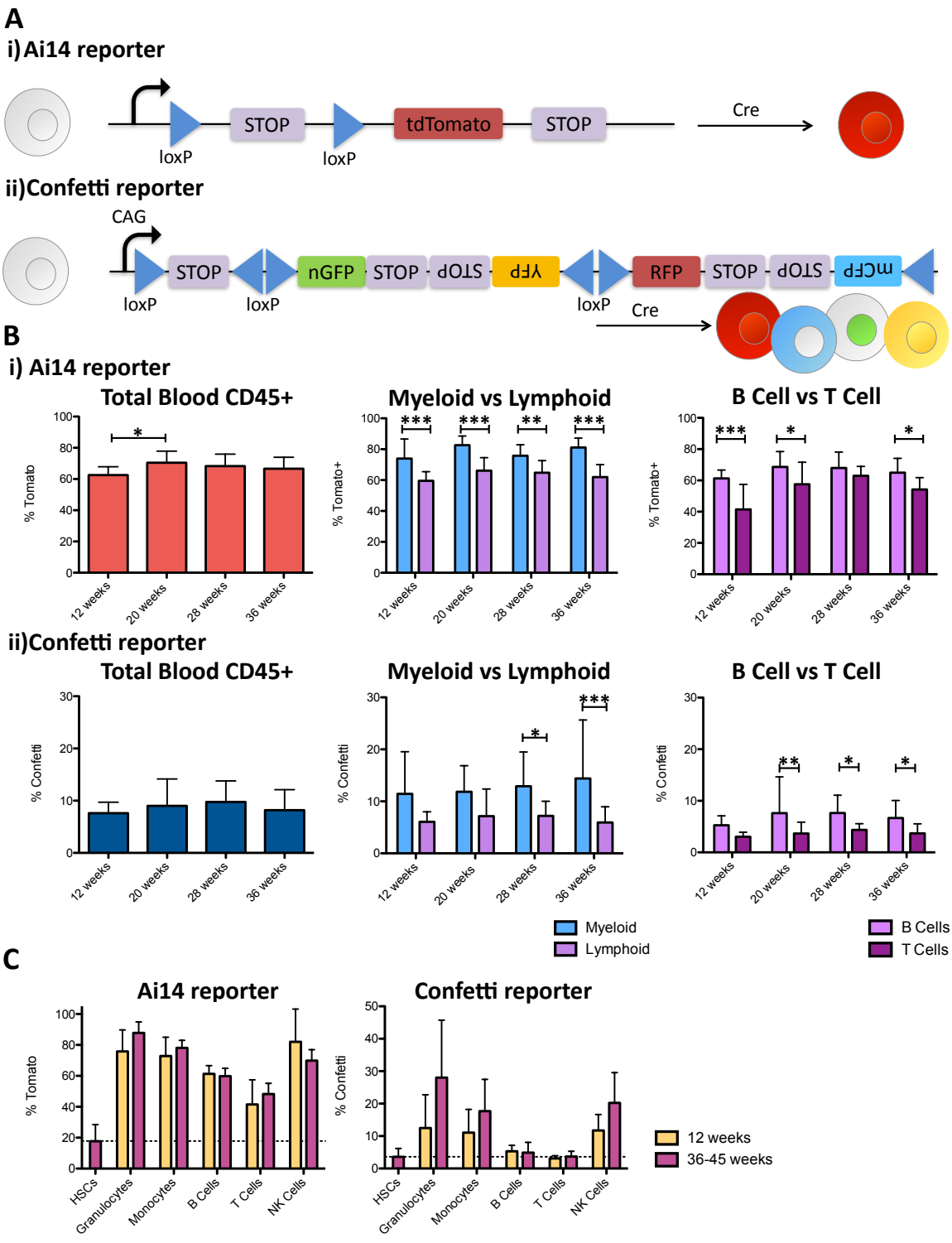
A
i) Ai14 reporter
STOP
tdTomato
STOP
loxP
loxP
Cre
ii) Confetti reporter
CAG
STOP
nGFP
STOP
YFP
RFP
STOP
mCFP
loxP
loxP
loxP
Cre
B
i) Ai14 reporter
Total Blood CD45+
Myeloid vs Lymphoid
B Cell vs T Cell
% Tomato
% Tomato+
12 weeks
20 weeks
28 weeks
36 weeks
ii) Confetti reporter
Total Blood CD45+
Myeloid vs Lymphoid
B Cell vs T Cell
% Confetti
Myeloid
Lymphoid
B Cells
T Cells
C
Ai14 reporter
Confetti reporter
% Tomato
% Confetti
HSCs
Granulocytes
Monocytes
B Cells
T Cells
NK Cells
12 weeks
36-45 weeks

Figure 3.4 LYVE1-derived T cell bias is not seen in other reporter systems
(A) Diagram of the Ai14 reporter system (i) and Confetti reporter system (ii).
(B) Flow cytometry analysis of LYVE1 labeling of hematopoietic populations in the Ai14 reporter (i) and Confetti reporter (ii) systems. Cells were gated on the same populations as described for the mTmG reporter system (Figure One). n= 14 for (i) and 18 for (ii)
(C) Comparison of reporter labeling of HSCs and the major blood lineages in the Ai14 and Confetti reporter systems. The line indicates the mean HSC labeling. n= 14 for (i) and 18 for (ii)
Statistical analysis: (B) 1 way ANOVA for CD45+ and 2 way ANOVA for Myeloid/Lymphoid and B/T, (C) 2 way ANOVA. *p<0.5, **p<0.01, ***p<0.001

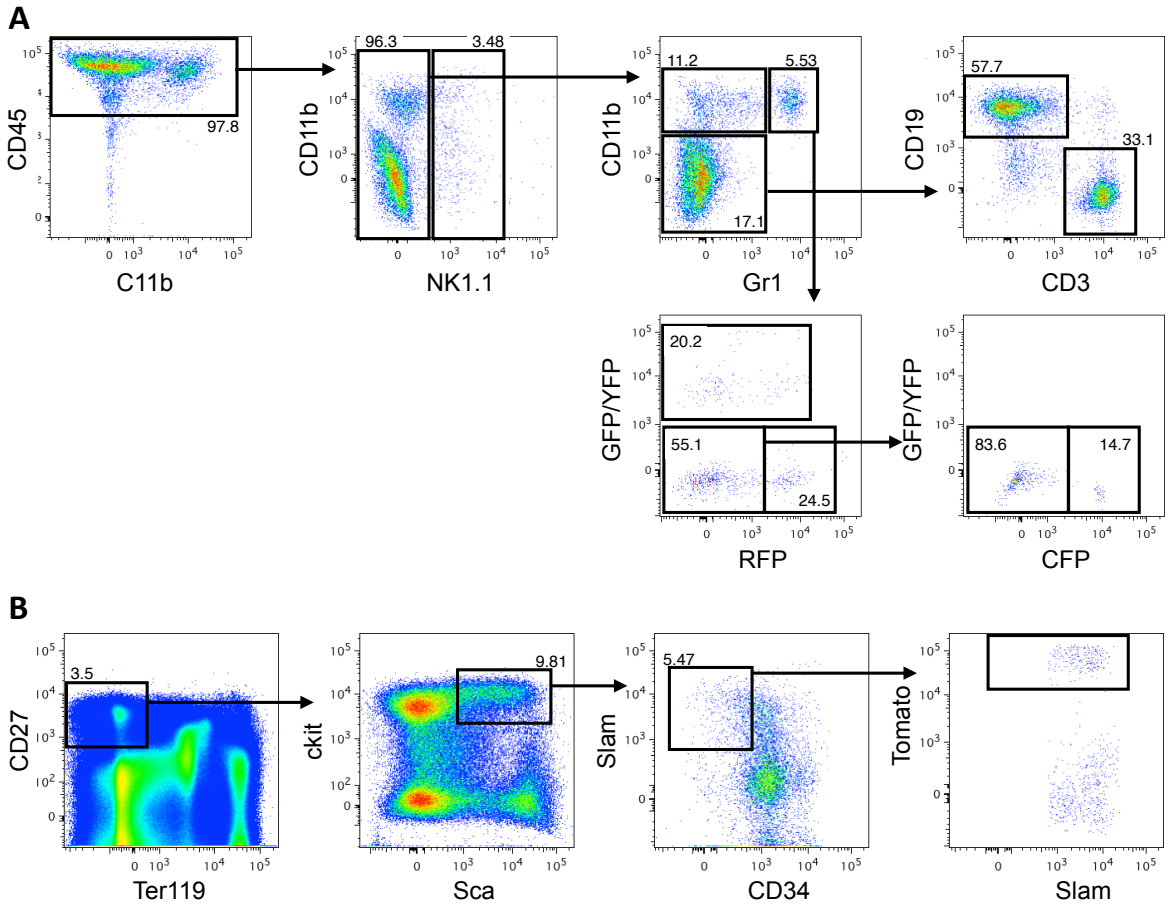

Supplemental Figure 3.2 Representative flow cytometry plots
(A) Lineage stain on peripheral blood from a Lyve1-Cre;Confetti mouse (gated on live, single cells).
(B) HSC stain on bone marrow from a Lyve1-Cre;Ai14 mouse (gated on live, single cells).

Discussion

In this study, we sought to determine if there are any lineage biases in the LYVE1-derived HSCs using three different reporter mouse strains. We found that each strain revealed a slightly different phenotype and that the Ai14 and Confetti strains have the most similarities. When homeostasis was disrupted via irradiation in the mTmG system, the hematopoietic compartment re-established the same levels of labeling indicating that the contribution from each type of HSC (GFP+ or Tomato+) is innate to the system. The mTmG system revealed only a CD8 cytotoxic T cell bias, whereas the Ai14 and Confetti systems appeared to have both a B cell over T cell and a slight myeloid over lymphoid cell bias.

The total percent of peripheral blood that was labeled by each system is a reflection of the complexity of the reporter and its effect on Cre. The Ai14 reporter, which is a single color reporter, is the least complex and has the greatest percent of labeled CD45+ cells (average of 67%). On the other hand, the Confetti reporter system is the most complex due to the random recombination events and has the least percent of labeled CD45+ cells (average of 8.6%). Of intermediate reporter complexity, the mTmG system has a percent of labeled CD45+ cells which falls in between the Ai14 and Confetti reporter systems (average of 27.6%). In a previous study, we determined the percent Cre efficiency for the Lyve1-Cre;mTmG system and calculated the percent of total CD45+ cells that are LYVE1-derived is about 49% which corresponds most closely to what is seen in the highest efficiency Cre system (Ai14). Similar levels of labeling were also seen by other studies (Ganuza et al. 2018).

Using the mTmG reporter system we found that the bias is not developmentally derived and instead appears in the periphery. However, it is an innate property as it remains after

resetting the hematopoietic system via irradiation, and is therefore not primarily due to influences in the environment. The differences between the labeling seen in each reporter system may be due to cell proliferation and its reflection of Cre efficiency on the reporter. The cells in the periphery divide more often than their quiescent precursors. This, taken together with the differences in the complexity of the reporter and the efficiency of the Cre, may explain the differences in labeling in each reporter system. The biases only appear in the peripheral cell subsets, which are the populations that divide more. They each reveal a slightly different bias because of their varied sensitivities. This does not however explain why there are more similarities between the most and least complex/efficient Cre/reporter system.

These different findings are not necessarily artifacts of the system. They may be true biases in that there are more LYVE1-derived myeloid than lymphoid cells, more B cells than T cells, and more cytotoxic T cells. The validity of these biases might be revealed by conducting RNAseq experiments on different developmental stages (including HSCs) and in peripheral cells to determine if there is a bias as seen by the genes expressed in these cells. ATAC-seq can also be done to determine if there are different epigenetic modifications that could contribute to a bias. The differences that we see may also be due to strain differences or due to differences in cell reactivity to the different fluorescent reporter systems used. This potential immunoreactivity may explain why there is a CD8 bias in the mTmG system. One of the fluorescent proteins (GFP or Tomato) may be immunoreactive and cause the cytotoxic T cells to become activated and proliferate in response to this stimulation.

This study highlights the importance of the use of different reporter systems in order to validate the identification of certain phenotypes. Results must be reproducible. This is not

limited to reproducibility from experiment to experiment or from lab to lab. This also means that the results need to be reproducible from system to system in order to determine if the observed phenotypes are due to the lineage tracer and not the reporter strain.

Materials and Methods

Mouse Models

All mice were obtained from Jackson Laboratories. Animals were housed in 12 hour light and dark cycles in the Gross Hall and Medical Sciences A vivarium facilities at the University of California, Irvine. All mice were given open access to food and water. The International Animal Care and Use Committee (IACUC) and the University Laboratory Animal Resources (ULAR) of the University of California, Irvine approved all animal procedures. The strains of mice that were used in this study were Lyve1-Cre (012601), mTmG (007576), Ai14 (007914), Confetti (017492), and C57 Bl/6 (00664).

Antibody staining

See table 3.1 for the antibodies used in flow cytometry.

Cell processing

Bone marrow was harvested via flushing or crushing of the femur and tibia. Spleens and thymi were processed using a glass tissue homogenizer. Peripheral blood was collected into EDTA via the tail vein. Red blood cells were lysed using 1X ACK Lysis Buffer and then washed with a

solution of PBS and 2% FBS to remove any residual lysis buffer. The cells were then ready for transplantation or staining for flow cytometry analysis/FACS.

Flow cytometry

Flow cytometry analysis was done on the BD LSR II or BD Fortessa X20 and data was analyzed using FlowJo.

Irradiation Stress

Briefly, 50 µL of blood was collected into EDTA from Lyve1Cre;mTmG adults via the tail vein. This was done to establish a baseline prior to irradiation, and for each time point after irradiation. The mice were irradiated at 750 cGy using a cabinet irradiator 2 weeks after the baseline bleed. They were then bled every week for 5 weeks post irradiation. Count bright beads were used to calculate absolute cell number.

Author Contributions

Conceptualization, M.A.I. and Y.G.; Methodology, M.A.I., Y.G; Investigation, Y.G., S.P., A.N., R.B.; Writing, Y.G. and M.A.I.; Visualization, Y.G., M.A.I.

Antibody	Fluorochrome	Clone	Dilution	Manufacturer	Catalog
B220	PE	RA3-6B2	1:200	BioLegend	103207
B220	APC	RA3-6B2	1:200	BioLegend	103211
B220	Brilliant Violet 605	RA3-6B2	1:200	BioLegend	103243
CD11a	PE	M17/4	1:200	BioLegend	101107
CD11a	Biotin	M17/4	1:200	BioLegend	101103
CD11b	APC	M1/70	1:200	BioLegend	101212
CD11b	APC-eFluor 780	M1/70	1:200	eBioscience	47-0112-82
CD135 (Flt3/Flk2)	PE	A2F10	1:100	BioLegend	135305
CD19	PerCP-Cyanine 5.5	eBio1D3	1:200	eBioscience	45-0193-82
CD19	Brilliant Violet 421	6D5	1:200	BioLegend	115537
CD19	Alexa Fluor 700	eBio1D3	1:200	eBioscience	56-0193-82
CD21	PE	eBio8D9	1:200	eBioscience	12-0211-81
CD23	PE/Cy7	B3B4	1:200	eBioscience	25-0232-81
CD25	APC	PC61	1:200	BioLegend	102011
CD27	APC	LG.7F9	1:200	eBioscience	17-0271-82
CD27	APC/Cy7	LG.3A10	1:100	BioLegend	124226
CD3	PE/Cy7	17A2	1:100	BioLegend	100220
CD3	PE	145-2C11	1:200	BioLegend	100307
CD3	PerCP-eFluor 710	17A2	1:200	Invitrogen	4338629
CD34	eFluor660	RAM34	1:50	Invitrogen	50-0341-82
CD4	PE/Cy7	RM4-5	1:200	BioLegend	100528
CD41	PE/Cy7	eBioMWReg30	1:50	Invitrogen	25-0411-80
CD43	APC	S7	1:200	BD Biosciences	560663
CD44	PE	IM7	1:200	BioLegend	103007
CD45	APC/Cy7	30-F11	1:200	BioLegend	103116

CD45	Alexa Fluor 700	30-F11	1:200	BioLegend	103128
CD45	PE/Cy7	30-F11	1:200	BioLegend	103114
CD61	PE	2C9.G2	1:50	BioLegend	104307
CD62L	APC	MEI-14	1:200	BioLegend	104411
CD8	APC/Cy7	53-6.7	1:200	BioLegend	100713
CD8	PE	53-6.7	1:200	Tonbo	50-0081-UO25
ckit	APC-eFluor 780	2B8	1:200	eBioscience	47-1171-82
ckit	Brilliant Violet 421	2B8	1:200	BioLegend	105827
ckit	PerCP-eFluor 710	2B8	1:200	eBioscience	46-1171-80
ckit	APC	ACK2	1:200	BioLegend	135108
ckit	PE/Cy7	2B8	1:200	BioLegend	105814
EPCR	PerCP-eFluor 710	eBio1560	1:200	eBioscience	46-2012-82
Gr1	Alexa Fluor 700	RB6-8C5	1:200	BioLegend	108422
Gr1	PE	RB6-8C5	1:200	Tonbo	50-5931-UO25
Gr1	Brilliant Violet 605	RB6-8C5	1:200	BioLegend	108439
IgD	Alexa Fluor 700	11-26c.2a	1:100	BioLegend	405729
IgM	APC/Cy7	RMM-1	1:200	BioLegend	406515
IL7Ra	Biotin	A7R34	1:100	eBioscience	13-1271-85
LYVE1	eFluor660	ALY7	1:50	Invitrogen	50-0443-80
NK1.1	PE	PK136	1:200	BioLegend	108708
NK1.1	APC	PK136	1:200	BioLegend	108710
Sca	PE/Cy7	E13-161.7	1:100	BioLegend	122514
Sca	Alexa Fluor 700	D7	1:200	BioLegend	108142
SLAM	PE	TC15-12F12.2	1:100	BioLegend	115904
Streptavidin	Qdot605	—	1:200	Invitrogen	Q10103MP
TCRab	APC	H57-597	1:200	BioLegend	109211

TCRyd	PE	GL3	1:200	BioLegend	118107
Ter119	PE/Cy5	TER-119	1:200	BioLegend	116210

Table 3.1 Antibodies

References

Ganuza, Miguel, Ashley Chabot, Xing Tang, Wenjian Bi, Sivaraman Natarajan, Robert Carter, Charles Gawad, Guolian Kang, Yong Cheng, and Shannon McKinney-Freeman. 2018. "Murine Hematopoietic Stem Cell Activity Is Derived from Pre-Circulation Embryos but Not Yolk Sacs." *Nature Communications* 9 (1). https://doi.org/10.1038/s41467-018-07769-8.

Lee, Lydia K., Yasamine Ghorbanian, Wenyuan Wang, Yanling Wang, Yeon Joo Kim, Irving L. Weissman, Matthew A. Inlay, and Hanna K.A. Mikkola. 2016. "LYVE1 Marks the Divergence of Yolk Sac Definitive Hemogenic Endothelium from the Primitive Erythroid Lineage." *Cell Reports* 17 (9): 2286–98. https://doi.org/10.1016/j.celrep.2016.10.080.

MD, Muzumdar, Tasic B, Miyamichi K, Li L, and Luo L. 2006. "A Global Double-Fluorescent Cre Reporter Mouse." *Genesis* 224 (September): 219–24. https://doi.org/10.1002/dvg.

Pham, Trung H.M., Peter Baluk, Ying Xu, Irina Grigorova, Alex J. Bankovich, Rajita Pappu, Shaun R. Coughlin, Donald M. McDonald, Susan R. Schwab, and Jason G. Cyster. 2010. "Lymphatic Endothelial Cell Sphingosine Kinase Activity Is Required for Lymphocyte Egress and Lymphatic Patterning." *The Journal of Experimental Medicine* 207 (1): 17–27. https://doi.org/10.1084/jem.20091619.

DISCUSSION

The origin(s) of definitive hematopoietic stem cells has become a contentious source of debate amongst those who study hematopoiesis. The field is often divided by those who believe that the AGM is the sole source of definitive HSCs and those who believe that the YS contributes to this population as well. When HSCs and their ontogeny were first studied, it was commonly believed that the YS gave rise to definitive HSCs which then matured and migrated into the embryo to seed the FL (Moore and Metcalf 1970). However, in the 1990's there came a wave of studies which pointed to the AGM as a source of definitive HSCs (A. L. Medvinsky et al. 1993; Müller et al. 1994; A. Medvinsky and Dzierzak 1996; A. L. Medvinsky and Dzierzak 1998). These were mostly fueled by studies that had been done earlier in the avian and amphibian blood systems, which pointed to the YS as the source of early, primitive HSCs and the AGM as the source of the later, definitive HSCs. These murine AGM studies relied heavily on an *in vitro* culture system in which only the AGM was shown to maintain and generate HSCs. Other tissues— the YS, FL, and placenta— were unable to generate HSCs in this artificial *in vitro* system, but were able to maintain HSC numbers (A. Medvinsky and Dzierzak 1996; Ottersbach and Dzierzak 2005). It is very possible that this *in vitro* culture system is only optimized for the intraembryonic AGM, which in the intact organism has a very different environment than the extraembryonic placenta and YS. This could be in part as to why these tissues do not produce any cells *de novo* in this system, a point that the authors concede when discussing the placenta (Ottersbach and Dzierzak 2005).

Studies that indicate that the YS is necessary for definitive HSPC generation show that circulation and migration are necessary to get HSPCs in the embryo, but do not affect the HSPCs

in the extraembryonic tissues (Lux et al. 2008; Ghiaur et al. 2008). However, cells from the AGM engraft into conditioned adult recipients a full day earlier than the YS, FL, and placenta (Müller et al. 1994; A. Medvinsky and Dzierzak 1996). Thus, this implies that the AGM and YS need each other in order to generate a complete pool of definitive HSCs and that circulation is a necessary component of this cooperative development. Metcalf suggested that the AGM is a "highly specialized finishing school" to which cells from the YS that have HSC potential migrate in order to receive signals to become definitive HSCs (Metcalf 2008). In support of this necessity for multiple sources of HSCs, it has been shown that the numbers of HSCs in the FL cannot be supplied solely by the AGM and that other sources, particularly extra-embryonic tissues, must contribute(Kumaravelu et al. 2002). Runx1 lineage tracing studies support this by showing that hematopoietic progenitors migrate to the FL and thymus from the YS (Samokhvalov, Samokhvalova, and Nishikawa 2007). Taken together, these studies indicate that the AGM may have a small initial source of HSCs and that the placenta and YS contribute to a later wave of HSCs that need to migrate into the embryo, either to the FL or to the AGM, in order to mature and give rise to fully functional (i.e. multipotent, self-renewing, and engraftable) HSCs.

Our studies, as shown in this dissertation, provide further evidence for this hypothesis that there are multiple sources and waves of definitive hematopoiesis. We show that there are at least two different pools of HSCs, LYVE1-derived and non-LYVE1-derived, and that these cells have different maturation kinetics. The non-LYVE1-derived pre-HSCs, as defined by their ability to engraft into conditioned neonatal recipients, mature before the LYVE1-derived pre-HSCs, which engraft a day later (E11.5) in almost all tissues. The exception to this is the LYVE1-derived pre-HSCs that are found in the AGM. A small portion of those were able to engraft at E10.5,

before LYVE1-derived cells found in other tissues. This points to the AGM as either a site in which these cell must migrate to and mature, or a site that already has a fully matured subset of pre-HSCs.

LYVE1 labels a much smaller population of endothelial cells in the AGM as compared to the YS in which LYVE1 labeling is abundant. This, along with the transplant data, could indicate that LYVE1 marks the rare hemogenic endothelial subset in the AGM that is efficient at creating mature pre-HSCs. That is not to say that the labeled endothelial cells in the YS are not hemogenic endothelium; however, the proportion of labeled cells in the YS that has hematopoietic potential is likely much lower than that of the AGM. The neonatal transplantation experiments provide evidence that the LYVE1-derived pre-HSCs found in tissues other than the AGM require longer to mature. This is a finding that is not exclusive to our studies. Limiting dilution analysis experiments were performed to quantify HSC/RUs in the FL and other tissues. Researchers found that the generation of HSC/RUs peaks in the AGM a day before it does so for the YS (Kumaravelu et al. 2002). All of this taken together provides strong evidence that the AGM has an environment that is conducive to earlier maturation of HSCs than that of other tissues. It cannot be concluded as to whether those cells have migrated or originated there. However, our data suggests that it is most likely the LYVE1-derived pre-HSCs that have come from the labeled endothelium in the AGM that mature first as opposed to cells that have migrated there. This is largely due to our *ex vivo* embryo culture data which shows that the labeled cells are not very migratory at these stages. Instead, they seem to be stuck in their environment and are either surveying the area or dividing in order to expand the population. It has been stated in other studies as well that the placenta and the YS are sites of

pre-HSC expansion, while the AGM and FL are sites of pre-HSC maturation (McGrath and Palis 2005; Ghiaur et al. 2008). Our data fits nicely with these hypotheses.

It would be important for future studies to determine the differences, if there are any, between the LYVE1-derived and non-LYVE1-derived hematopoietic cells. Our neonatal transplant studies already indicate that the non-LYVE1-derived pre-HSCs mature earlier than their LYVE1-derived counterparts. However, once they are fully matured adult HSCs, they are able to engraft equally well into conditioned adult recipients. For the FL HSC population, when the LYVE1-derived and non-LYVE1-derived HSCs are transplanted at their native ratios, they engraft at levels that recapitulate their contribution to the total HSC pool in Lyve1-Cre;mTmG mice. This is strong evidence that there is an innate level of homeostasis in the system, which may have implications for the clinical use of these cells. It would also be interesting to determine if one population is more prone to disease or to mutagenesis and therefore more likely to cause a hematological malignancy or cancer. This could have major implications for if one population should be sorted to use in BMT over another, or if it is important to keep both as they might keep the system in some sort of homeostatic check. This could be an additional consideration for the *in vitro* differentiation of HSCs either for clinical therapies or for research.

A way to determine these differences would be to perform RNAseq of adult LYVE1-derived/non-LYVE1-derived HSCs and embryonic LYVE1-derived/non-LYVE1-derived endothelial cells, pre-HSCs, and HSCs. The embryonic populations would be separated based on tissue (AGM, YS, VV, placenta, and FL) and harvested at different stages (E8.5-E11.5 and E14.5). This analysis would allow us to determine if these populations differ in gene expression. Of particular interest would be to ascertain if there is expression of certain promoting or inhibitory

genes for differentiation that differ between the AGM and the other tissues in the embryonic endothelial cells.

We attempted to look into the differences between the two populations of cells by determining if there was a lineage bias for either of the HSC populations. At first we believed that the LYVE1-derived HSCs had a T cell bias, and spent a great deal of effort in an attempt to characterize this bias and uncover its source. It was not developmentally derived and in fact, it was only seen when using the mTmG reporter strain. The use of the Confetti and Ai14 reporter strains revealed different biases (myeloid and B cell). This was an important lesson to learn in that phenotypes found in certain reporter systems must be confirmed in others in order to ensure reproducibility.

The *ex vivo* embryo cultures are one of the most exciting set of experiments that were done for this dissertation. This is the first time that intact murine embryos have been successfully cultured and imaged as they develop. It is important to note that their development is normal during the time that they are viable. These experiments lay the groundwork for many more exciting experiments that can be done. Manipulation of hematopoiesis by either inhibition or promotion of this process can help to yield insights into how these cells develop. Can we recapitulate the AGM microenvironment to get early maturation of YS LYVE1-derived pre-HSCs? This system can also be utilized to ascertain how different drugs can affect the hematopoietic compartment.

A noteworthy observation from the *ex vivo* embryo culture movies, and one that would be important to follow up on for future experiments, would be the appearance of LYVE1-labeled myeloid cells. It looks like these cells are very motile and are perhaps involved in

vascular remodeling. A recent study suggested that inflammatory macrophages are important for the maturation of pre-HSCs in the AGM (Mariani et al. 2019). It would be interesting to determine if the myeloid cells that we are seeing in the YS are inflammatory, and if they are not, induce an inflammatory environment in an effort to accelerate pre-HSC maturation in the YS.

It is still unclear as to why LYVE1 would mark a specific subset of hemogenic endothelium that ultimately gives rise to definitive HSCs. The role of LYVE1 is still being researched, but currently it has been implicated in the transport of HA from the tissues and into the lymphatics. HA is important for tissue repair, wound healing, and embryogenesis so it would be interesting to determine if HA has an active role in hematopoiesis. It is an inflammatory molecule and because of the recent implications that inflammation is necessary for HSC maturation, perhaps this concept applies in this situation as well. However, it is more likely that HA has a role in vascular remodeling since our *ex vivo* embryo cultures show that the vasculature is constantly changing from E8.5-E10.5.

Overall, the work in this dissertation provides strong evidence that LYVE1 is a marker for definitive hematopoietic stem cell ontogeny. It identifies a subset of definitive hemogenic endothelial cells that give rise to definitive HSCs that are multipotent, self-renewing, and engraftable. More research still needs to be done to determine if there differences between the LYVE1-derived and non-LYVE1-derived HSCs. However, it is important that we have revealed a possible source of heterogeneity in the HSC pool and this could have strong implications for the study and treatment of hematopoietic malignancies. It also reveals that it is

perhaps not necessarily the tissue of origin that we should focus on for studying the ontogeny of HSCs, but the cell populations and the microenvironments that they are located in instead.

References

Auerbach, Robert, Hua Huang, and Lisheng Lu. 1996. "Hematopoietic Stem Cells in the Mouse Embryonic Yolk Sac." *Stem Cells* 14 (3): 269–80. https://doi.org/10.1002/stem.140269.

Ghiaur, Gabriel, Michael J. Ferkowicz, Michael D. Milsom, Jeff Bailey, David Witte, Jose A. Cancelas, Mervin C. Yoder, and David A. Williams. 2008. "Rac1 Is Essential for Intraembryonic Hematopoiesis and for the Initial Seeding of Fetal Liver with Definitive Hematopoietic Progenitor Cells." *Blood* 111 (7): 3322–30. https://doi.org/10.1182/blood-2007-09-078162.

Jackson, David G. 2004. "Biology of the Lymphatic Marker LYVE-1 and Applications in Research into Lymphatic Trafficking and Lymphangiogenesis." *Apmis* 112 (7–8): 526–38. https://doi.org/10.1111/j.1600-0463.2004.apm11207-0811.x.

Kumaravelu, Parasakthy, Lilian Hook, Aline M. Morrison, Jan Ure, Suling Zhao, Sergie Zuyev, John Ansell, and Alexander Medvinsky. 2002. "Quantitative Developmental Anatomy of Definite Haematopoietic Stem Cells/Long-Term Repopulating Units (HSC/RUs): Role of the Aorta-Gonad-Mesonephros (AGM) Region and the Yolk Sac in Colonisation of the Mouse Embryonic Liver." *Development* 129 (21): 4891–99.

Lux, Christopher T., Momoko Yoshimoto, Kathleen McGrath, Simon J. Conway, James Palis, and Mervin C. Yoder. 2008. "All Primitive and Definitive Hematopoietic Progenitor Cells Emerging before E10 in the Mouse Embryo Are Products of the Yolk Sac." *Blood* 111 (7): 3435–38. https://doi.org/10.1182/blood-2007-08-107086.

Mariani, Samanta Antonella, Zhuan Li, Siobhan Rice, Carsten Krieg, Stamatina Fragkogianni, Mark Robinson, Chris Sebastiaan Vink, Jeffrey William Pollard, and Elaine Dzierzak. 2019. "Pro-Inflammatory Aorta-Associated Macrophages Are Involved in Embryonic Development of Hematopoietic Stem Cells." *Immunity* 50 (6): 1439-1452.e5. https://doi.org/10.1016/j.immuni.2019.05.003.

McGrath, Kathleen, and James Palis. 2005. "Hematopoiesis in the Yolk Sac: More than Meets the Eye." *Experimental Hematology* 33 (9): 1021–28. https://doi.org/10.1016/j.exphem.2005.06.012.

Medvinsky, Alexander, and Elaine Dzierzak. 1996. "Definitive Hematopoiesis Is Autonomously Initiated by the AGM Region." *Cell* 86 (6): 897–906. https://doi.org/10.1016/S0092-8674(00)80165-8.

Medvinsky, Alexander L., and Elaine A. Dzierzak. 1998. "Development of the Definitive Hematopoietic Hierarchy in the Mouse." *Developmental & Comparative Immunology* 22 (3): 289–301. https://doi.org/10.1016/S0145-305X(98)00007-X.

Medvinsky, Alexander L., Nina L. Samoylina, Albrecht M. Müller, and Elaine A. Dzierzak. 1993. "An Early Pre-Liver Intraembryonic Source of CFU-S in the Developing Mouse." *Nature* 364 (6432): 64–67. https://doi.org/10.1038/364064a0.

Metcalf, Donald. 2008. “AGM: Maternity Ward or Finishing School?” *Blood*. American Society of Hematology. https://doi.org/10.1182/blood-2007-11-124412.

Moore, Malcolm A.S., and Donald Metcalf. 1970. “Ontogeny of the Haemopoietic System: Yolk Sac Origin of In Vivo and In Vitro Colony Forming Cells in the Developing Mouse Embryo.” *British Journal of Haematology* 18 (3): 279–96. https://doi.org/10.1111/j.1365-2141.1970.tb01443.x.

Müller, Albrecht M., Alexander Medvinsky, John Strouboulis, Frank Grosveld, and Elaine Dzierzakt. 1994. “Development of Hematopoietic Stem Cell Activity in the Mouse Embryo.” *Immunity* 1 (4): 291–301. https://doi.org/10.1016/1074-7613(94)90081-7.

Ottersbach, Katrin, and Elaine Dzierzak. 2005. “The Murine Placenta Contains Hematopoietic Stem Cells within the Vascular Labyrinth Region.” *Developmental Cell* 8 (3): 377–87. https://doi.org/10.1016/j.devcel.2005.02.001.

Palis, J. 2001. “Yolk-Sac Hematopoiesis The First Blood Cells of Mouse and Man.” *Experimental Hematology* 29 (8): 927–36. https://doi.org/10.1016/S0301-472X(01)00669-5.

Peeters, Marian, Katrin Ottersbach, Karine Bollerot, Claudia Orelino, Marella de Bruijn, Mark Wijgerde, and Elaine Dzierzak. 2009. “Ventral Embryonic Tissues and Hedgehog Proteins Induce Early AGM Hematopoietic Stem Cell Development.” *Development* 136 (15): 2613–21. https://doi.org/10.1242/dev.034728.

Samokhvalov, Igor M., Natalia I. Samokhvalova, and Shin-ichi Nishikawa. 2007. “Cell Tracing Shows the Contribution of the Yolk Sac to Adult Haematopoiesis.” *Nature* 446 (7139): 1056–61. https://doi.org/10.1038/nature05725.